

a. Mechanical Properties Engineering

Anisotropy in Woven Fabric Stress and Elongation at Break

Radko Kovar
*Technical University of Liberec
Czech Republic*

1. Introduction

Anisotropy is a characteristic of most fabrics, especially woven; the impact of the direction of loading on tensile properties can be enormous and is frequently examined, for example in (Dai & Zhang, 2003; Hu, 2004; Kilby, 1963; Kovar & Dolatabadi, 2009; Kovar, 2003; Lo & Hu, 2002; Pan & Yoon, 1996; Postle et al., 1988 etc.). Anisotropy of properties comes out of anisotropy of the structure, based on longitudinal fibers. For woven fabric there are two principal directions – warp and weft (fill), in which yarns and majority of fibres are oriented. Load in principal directions results in minimum breaking elongation and maximum initial modulus. For arbitrary load direction the values of tensile properties change and fabric deformation becomes more complex, often incorporating fabric shear and bend deformation.

Although weave anisotropy is well known, tensile properties are usually theoretically and experimentally investigated namely for principal directions; the main reason is probably complexity of deformation and stress distribution when the load is put at non-principal direction. In this section we shall try to make a step to describe and perhaps to overcome some of these problems.

In practical use, the fabrics are often imposed load in arbitrary direction, bi-axial load or complex load composed of elongation, bend, shear and lateral compression. To predict tensile properties becomes more and more important with development of technical textiles. Now only main difficulties, connected with the topic of this section, will be outlined:

- a. At diagonal load great lateral contraction occurs. It causes complex distribution of stresses. It results in stress concentration at jaws when experiment in accordance with EN ISO 13934-1 is used.
- b. There are yarns cut ends in the sample where tensile stress starts from zero.
- c. Shear deformation causes jamming of yarns, what can change yarn properties. Strength of the yarn in the fabric can be higher than the strength of free yarn.

There are not available many publications, based on real fabric structure and solving the problem of woven fabric tensile properties in different directions. The reason is mentioned long range of problems and difficulties. Monographs (Hearle et al., 1969 and Postle et al., 1988) are involved in problems of bias fabric load only marginally. (Hu, 2004) is oriented on influence of direction on properties such as tensile work, tensile extension, tensile linearity etc. and uses another approach. Fabric shear at bias extension is investigated in (Du & Yu, 2008). Model of all stress-strain curve of fabric, imposed bias load, is introduced for example in (King, M. J. et al., 2005) with the respect to boundary conditions (stress concentration at

jaws). In (Peng & Cao, 2004) is area of fabric sample separated into 3 zones with different characteristics of bias deformation. Experimental models of woven fabric deformation in different directions are presented by (Zouari et al., 2008). Often the mechanics of continuum approach, coming out of prediction of Hook's law validity, is used, for example, in (Du & Yu, 2008; Hu, 2004; Peng & Cao, 2004 and Zheng et al., 2008). A new method of anisotropy measuring is proposed by (Zheng, 2008) etc.

This section is oriented first of all on anisotropy of rupture properties of weaves, imposed uniaxial load in different directions. The main goal is to develop algorithm for calculation of plain weave fabric breaking strain and stress under conditions of simulated idealized experiment. There are two ways of ideal uni-axial woven fabric loading (details are in section 2): (a) Keeping stable lateral (i.e. perpendicular to direction of load) dimension, (b) Keeping lateral tension on zero (i.e. allowing free lateral contraction).

In this chapter rupture properties will be analyzed for plane weave structure.

2. Nomenclature

β_0, β - angle of warp yarns orientation to the load direction before and after load [rad].

γ - shear angle [rad].

ε - relative elongation or strain [1].

μ - yarn packing density, a share of volume of fibrous material and volume of yarn [1].

ν - Poisson's ratio [1]

b - width of the fabric sample [m].

c - yarn crimp [1]

d - diameter of yarn [m].

F - force [N].

h_0, h - length of the fabric, taken for calculation, before and after fabric elongation [m].

l_0, l - length of the yarn in a crimp wave [m].

L_0, L - projection of the length of the yarn in fabric plane before and after load [m].

s_0, s - component of yarn length L into direction perpendicular to load [m].

p - spacing of yarns (pitch) [m].

S - fabric sett (yarn density) [m⁻¹].

t - fabric thickness [m⁻¹].

T - yarn linear density [Mtex].

Main subscripts: y - yarn, f - fabric, 1 - warp yarn or direction of warp yarns, 2 - weft yarn or direction of weft yarns, 1,2 - warp or weft yarns, 0 - status before load (relaxed fabric), b - status at break, d - diagonal direction (45 °), n - not-broken yarn, h - horizontal or weft direction, v - vertical or warp direction.

3. Models of woven fabrics rupture properties

Modelling always means simplification of reality and, in our case, idealizing the form of the load. When we wish to simulate experimental investigation of similar property, we should start with brief description of standard fabric rupture properties measuring with the use of EN ISO 13934-1 (strip test) standard. Fast jaws keep the sample in original width (width before load) what results in tension concentration at these jaws. Break usually occurs near the sample grip sooner then real fabric strength is reached. In Fig. 1 a, b are these critical points of the sample marked by circles.

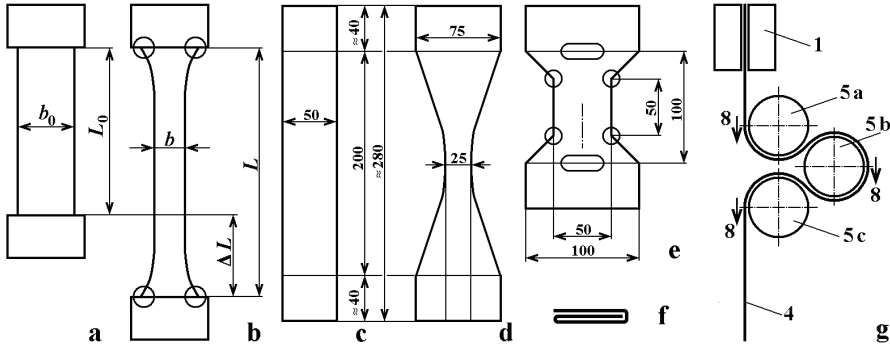


Fig. 1. Tension concentration at jaws and methods of its elimination

There are two main ways how to avoid the problem of tension concentration that occurs when using standard method; sample dimensions are in Fig. 1 c. First is reduction of fabric tension at jaws by narrowing the sample in central part, Fig. 1 d (Zborilova & Kovar, 2004) and 1 e (CSN standard 80 0810). This solution improves the results but some places with tension concentration stay. Till now the best results provides a new method (Kovar & Dolatabadi, 2010), Fig. 1 g; details of the method will be described in section 4.1.

When we wish to model fabric rupture properties and to avoid the problems with uneven tension distribution, we need to analyze a part of the fabric imposed constant load. Virtually there are two idealized situations:

- To prevent sample from lateral contraction, i.e. to keep the fabric at original width b_0 . This can simulate an experiment with infinite fabric width, when the influence of the sample margins becomes negligible. Restriction of lateral contraction must be, in practical experiments, connected with biaxial load, because some complementary load arises in the direction perpendicular to the direction of main load.
- To allow free lateral contraction of the fabric. This model can simulate an experiment with flexible jaws that change the width simultaneously with fabric lateral contraction, or partly infinite fabric length, where the effect of fast jaws will not change sample relative elongation at break. This model is more complicated owing to fabric jamming and cut ends of yarns under load. Tensile stress in yarn at the cut end is zero and increases gradually due to yarn-to-yarn friction.

Yarn parameters and properties

From parameters and properties of yarn are, for fabric tensile properties investigation, most important: (a) Yarn cross-section as variable parameter. For simplification we can use yarn diameter d . For rough estimation of d can be used well known formula (1), where ρ is density of fibrous material and μ is average yarn packing density, the most problematic parameter. Its average value in free yarn used to be around $\mu_0 \approx 0.5$. This could be used for fabric with low packing density (lose fabric). At tight fabric yarn cross-section becomes flat and packing density increases. Here can be used effective yarn diameter d_{ef} . It is variable parameter, described as distance of yarns neutral axes in cross-over elements. In tight fabric can packing density reach, near warp and weft yarn contact, approximately $\mu_{ef} \approx 0.8$. In fabric near the break, mainly at diagonal load, yarn packing density reaches maximum possible value $\mu_b \approx 0.9$. (b) Yarn stress-strain curve, which can be for some purposes replaced by yarn breaking stress F_{yb} (strength) and strain ϵ_{yb} . Due to yarn jamming breaking

stress can increase and strain decrease. (c) Unevenness of yarn geometry and other properties. In this section this will be neglected.

$$d = \sqrt{\frac{4T}{\pi \cdot \rho \cdot \mu}}, \quad d_{ef} = \sqrt{\frac{4T}{\pi \cdot \rho \cdot \mu_{ef}}} \quad (1)$$

3.1 Model for infinite sample width

Restriction of lateral contraction makes the models relatively simple. This model and its experimental verification have been described in (Kovar & Gupta 2009). A conception of this theory is the test with infinite sample width that does not allow fabric lateral contraction. Experimental verification was based on keeping the tubular sample in original width by two fast wires (see Fig. 19). The yarns in model fabric are shown in Fig. 2; 1 is upper jaw, 2 bottom jaw before and 3 after elongation or at break.

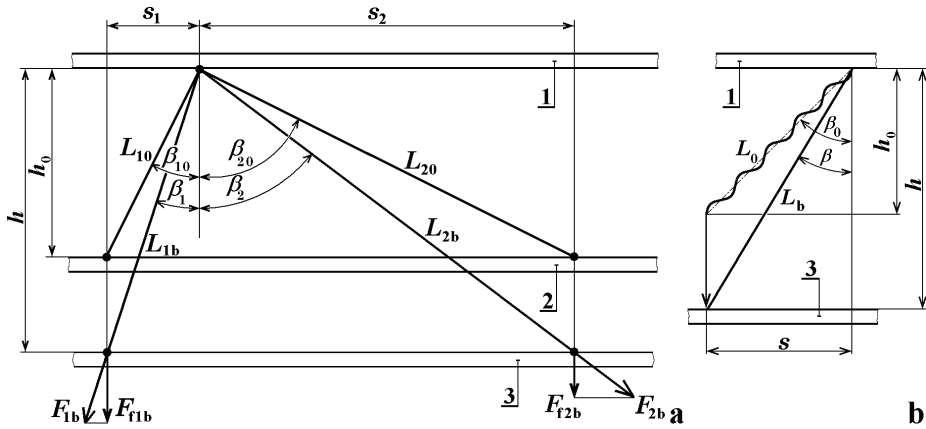


Fig. 2. Warp and weft yarns dimensions before load and at break

Relative fabric elongation, ε_f , and warp and weft yarns elongations, $\varepsilon_{1,2}$, are defined as

$$\varepsilon_f = \frac{h - h_0}{h_0} = \frac{h}{h_0} - 1 \quad \text{and} \quad \varepsilon_{1,2} = \frac{L_{1,2b} - L_{1,20}}{L_{1,20}} = \frac{L_{1,2b}}{L_{1,20}} - 1 \quad (2)$$

Original lengths of warp L_{10} and weft L_{20} yarns before elongation between the jaws are

$$L_{10} = \frac{h_0}{\cos \beta_{10}} \quad \text{and} \quad L_{20} = \frac{h_0}{\cos \beta_{20}} = \frac{h_0}{\sin \beta_{10}} \quad (3)$$

where β_0 is the angle between direction of warp or weft yarns and direction of load. After fabric elongation from h_0 on h yarn angles decrease from $\beta_{1,20}$ to $\beta_{1,2}$.

Note: subscripts 1, 2 denotes validity of expression either for warp or for weft yarns, valid are either the first or the second subscripts, so often one expression contains two equations.

The final lengths of yarn segments will be L_{1b} and L_{2b} . As lateral contraction is restricted, horizontal projections of yarn segments will not change and so $s_{1,2} = s_{1,20}$. Fig. 2 b describes two main means of each yarn elongation, i.e. decrimping and yarn axial elongation.

With the exception of one particular load angle β_0 only one system of yarns reaches breaking elongation; in so called square fabric, when all the parameters are for warp and weft directions the same, first break yarns with $\beta_0 < 45^\circ$. For these broken yarns their lengths at fabric break will be $L_{1,2b} = L_{1,20} \cdot (1 + \varepsilon_{1,2b}) \cdot (1 + c_{1,20})$, where $\varepsilon_{1,2b}$ is yarn relative elongation at break and $c_{1,20}$ is crimp of the yarn, see Fig. 6 and Equation (7). As in this case it is $s = \text{const.}$ we shall obtain, using Pythagorean Theorem, the length of the fabric at break $h = \sqrt{L_{1,2b}^2 - s_{1,2}^2}$ and fabric breaking elongation ε_{fb} will be

$$\varepsilon_{fb} = \frac{h}{h_0} - 1 = \frac{\sqrt{(L_{1,20} \cdot (1 + \varepsilon_{1,2b}) \cdot (1 + c_{1,20}))^2 - s_{1,2}^2}}{h_0} - 1 \quad (4)$$

where $s_{1,2} = h_0 \cdot \tan \beta_{1,20}$.

Characteristics of this formula is shown, for one value of warp yarns extensibility $\varepsilon_{1b} = 0.2$ and five values of weft yarns extensibility $\varepsilon_{2b} = 0.1; 0.15; 0.2; 0.25$ and 0.3 , in Figure 3. As it was mentioned, with the exception of one critical angle only yarns of one system (warp ore weft) will break. The critical angle can be found as crossing points of the curves for warp and weft yarns.

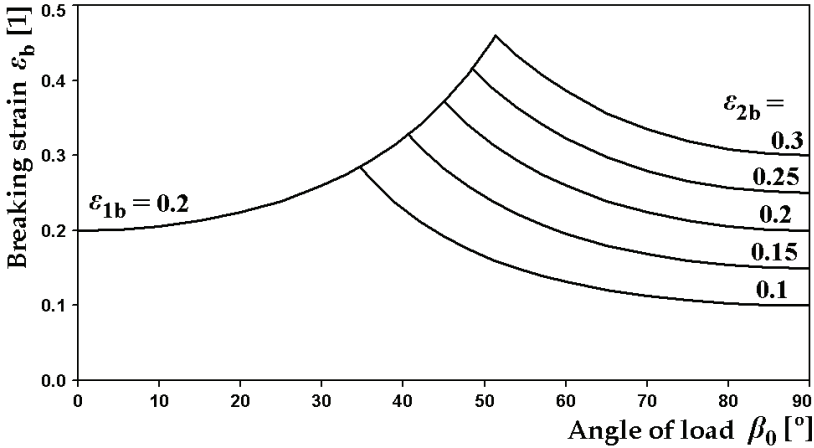


Fig. 3. Influence of angle load on breaking elongation for different yarn

Breaking stress, i.e. force necessary for damage of 1 m width of the fabric, can be calculated as the sum of the stresses from all yarns in 1 m of fabric width. Number of yarns in fabric width unit is $n = n_1 + n_2 = S_1 \cdot \cos \beta_{10} + S_2 \cdot \cos \beta_{20}$, where $S_{1,2}$ are fabric setts. The component of yarns axial stresses to the direction of external load from one broken yarn is $F_{fl,2b} = F_{1,2b} \cdot \cos \beta_{1,2}$ (see Fig. 2), $F_{1,2b}$ is strength of one yarn (axial force at break). The force from one non-broken yarn $F_{1,2n}$ depends on this yarn elongation at fabric break $\varepsilon_{1,2n}$ and on yarn stress-strain curve. For simplification we shall assume linear yarn deformation and so $F_{1,2n} = F_{1,2b} \cdot \frac{\varepsilon_{1,2n}}{\varepsilon_{1,2b}}$. The final result, the force necessary for breakage of 1 m fabric width is

$$F_{fb} = F_{f1,2b} + F_{f2,1n} = F_{1,2b} \cdot \cos \beta_{1,2} \cdot S_{1,2} \cdot \cos \beta_{1,20} + F_{2,1b} \cdot \cos \beta_{2,1} \cdot S_{2,1} \cdot \cos \beta_{2,10} \cdot \frac{\varepsilon_{2,1n}}{\varepsilon_{2,1b}} \quad (5)$$

where $F_{f1,2b}$ is the force in 1 m fabric width from all broken yarns, $F_{f2,1n}$ is the same from non-broken yarns. If change of angle of yarn incline during the elongation is neglected, i.e. if $\beta_{1,2} = \beta_{1,20}$, equation (5) would be simplified as

$$F_{fb} = F_{1,2b} \cdot \cos^2 \beta_{1,20} \cdot S_{1,2} + F_{2,1b} \cdot \cos^2 \beta_{2,10} \cdot S_{2,1} \cdot \frac{\varepsilon_{2,1n}}{\varepsilon_{2,1b}} \quad (6)$$

Examples of results of calculation are shown in the following charts. In Fig. 4 is set warp and weft yarns extensibility at break, that includes de-crimping and yarns breaking elongation, on $\varepsilon_{1b} = \varepsilon_{2b} = 0.2$, warp yarn strength $F_{1b} = 8$ and weft yarn strengths are variable. Warp and weft yarns set is $S_1 = S_2 = 1000 \text{ m}^{-1}$. Similarly in Fig. 5 is shown influence of yarn extensibility on fabric breaking stress for $\varepsilon_{1b} = 0.2$, variable ε_{2b} , $F_{1b} = 8 \text{ N}$ and $F_{2b} = 6 \text{ N}$. In Figs. 4 and 5 thick lines represent calculation according to equation (5) and thin lines follows equation (6).

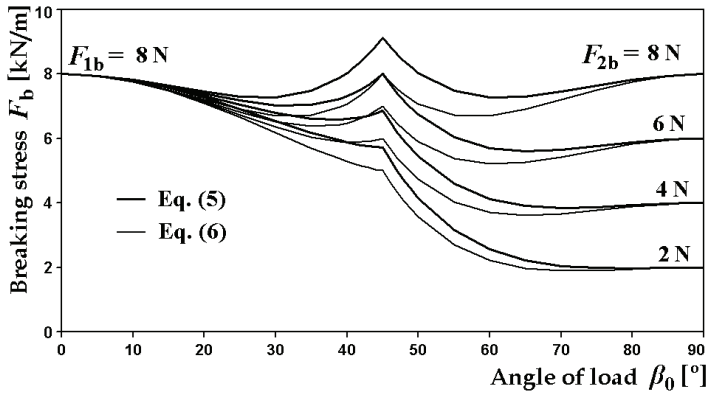


Fig. 4. Influence of angle β_0 on breaking stress for $F_{1b} = 8 \text{ N}$, different F_{2b} , $\varepsilon_{1b} = \varepsilon_{2b} = 0.2$

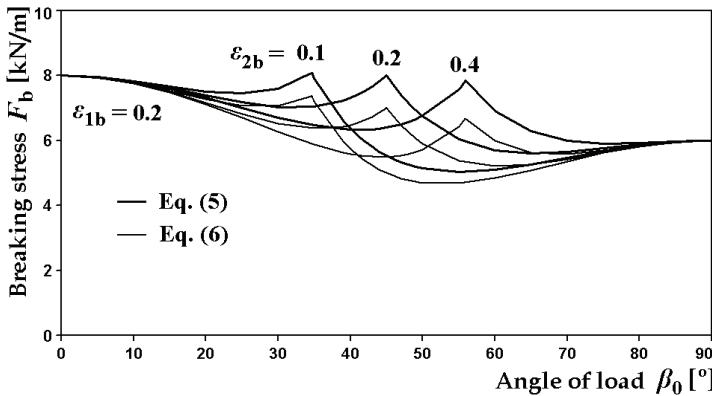


Fig. 5. Influence of angle β_0 on breaking stress for $\varepsilon_{1b} = 0.2$, different ε_{2b} , $F_{1b} = 8$ and $F_{2b} = 6 \text{ N}$

Figures 3, 4 and 5 show significant peaks at critical angle where lines for warp yarns and weft yarns meet; this is not recognized in experimental results. This disagreement is caused by simplified model approach that assumes ideally even yarn properties. In real fabric, variability in yarn breaking strain and in other parameters causes, near mentioned critical point, break of some warp and some weft yarns together.

3.2 Model for infinite sample length

Models of ideally uni-axial woven fabric load in variable directions are rather complicated, first of all from the next reasons: (a) Substantial change in yarns incline (angle β) toward load direction during fabric elongation results in combination of tensile and shear deformation. The change of angle β allows itself certain fabric elongation and so its diagonal extensibility and lateral contraction is greater. (b) Reduction of yarns crimp in bias directions is limited, whereas at load in principal directions crimp of the yarns, imposed load, could be practically zero. (c) Change in fabric properties caused by jamming of yarns at diagonal load is great. The jamming could improve utilization of fibers strength and so the strength of the yarn could become better than that at load in principal directions. (d) There are cut ends of the yarns, bearing fabric load, what changes the results when the fabric width is limited. In the next steps will be modeled relaxed fabric, fabric at load in principal and in different directions.

3.2.1 Relaxed fabric

Investigation of fabric tensile properties starts at definition of relaxed state. It is described in (Lomov et al, 2007) etc. Simple model of plain weave balanced fabric is shown in Figure 6. Wavelength λ_1 of warp is defined by weft pitch p_2 and vice versa. Fabric thickness is t ; average p value corresponds with reciprocal value of fabric sett S of the opposite yarn system and so $\lambda_{1,20} = 2p_{2,10} = \frac{2}{S_{2,10}}$. Main parameters of crimp wave are: wavelength λ , wave

amplitude a and length of the yarn axis l . Wave amplitudes a are dependent on yarn diameters and in non-square fabric (i.e. $S_1 \neq S_2$, $d_{10} \neq d_{20}$, $l_{10} \neq l_{20}$ etc.) as well on fabrics setts, yarns diameters, imposed load (contemporary or in fabric history) and so on.

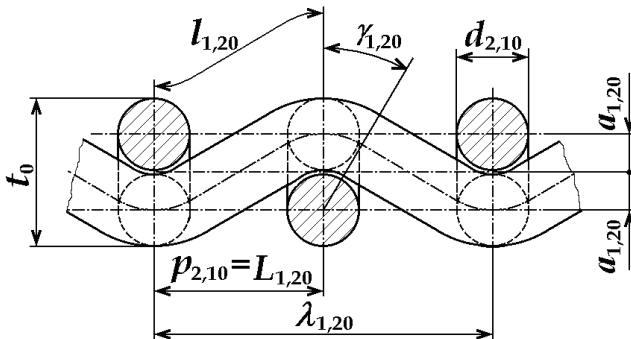


Fig. 6. Definition of yarn crimp in a woven fabric.

Crimp of the yarns in woven fabric as numeric parameter c is defined by equation (7); wavelength of warp λ_1 corresponds with pitch of weft p_2 and vice versa.

$$c_{1,20} = \frac{l_{1,20}}{p_{2,10}} - 1 \quad \text{or} \quad l_{1,20} = (c_{1,20} + 1) \cdot p_{2,10} \quad (7)$$

Lengths of the yarn in a crimp wave l will be counted with the help of equation (8). This formula approximates crimp c of loose fabrics (low packing density) using sinusoid crimp wave model and of tight fabrics (high packing density) using Peirce's model.

$$c_{1,20} = 2.52 \cdot \left(\frac{a_{1,20}}{p_{2,10}} \right)^2 \quad \text{or} \quad c_{1,2} = 2.52 \cdot \left(\frac{a_{1,2}}{p_{2,1}} \right)^2 \quad (8)$$

Relative crimp wave amplitude a/p can reach maximum value of 0.57735 at so called fabric limit packing density (maximal available fabric sett) for square fabric construction. In Figure 7 is curve, following equation 8, compared with calculation of crimp using sinusoid and Peirce crimp wave models (Kovar & Dolatabadi 2008).

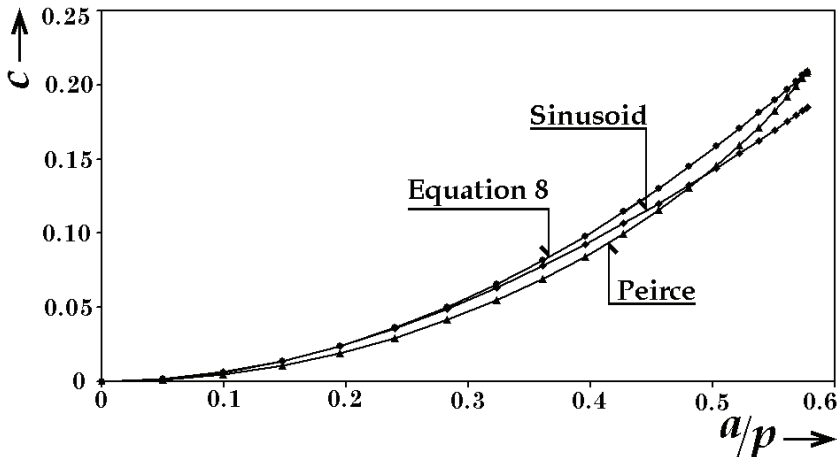


Fig. 7. Dependence of crimp c on relative crimp amplitude a/p .

Using equations 7 and 8 one get for length of the yarn in a crimp wave l :

$$l_{1,20} = \left(2.52 \cdot \left(\frac{a_{1,20}}{p_{2,10}} \right)^2 + 1 \right) \cdot p_{2,10} = 2.52 \cdot a_{1,20}^2 + p_{2,10}^2 \quad \text{or} \quad l_{1,2} = 2.52 \cdot a_{1,2}^2 + p_{2,1}^2 \quad (9)$$

Note: equations 7, 8 and 9 are valid both for fabric status before (with subscript 0) and after load. Parameters p_0 are known (reciprocal values of setts S) and height of the crimp wave can be, for square fabric, estimated as $a_{10} = a_{20} = 0.5 d$.

3.2.2 Load in principal directions

These directions are analyzed in different publications (Hearle et al., 1969; Hu, 2004; Pan, 1996 etc.) sufficiently and so this paragraph will describe only few important parameters.

- Fabric breaking force** $F_{1,2}$ (subscripts 1, 2 specify warp or weft direction of imposed load). For its calculation simple equation (10) can be used (Kovar, 2003), in which $F_{1,2b}$

are breaking forces of one warp or weft yarn and $C_{1,2u}$ are coefficients of utilization of these forces at fabric break. We shall assume, that in principal directions it will be $C_{1,2u} \approx 1$, as there are two opposite tendencies; yarn and fabric unevenness results in decreasing of $C_{1,2u}$ and fabric jamming can, on the contrary, this parameter increase.

$$F_{f1,2} = S_{1,2} \cdot F_{1,2b} \cdot C_{1,2u} \quad (10)$$

- b. **Fabric breaking strain**, $\varepsilon_{f1,2}$. There are two main resources of fabric elongation (Kovar & Gupta, 2009): yarn straightening (de-crimp) and yarn axial elongation. For principal direction it will be assumed that all yarns at break are straight and so in equation (8) $a_{1,2} = 0$. For yarn axial elongation experimental results of yarn at breaking strain, $\varepsilon_{1,2b}$, can be used.

$$\varepsilon_{f1,2} = (1 + \varepsilon_{1,2b}) \cdot (1 + c_{1,20}) - 1 \quad (11)$$

Explanation: equation (11) can be derived from general definition of relative elongation with the use of (7) and Fig. 6:

$$\varepsilon_{f1,2} = \frac{l_{1,2} - p_{2,10}}{p_{2,10}}, \quad \text{in which} \quad l_{1,2} = p_{2,10} \cdot (\varepsilon_{1,2b} + 1) \cdot (c_{1,20} + 1),$$

where $l_{1,2}$ are lengths of the yarn in a crimp wave after straightening and elongation.

- c. **Fabric width**. Fabric elongation in principal directions is attached with straightening (de-crimping) of the yarns imposed load, whereas opposite yarns crimp amplitude increases and fabric contracts. We shall assume that lateral contraction is similar as elongation in lateral direction. There are two opposite tendencies again: quicker increase of yarn crimp at greater a/p , Fig. 7, and yarn cross-section deformation (flattening). Original width of the sample b_0 will be changed into $b_{b1,2}$:

$$b_{b1,2} = \frac{b_0}{1 + \varepsilon_{fb1,2}} \quad \text{and} \quad b_0 = b_{b1,2} \cdot (1 + \varepsilon_{fb1,2}) \quad (12)$$

- d. **Lateral contraction**. Fabric Poisson's ratio ν can be counted using

$$\nu_{1,2} = \frac{b_0 - b_{b1,2}}{b_0} = \frac{b_{b1,2} \cdot (1 + \varepsilon_{fb1,2}) - b_{b1,2}}{b_{b1,2} \cdot (1 + \varepsilon_{fb1,2})} = \frac{\varepsilon_{fb1,2}}{1 + \varepsilon_{fb1,2}} \quad (13)$$

3.2.3 Load in diagonal direction (45 °) for structural unit

Load at diagonal directions is connected with shear deformation and lateral contraction (Sun & Pan, 2005 a, b). This analysis helps with recognition of yarns spacing p_d and angle of yarns incline β_d at fabric break, Fig. 8. Elongation of woven fabric in principal directions is restricted by the yarn system that lays in direction of imposed load, whereas load in angle of 45 ° with free lateral contraction enables greater breaking strain thanks to shear deformation. For description of fabric geometry at break it is necessary to describe jamming in the fabric; break can't occur sooner than maximum packing density is reached.

There are two opposite trends for originally circular yarn cross-section change: (a) Fabric lateral contraction is connected with increase of compressive tension between neighboring

yarns. This tension causes tendency to increase the fabric thickness. (b) Crimp of the yarns could not be near zero as it was at loading in warp or weft directions, because now both yarn systems are imposed load. Axial stress in all yarns leads to tendency of de-crimping and so to reduction of fabric thickness.

The situation for initial value of warp and weft yarns decline $\beta_{1,20} = \beta_{d0} = 45^\circ$ is shown in Figure 8 (a before, b after uniaxial elongation), where $p_{1,2} = p_d$ describes yarn perpendicular spacing, p_h and p_v are projections of these parameters in horizontal and in vertical direction, respectively.

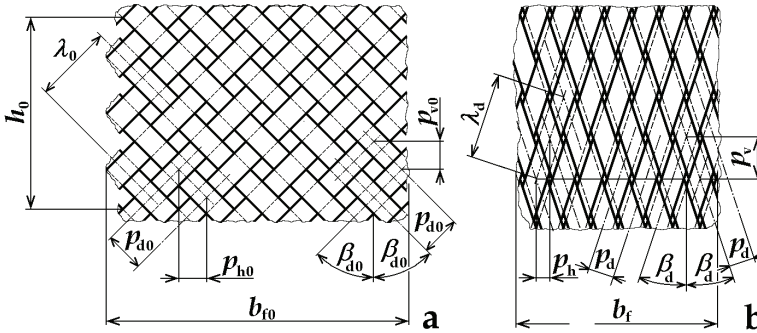


Fig. 8. Diagonal fabric deformation at ideally uniaxial load for $\beta_0 = 45^\circ$ for square fabric.

Spacing of yarns, p_0 , is independent parameter corresponding with reciprocal value of fabric sett ($p_0 = 1/S$). During diagonal deformation p decreases and at fabric break it reaches minimum value that restricts fabric lateral contraction and breaking elongation. A hypothesis of even packing density μ distribution in all fabric thickness at break is accepted and so profiles of yarns in crossing points can be as shown in Fig. 9 a for the same material in warp and in weft or in Fig. 8 b for different diameters in warp and weft. Parameter δ , defined as $\delta = \frac{p_d}{t_d}$, can be variable, or another hypothesis of maximum area $p_d \cdot t_d$ can be

incorporated and then $\delta = \frac{p_d}{t_d} = 1$ (Figs 9 a and b; Fig. c is for $\delta \neq 1$).

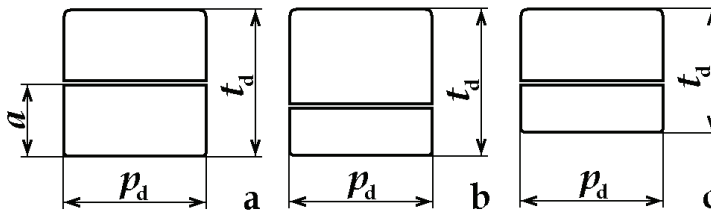


Fig. 9. Model profiles of warp and weft yarns in crossing elements.

If A_0 is original area of warp and weft yarns cross-section at packing density μ_0

($A_0 = \frac{\pi \cdot (d_{10}^2 + d_{20}^2)}{4}$, approximately $\mu_0 = 0.5$), final area $A = p_d \cdot t_d$ after yarn compression (at

packing density $\mu = 0.8$) will be $A = A_0 \cdot \mu_0 / \mu$. Then yarn spacing will be, for $p_d = t_d$:

$$p_d = \frac{A}{p_d} = \frac{A_0 \cdot \frac{\mu_0}{\mu}}{p_d} = \frac{\pi \cdot (d_{10}^2 + d_{20}^2)}{4} \cdot \frac{\mu_0}{\mu} \quad \text{and so} \quad p_d = \sqrt{\frac{\pi \cdot (d_{10}^2 + d_{20}^2)}{4} \cdot \frac{\mu_0}{\mu}} \quad (14)$$

Note: experiments show, that $p_1 = p_2 = p_d$ also for fabric in which $S_1 \neq S_2$. When yarn diameters are different ($d_1 \neq d_2$), then p_1 and p_2 , β_1 and β_2 will be different, but these changes will be small.

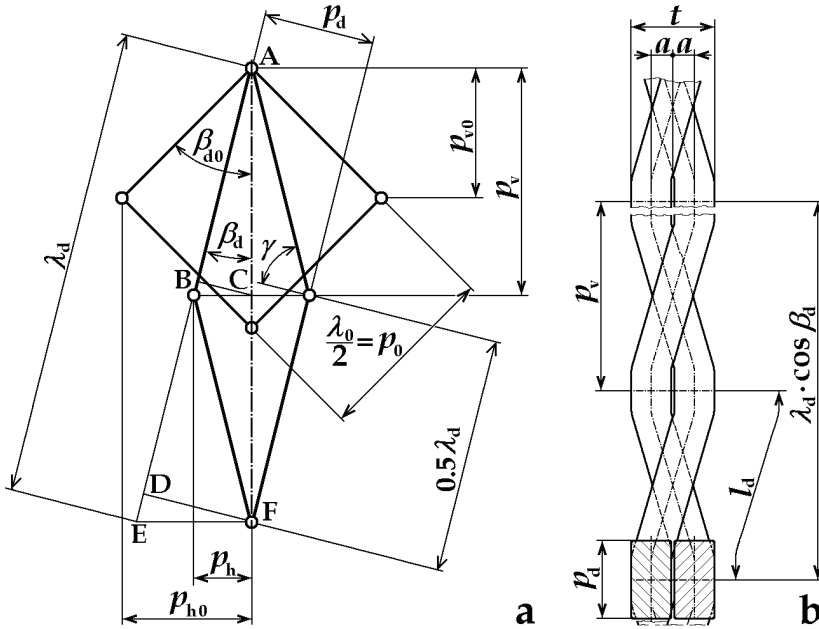


Fig. 10. Geometrical analysis of structural unit deformation at $\beta_0 = 45^\circ$ for square fabric.

Geometrical changes, connected with shear fabric deformation at diagonal load of one fabric structural element (this is a square connecting four adjacent crossing points), are described using Figure 10 a, where β_{d0} , β_d are angles of yarns incline before deformation and at break ($\beta_{d0} = 45^\circ$), γ is shear angle ($\gamma = \frac{\pi}{2} - 2\beta_d$, $\gamma_0 = 0$), p_0 , p_d is spacing (pitch) of yarns before and after deformation. Parameter p_0 corresponds with fabric sett and with $\frac{1}{2}$ of wavelength of crimped yarns λ_0 (Figs. 6 and 8). λ_d is wavelength of crimped yarns at break. Elongation of λ_0 is enabled both by yarns straightening and by yarn axial elongation, residual crimp of warp and weft yarns can be counted using parameter $a = 0.5 t_d = 0.5 p_d$ (Figures 9, 10 b) or neglected, because for $a/p < 0.1$ is $c < 0.006$, Fig. 7. p_{h0} and p_h are horizontal projections of yarn spacing p_0 and p_d before and after deformation and similarly p_{v0} and p_v are vertical projections of p_0 and p_d before and after deformation; these parameters are necessary for calculation of fabric breaking elongation and of maximum shear angle γ , see as well Fig. 10 b (view in direction perpendicular to the load).

Length of the yarn in a crimp wave, l_d , increases in the course of elongation, but due to jamming not so much as in free yarn. We shall assume that yarn axial elongation at break is reduced on axial elongation at break of fibers ε_{fib} and so it will be, see Fig. 6 and equation (9):

$$l_{1,2d} = l_{1,20} \cdot (1 + \varepsilon_{\text{fib}}) = (2.52 \cdot a_{1,20}^2 + p_{2,10}^2) \cdot (1 + \varepsilon_{\text{fib}}) \quad (15)$$

Experimentally such yarn breaking elongation can be measured with a very short test length (shorter than is the length of the fibers) to simulate status of fibers and yarn in the fabric.

Getting wavelength of crimped yarn at break, λ_d , needs to know crimp wave amplitude a (Figs. 9, 10 b); it is assumed, that $a = \frac{t_d}{4} = \frac{p_d}{4}$. Using crimp definition $c_{1,2} = \frac{l_{1,2}}{p_{2,1}} - 1$ and

replacing $p_{2,1}$ for $0.5 \cdot \lambda_{1,2}$ we get $0.5 \cdot \lambda_{1,2d} = \frac{l_{1,2d}}{c_{1,2d} + 1}$. Parameter $c_{1,2d}$ can be counted with the

help of equation (8): $c_{1,2d} = 2.52 \left(\frac{a}{0.5 \cdot \lambda_{1,2d}} \right)^2$. After connection and conversion we get

quadratic equation $0.5 \lambda_{1,2d}^2 - l_{1,2d} \cdot 0.5 \lambda_{1,2d} + 2.52 \cdot a^2 = 0$ that leads to the result

$$0.5 \cdot \lambda_{1,2d} = \frac{l_{1,2d} + \sqrt{l_{1,2d}^2 - 4 \cdot 2.52 \cdot a^2}}{2} \quad (16)$$

Using Fig. 10 one can calculate horizontal and vertical projection of the yarn spacing before deformation, p_{h0} and p_{v0} , and after deformation (triangle ABC), p_h and p_v :

$$p_{h0} = 0.5 \cdot \lambda_0 \sin \frac{\pi}{4} = 0.5 \cdot p_0 \cdot \sqrt{2} \quad \text{and} \quad p_h = 0.5 \cdot \lambda_d \cdot \sin \beta_d \quad (17)$$

$$p_{v0} = 0.5 \cdot \lambda_0 \cos \frac{\pi}{4} = 0.5 \cdot p_0 \cdot \sqrt{2} \quad \text{and} \quad p_v = 0.5 \cdot \lambda_d \cdot \cos \beta_d \quad (18)$$

Minimum yarn spacing, p_d , has already been known from equation (14). It can help with calculation of p_v and p_h that give fabric breaking elongation and lateral contraction. From Fig. 10, triangles AEF and DEF, it will be $\sin \beta_d = \frac{2p_h}{\lambda_d}$ and $\sin \beta_d = \frac{p_d}{2p_h}$ and hence

$\frac{2p_h}{\lambda_d} = \frac{p_d}{2p_h}$, $p_h = \frac{\sqrt{p_d \lambda_d}}{2}$, what results in angle of yarn incline at break β_d :

$$\sin \beta_d = \frac{\sqrt{p_d \cdot \lambda_d}}{\lambda_d} \quad \text{and} \quad \beta_d = \arcsin \frac{\sqrt{p_d \cdot \lambda_d}}{\lambda_d} \quad (19)$$

Fabric elongation at diagonal break ε_{db} is, using eq. (18):

$$\varepsilon_{\text{db}} = \frac{p_v - p_{v0}}{p_{v0}} = \frac{\lambda_d \cdot \cos \beta_d - p_0 \cdot \sqrt{2}}{p_0 \cdot \sqrt{2}} \quad (20)$$

Maximum value of shear angle γ_d will be $\gamma_d = \frac{\pi}{2} - 2 \cdot \cos \beta_d$

3.2.4 Load in diagonal direction (45 °) for fabric strip

Strip of the tested fabric of original width b_0 at angle of warp and weft yarns decline to vertical load direction $\beta_{10} = \beta_{20} = 45^\circ$ is shown in Figure 11 (a before load, b after load for square fabric, c after load for non-square fabric with $S_1 \neq S_2$ or/and $\varepsilon_{1b} \neq \varepsilon_{2b}$).

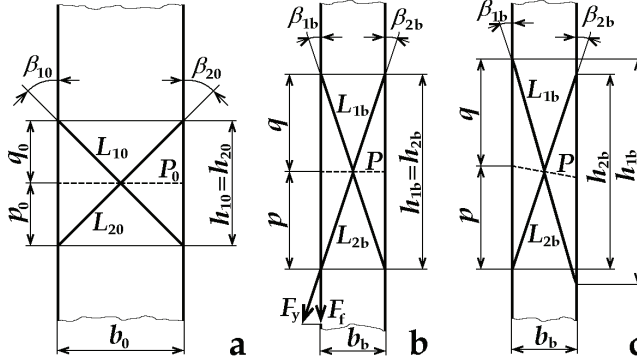


Fig. 11. Geometrical analysis of sample deformation at $\beta_0 = 45^\circ$.

Lengths of the weft and the warp yarns in fabric plane before elongation, L_{10} and L_{20} , are

$L_{1,20} = \frac{b_0}{\sin \beta_{1,20}}$, where for $\beta_{10} = \beta_{20} = \beta_0 = 45^\circ$ is $\sin \beta_{1,20} = \frac{\sqrt{2}}{2}$. The width of the sample at

break, b_b , and fabric lateral contraction, ν , can be counted using equation (17), in which p_h

corresponds with b ($\frac{p_h}{p_{h0}} = \frac{b_b}{b_0}$):

$$b_b = b_0 \cdot \frac{p_h}{p_{h0}} = b_0 \cdot \frac{0.5 \cdot \lambda_d \cdot \sin \beta_d}{p_0 \cdot \sqrt{2}} \quad \text{and} \quad \nu_b = \frac{b_0 - b_b}{b_0} \quad (21)$$

Note: equation (21) gives, for non-square fabric (Figure 11 c), different results for weft and warp yarns ($b_{1b} \neq b_{2b}$). In this case we shall assume that minimum value of b and maximum value of ν is valid; the reason is that maximum load is only in one yarn system, the opposite systems of yarns with lower or negative load cannot keep fabric strip wider as the yarns are able to bear only negligible compressive load.

Now we shall count fabric breaking elongation, using knowledge of sample width b_b , equation (21), and determination of projections of lengths of the yarns axes l_1 and l_2 into fabric plane L_1 and L_2 (Figs. 6, 11):

$$l_{1,20} = L_{1,20} (1 + c_{1,20}) \quad \text{and} \quad l_{1,2b} = l_{1,20} (1 + \varepsilon_{fib}) = L_{1,20} \cdot (1 + c_{1,20}) \cdot (1 + \varepsilon_{fib}) \quad (22)$$

Relation between lengths of yarns axes calculation before load, l_{10} and l_{20} , and at break, l_{1b} and l_{2b} , is described by equation (9). The lengths of yarns axes projection into fabric plane, L_{1db} and L_{2db} , will be from (22)

$$L_{1,2b} = \frac{l_{1,2b}}{1 + c_{1,2b}} = \frac{L_{1,20} \cdot (1 + c_{1,20}) \cdot (1 + \varepsilon_{fib})}{1 + c_{1,2b}} \quad (23)$$

Yarns elongation at break is reduced on the value, corresponding with elongation at break of fibers. Crimp of yarns at break is taken from equation (8), where p is replaced with 0.5λ :

$$c_{1,2db} = 2.52 \cdot \left(\frac{a}{0.5 \cdot \lambda_{1,2}} \right)^2 \quad (24)$$

Horizontal projections of lengths L_{1b} and L_{2b} are $h_{1,2} = \sqrt{L_{1,2b}^2 - b_{db}^2}$.

Finally fabric sample breaking elongation ε_{fbd} is (Fig. 11) for $h_{1b} = h_{2b} = h_b$ and $h_0 = b_0$:

$$\varepsilon_{fbd} = \frac{h_b - h_0}{h_0} = \frac{h_b - b_0}{b_0} \quad (25)$$

More complex is breaking elongation calculation for non-square fabric (Fig. 11 c) when $L_1 \neq L_2$. It leads to skewed fabric in which originally horizontal line P_0 will get some another angle to load direction. In this case it could be assumed, that thanks to possibility of reaching new equilibrium, fabric breaking elongation will be average of the values, get from equation (24) for weft and warp yarns; this assumption is in good agreement with experimental results.

Breaking stress of the fabric, F_{fb} , equation (26), can be got by modification of equation (10). The role of both warp and weft yarns strength is for one critical angle β_{0c} identical (for square fabric $\beta_{0c} = 45^\circ$, for other fabrics it is near 45°). Incline of yarns is as well considered; only component of yarn axial stress F_y into direction of fabric load F_f supports fabric strength (it is shown in Fig. 11 b). Prediction of coefficients of yarn strength utilization C_u is in this case difficult, because due to jamming strength of the yarn can be higher than the strength of free yarn. On the contrary, cut yarn ends causes gradual tensile stress increase from zero at sample edge to maximum value (it will be described later).

$$F_{fb} = S_1 \cdot F_{1b} \cdot C_{1u} \cdot \cos \beta_{1b} + S_2 \cdot F_{2b} \cdot C_{2u} \cdot \cos \beta_{2b} \quad (26)$$

3.2.5 Load in variable directions – breaking strain

Example for angle of load $\beta_{10} = 30^\circ$ is described in Fig. 12. The lengths of warp and weft yarns projections into fabric plane within the sample width b_0 before elongation, L_{10} and L_{20} , can be counted similarly as in previous paragraph.

For further calculations it is necessary to know sample width b_b at break as variable, dependent on angle β_0 . We shall assume, in accordance with experimental results, that the change of b is slower near the critical angle β_{0c} ($\beta_{0c} \approx 45^\circ$, value of b is here at minimum) and quicker near $\beta_0 = 0^\circ$ and 90° . This is the reason, why parabolic approximation in equation (27) is used. In this, $b_{1,2b}$ is sample width at break for angle of load 0° or 90° and b_{db} is the same for angle of load 45° .

$$b_b(\beta_0) = (b_{1,2b} - b_{db}) \cdot \left(1 - \frac{4}{\pi} \cdot \beta_0 \right)^2 + b_{db} \quad (27)$$

Sample strain at break is, with the exception of critical angle β_{0c} , restricted namely by yarns of one system (warp or weft), usually by that with smaller value of β_0 . Elongation at break near β_{0c} is influenced first of all by: (a) Crimp interchange. At mentioned β_{0c} both warp and

weft yarns are crimped and so an important crimp interchange occurs; yarns of one system get straight whereas crimp of the opposite yarns grows. This mechanism enables, in some range of angles β_0 , to utilize strength of warp and weft yarns simultaneously. Out of this range, stress in the yarn of the system with greater β_0 becomes negligible or even negative (compression). (b) Effect of yarn jamming, that increases yarn breaking stress, is maximum at β_{0c} and minimum for $\beta_0 = 0^\circ$ or 90° .

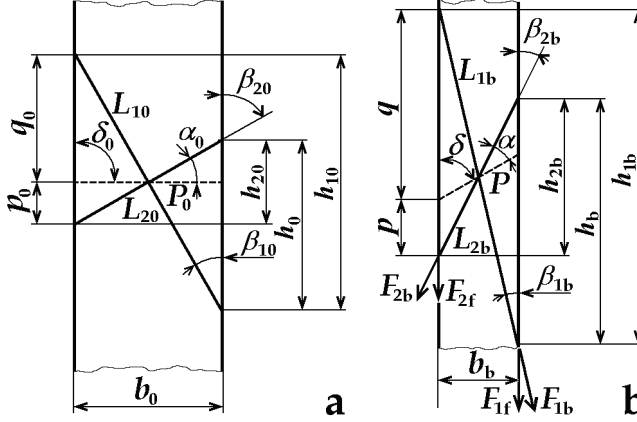


Fig. 12. Deformation of a fabric strip before deformation (a) and at break (b).

One of the results of different stresses in warp and weft yarns is that originally horizontal line P_0 changes after load its direction δ_0 for δ , see Fig. 12 (dash lines) and (Zouari, Amar & Dogui, 2008). Lengths of the yarn axis projections at break, $L_{1,2b}$, corresponding with the lengths $L_{1,20}$ before load, can be counted similarly as in equation (23). Crimps $c_{1,2b}$ are variable near critical angle β_{0c} , near principal directions are crimps of broken yarns neglected. Yarn elongations at break $\varepsilon_{1,2b}$ are as well variable; near angle β_{0c} it is $\varepsilon_{1,2b} = \varepsilon_{fib}$.

$$L_{1,2b} = \frac{L_{1,20} \cdot (1 + c_{1,20}) \cdot (1 + \varepsilon_{1,2b})}{1 + c_{1,2b}} = \frac{b_0 \cdot (1 + c_{1,20}) \cdot (1 + \varepsilon_{1,2b})}{\sin \beta_{1,20} \cdot (1 + c_{1,2b})} \quad (28)$$

For fabric breaking strain it is necessary to know vertical projections of $L_{1,2b}$, parameters $h_{1,2b}$ (Fig. 12). Using Pythagorean Theorem and equations (27) and (28) it will be

$$h_{1,2b} = \sqrt{L_{1,2b}^2 - b_b^2} \quad (29)$$

The same parameters before load, $h_{1,20}$, are

$$h_{1,20} = L_{1,20} \cdot \cos \beta_{1,20} \quad (30)$$

Now we can count, separately for warp and weft yarns, fabric breaking elongation, $\varepsilon_{1,2b}$. Smaller of the results will be valid (break yarns of only one system).

$$\varepsilon_{1,2b} = \frac{h_{1,2b} - h_{1,20}}{h_{1,20}} \quad (31)$$

In Fig. 13 is shown an example of results for calculated and measured breaking elongation. Fabric was plain weave, cotton yarn linear density 35 tex (warp and weft), warp sett 2600 ends/m, weft sett 2500 ends/m, finished fabric. Experiment 1 was carried on in accordance with the standard EN ISO 13934-1, experiment 2 is in accordance with (Kovar & Dolatabadi, 2010).

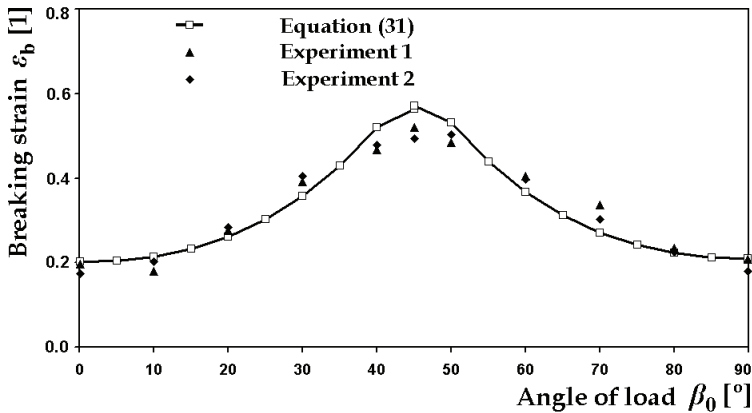


Fig. 13. Example of calculated and measured fabric strain at break.

3.2.6 Load in variable directions – breaking stress

Force from one broken yarn. Basic algorithms for breaking stress calculation were explained sooner, equations (10) and (26). For variable β_0 it is necessary to consider that only component of yarn axial stress F_1 and F_2 aims in direction of load, Fig. 12. Components of axial tensile force of one yarn at fabric break, $F_{1,2b}$, into fabric load direction, $F_{1,2f}$, are $F_{1,2f} = F_{1,2b} \cdot \cos \beta_{1,2b}$, where angles of yarns incline at break $\beta_{1,2b}$ can be counted using (27) and (29):

$$\tan \beta_{1,2b} = \frac{b_b}{h_{1,2b}} \quad \text{and} \quad \beta_{1,2b} = \arctan \frac{b_b}{h_{1,2b}} \quad (32)$$

Force from all broken yarns. Number of broken yarns in fabric width at break corresponds with fabric sett S , width b and angle of load β_0 and so comprehensive force from all warp or weft yarns in fabric strip, $F_{a1,2b}$, is

$$F_{a1,2b} = S_{1,2} \cdot b_0 \cdot \cos \beta_{1,20} \cdot F_{1,2f} = S_{1,2} \cdot b_0 \cdot \cos^2 \beta_{1,20} \cdot F_{1,2b} \quad (33)$$

where $n_{1,2} = S_{1,2} \cdot b_0 \cdot \cos \beta_{1,20}$ is number of yarns in sample width.

Correction for fabric jamming

At diagonal load, utilization of fibers strength can be better then at load in principal directions. It will be described by coefficient C_{fu} , equation (10). In this chapter only rough estimation will be presented. Fibers strength utilization, by other words a share of broken fibers to all fibers in yarn cross-section, can be: (a) In free spun yarn around value of $C_{fuy} =$

0.5; it depends on fibers length (staple), friction coefficients, yarn twist etc. (b) In fabric at break in principal directions, C_{fup} is similar or slightly higher; it depends on fabric packing density and on other parameters. (c) In fabric at break in diagonal directions, C_{fud} is maximal due to jamming. Extremely it can be near to 1. From these reasons, final parameters $C_{fu1,2}$ as a function of β_0 , will be predicted as parabolic relation (without derivation):

$$C_{fu1,2}(\alpha_0) = (C_{fud} - C_{fup}) \cdot \left(\frac{\beta_0}{\frac{\pi}{4}} \right)^2 + C_{fup} \quad (34)$$

Fabric strip strength from broken yarns with implementation of jamming, $F_{j1,2b}$, is from (33) and (34):

$$F_{j1,2b} = C_{fu1,2} \cdot F_{a1,2b} = C_{fu1,2} \cdot S_{1,2} \cdot b_0 \cdot \cos^2 \beta_{1,20} \cdot F_{y1,2b} \quad (35)$$

Correction for cut yarn ends

With the exception of $\beta_0 = 0$ and $\beta_0 = 90^\circ$ there are yarns, bearing fabric load, having one or two free ends (Kovar & Dolatabadi, 2007). Near cut yarn end axial stress is zero and gradually increases (linear increase is assumed) due to friction till it reaches yarn strength in length l , see Fig. 14 a. In this area fabric jamming is not as important as in sample inner parts and shear angle is smaller. This length l is hardly predictable and depends on many parameters (setts, yarn properties including frictional, fabric finishing, shear deformation, angle of load, jamming etc.). It can be evaluated experimentally by testing yarn pullout force from the fabric (Pan & Yoon, 1993) or testing the samples of variable widths. By this effect, some width on each side of fabric $b_{in} = l \cdot \sin \beta_{1,20}$ is inefficient; this is important mainly for broken yarns. This strip b_{in} can bear only about 50 % of full load. It results in reduction of original sample width to effective one $b_{ef} = b_{b0} - l \cdot \sin \beta_{1,20}$.

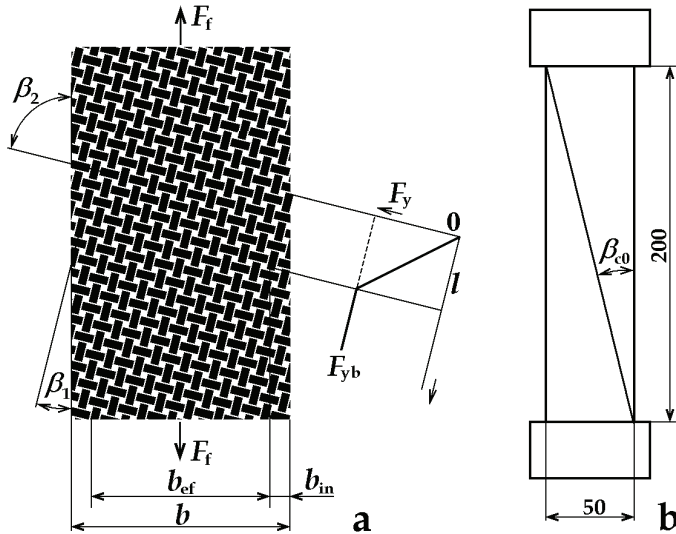


Fig. 14. Free ends of yarns in fabric at bias load.

Total effective force from broken yarns with reduced fabric width, $F_{f1,2b}$, is then from (35)

$$F_{f1,2b} = C_{fu1,2} \cdot S_{1,2} \cdot b_{ef} \cdot \cos^2 \beta_{1,20} \cdot F_{y1,2b} = C_{fu1,2} \cdot S_{1,2} \cdot (b_{b0} - l \cdot \sin \beta_{1,20}) \cdot \cos^2 \beta_{1,20} \cdot F_{y1,2b} \quad (36)$$

Correction for critical angles

In our theory, unlimited sample length is assumed and the effect of critical angles is neglected. Nevertheless for comparison with real experiments it should be mentioned; tension concentration at jaws reaches high value for critical angles, at which only 1 yarn is kept simultaneously by both pair of jaws and all others yarns have 1 end free. For critical angle β_{c0} it will be: $\tan \beta_{c0} = 50 : 200$, see Fig. 14 b (sample width is 50 mm, test length 200 mm). Near this angle an important drop in tested fabric strength is observed.

Example of results for plain weave fabric, warp and weft yarns are polypropylene/cotton 35/65 %, linear density $T = 29.5$ tex, warp sett $S_1 = 2360$ ends/m, weft sett $S_2 = 1920$ (lines 1 and 3) and $S_2 = 1380$ ends/m (lines 2 and 4) is shown in Fig. 15. Lines 3, 4 describes standard experiment (EN ISO 13934-1), lines 1, 2 results of the new method (Kovar & Dolatabadi, 2010) with the same size of samples. Drop in the sample strength near critical angles is evident.

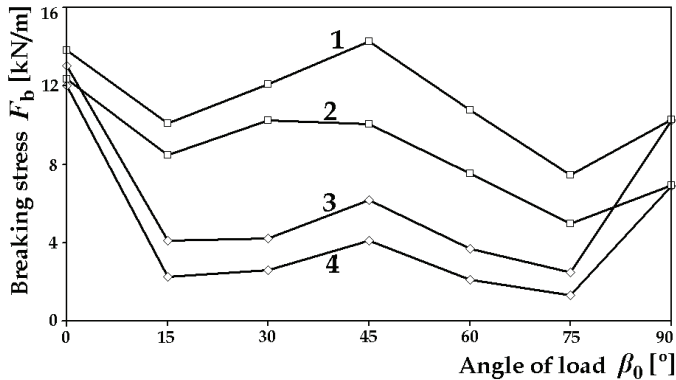


Fig. 15. Influence of critical angles on fabric breaking stress.

Note: linear connection of measured points only assembles these points together; in any case it does not mean approximation of the results.

Force from unbroken yarns at fabric break

These yarns are, for fabric strength, important only near critical angle β_{0c} (near 45 °). At other load angles, tensile stress in these yarns is low or negative. We shall assume, that maximum force corresponds with maximum length $L_{1,2b}(\beta_0)$, Fig. 12, and that it can be calculated using formula (33) on condition of similar tensile properties of warp and weft yarns.

Vertical projection of unbroken yarn length at fabric break, $h_{u1,2}$, depends on this parameter before load ($h_{1,20}$) and on sample elongation at break (elongation of sample is proportional), identified by broken yarns of the opposite system: $h_{u1,2} = h_{1,20} \cdot (1 + \varepsilon_{2,1b})$. Length of unbroken

yarns in fabric width before load is $L_{1,20} = \frac{b_0}{\sin \beta_{1,20}}$, corresponding length of unbroken yarns

at fabric break (Fig. 12), $L_{u1,2}$, is using (29), $L_{u1,2} = \sqrt{b_b^2 + h_{1,2b}^2}$.

Relative elongation of unbroken yarns is then

$$\varepsilon_{u1,2} = \frac{(L_{u1,2} - L_{1,20})}{L_{1,20}} \quad (37)$$

and hence force, by which unbroken yarns contribute to sample strength, will be:

$$F_{u1,2b} = F_{a1,2d} \cdot \frac{L_{u1,2}}{L_{u1,20}} \quad (38)$$

where $F_{a1,2d}$ is breaking load, calculated in accordance with (33) for $\beta_0 = 45^\circ$.

Final results

Force $F_{12,b}$ is the sum of the forces from broken and unbroken yarns, equations (36) and (38):

$$F_{1,2b} = F_{f1,2b} + F_{u1,2b} \quad (39)$$

In Fig. 16 is an example of results, carried on the same fabric and with the same experimental methods as shown in Fig. 13. Agreement is not excellent; it is caused by simplifications in calculation and as well by imperfection of known experimental methods. Results of patented method (experiment 2, Kovar & Dolatabadi, 2010) shows, with exception of principal directions, higher breaking stress than does standard method (experiment 1, EN ISO 13934-1). Important drop is observed near previously mentioned critical angles β_0 14 and 76 °. Slower decrease of breaking stress near angle $\beta_0 = 45^\circ$ is due to interactions between warp and weft yarns that were not implemented into calculation yet.

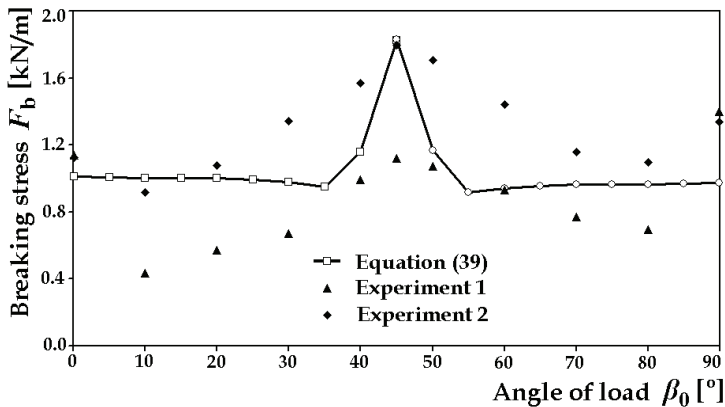


Fig. 16. Example of calculated and measured fabric stress at break.

4. Measuring of rupture properties

Experiments always mean some scale of unification and simplification in comparison with fabric real loading at the use. To simulate real practical situations is not possible – it would result in too many different experimental methods. In general, the load put on textile fabric, can be (a) tensile uniaxial, (b) tensile biaxial or (c) complex as combination of different form

of the load (elongation, bend, shear etc.). Nevertheless uniaxial and biaxial stresses are the most important forms of load for investigation of textile fabrics rupture properties. Other forms of deformation (bending, shear, lateral pressure etc.) seldom result in fabric break.

4.1 Uniaxial stress

The problems, connected with breaking test of woven fabrics due to great lateral contraction that accompanies load in diagonal directions, have already been described in section 2 (Fig. 1). The principle of a new method (Kovar & Dolatabadi, 2010) is sample tension reduction by fabric capstan friction, Fig. 17 (scheme and photographs at three stages of sample elongation). A set of fast cylinders 5, 6 is connected with each pair of dynamometer jaws 1, 2. At sample elongation fabric slips towards central fabric part 4 in directions 8, what results in tension reduction due to capstan friction; however, fabric lateral contraction on cylinders is enabled. Total angle of contact is on each sample side is approximately 8.03π (460°) and for friction coefficient $f = 0.17$ (this is low value of f , valid for fabric to smooth steel surface friction at high load near break of the sample) decrease of sample tension will be

$\frac{F_c}{F_j} = e^{\alpha \cdot f} \doteq 3.9$ (390 %). In Fig. 17 right is example of tested sample before elongation (a), at elongation of 40 % (b) and 90 % near the break point (c).

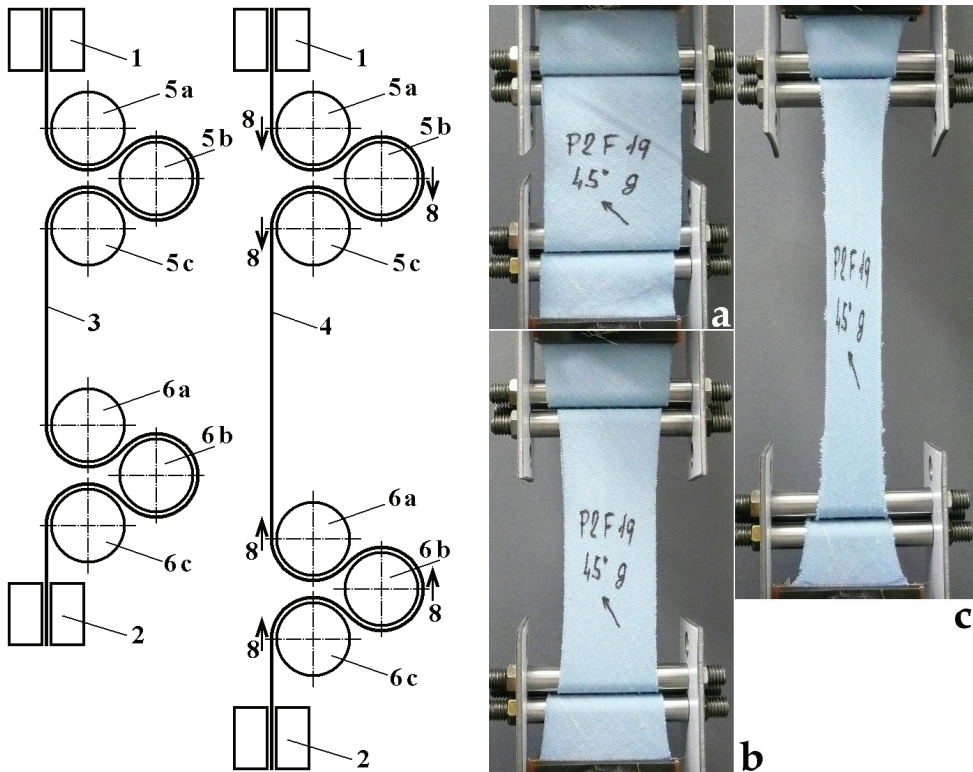


Fig. 17. Patented method for fabric tensile properties measuring

4.2 Biaxial stress

Measuring of fabric tensile properties at biaxial stress is more complicated task, described for example in (Bassett, Postle & Pan, 1999). If fast jaws 1 are used, Fig. 18 a, fabric would soon break at sample corners as relative elongation of L_2 is many times greater than that of sample length and width L_1 . MA is measured area of the sample. Two of solutions are shown. In Fig. b are fast jaws replaced with sets of individual narrow free grippers and in Fig. c is measured sample MA connected with four auxiliary fabrics cut into strips that enable 2-D sample elongation, although jaws 1 are fast. Two mentioned methods are suitable for measuring fabric anisotropy, nevertheless they need special equipment and much of labor. It is not easy to investigate rupture properties by these methods. As the load in two directions can be different, it would be useful to reduce number of tested samples by election of only some variants such as: (a) uniaxial load (but different than at standard methods, lateral contraction is now enabled), (b) restriction of lateral contraction similarly with chapter 2.2, (c) the same load (absolutely or recounted per one yarn in the sample width) or tension in two directions, (d) the same elongation in two directions.

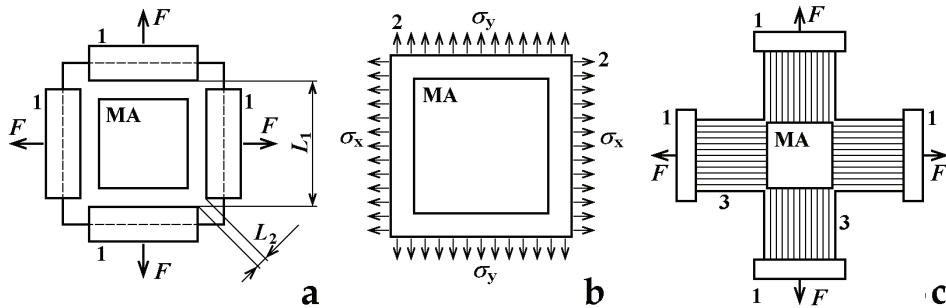


Fig. 18. Principles of tensile properties measuring at biaxial load

The principle of measuring tensile properties when fabric lateral contraction is restricted (simulation of sample infinite width, section 2.1) is shown in Fig. 19. The sample 1 is sewn by several individual stitches into tubular form and by wires 3, placed beside jaws 2, is kept in original width.

5. Discussion, current trends and future challenges in investigated problems

The problems of anisotropy of woven fabric rupture properties are very complex and till now not in the gravity centre of researches. This section could make only a short step in bringing new knowledge on this field. Partly another approach to similar problem solution is used in (Dolatabadi et al., 2009; Dolatabadi & Kovar, 2009). Anisotropy of different fabric properties is often investigated for textile based composites, where rupture properties are very important, for example in (Hofstee & van Keulen, 2000).

There are lots of possibilities how to go on in research on this topic, for example:

- Investigation of influence of sample width on tensile properties with the goal to specify better impact of cut yarn ends (Fig. 14).
- Research on biaxial and combined fabric load, the aim could be, for example, better description of fabric behaviour at practical usage.

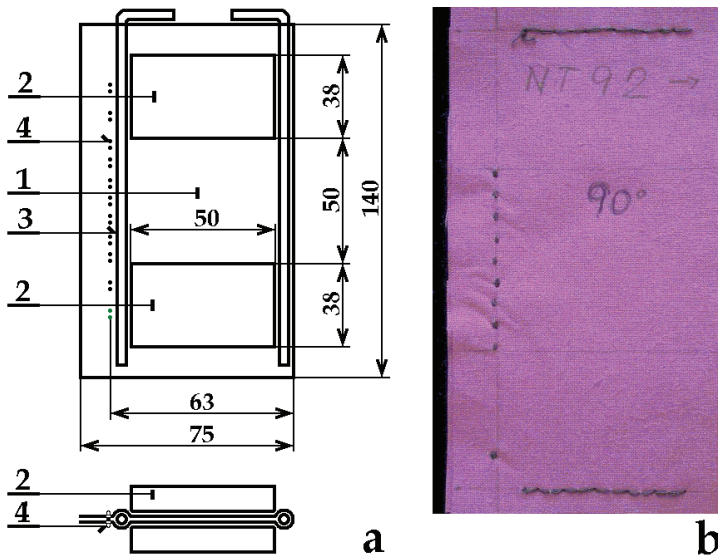


Fig. 19. Measuring of tensile properties at restricted lateral contraction (scheme, sample)

- c. Development of suitable experimental methods and its standardization; till now there is no standard method for measuring rupture properties of fabrics with great lateral contraction.
- d. Implementation of other variable parameters into calculation, such as variability in yarns properties, unevenness of fabric structure etc.
- e. Research of another weaves (twill, sateen...), influence of structure on utilization of strength of used fibres.
- f. Developing of suitable methods for simulation of fabric tension distribution at particular load with the stress to be put on a great and variable Poisson's ratio of fabrics etc.

There are other important anisotropic forms of fabric deformation, which are not described in this chapter, such as bend (Cassidy & Lomov, 1998) and shear. Lateral contraction is as well very important.

6. Acknowledgement

This work was supported by the research project No. 106/09/1916 of GACR (Grant Agency of Czech Republic).

7. References

- Bassett, R. J.; Postle, R. & Pan, N. (1999). Grip Point Spacing Along the Edges of an Anisotropic Fabric Sheet in a Biaxial Tensile Test. *Polymer composites*, Vol. 20, No. 2
- Cassidy, C. & Lomov, S. V. (1998). Anisotropy of fabrics and fusible interlinings. *International Journal of Clothing Science and Technology*, Vol. 10 No. 5, pp. 379-390

- Dai, X.; Li, Y. & Zhang, X. (2003). Simulating Anisotropic Woven Fabric Deformation with a New Particle Model, *Textile Res. J.* 73 (12), 1091-1099
- Dolatabadi, K. M.; Kovar, R. & Linka, A. (2009). Geometry of plain weave fabric under shear deformation. Part I: measurement of exterior positions of yarns. *J. Text. Inst.*, 100 (4), 368-380
- Dolatabadi, K. M. & Kovar, R. (2009). Geometry of plain weave fabric under shear deformation. Part II: 3D model of plain weave fabric before deformation and III: 3D model of plain weave fabric under shear deformation. *J. Text. Inst.*, 100 (5), 381-300
- Du, Z., & Yu, W. (2008). Analysis of shearing properties of woven fabrics based on bias extension, *J. Text. Inst.*, 99, 385-392
- Hearle, J. W. S.; Grosberg, P. & Backer, S. (1969). *Structural Mechanics of Fibres, Yarns and Fabrics*. Vol. 1. New York, Sydney, Toronto
- Hofstee, J. & van Keulen, F. (2000). Elastic stiffness analysis of a thermo-formed plain-weave fabric composite. Part II: analytical models. *Composites Science and Technology*, 60, 1249-1261
- Hu, J. (2004). *Structure and mechanics of woven fabrics*. Woodhead Publishing Ltd. P 102, ISBN 0-8493-2826-8
- Kilby, W. F. (1963). Planar stress-strain relationships in woven fabrics. *J. Text. Inst.*, 54, T 9-27
- King, M. J.; Jearanaisilawong, P. & Socrate, S. (2005). A continuum constitutive model for the mechanical behavior of woven fabrics. *International Journal of Solids and Structures* 42, 3867-3896
- Kovar, R. & Gupta, B. S. (2009). Study of the Anisotropic Nature of the Rupture Properties of a Woven Fabric. *Textile Research Journal* Vol 79(6), pp. 506-506
- Kovar, R. & Dolatabadi, M. K. (2010). The way of measuring of textile fabric deformation and relevant equipment. Czech patent No. 301 314
- Kovar, R. & Dolatabadi, M. K. (2008). Crimp of Woven Fabric Measuring. Conference Strutex 2008, TU of Liberec 2008, ISBN 978-80-7372-418-4
- Kovar, R. & Dolatabadi, M. K. (2007). Impact of yarn cut ends on narrow woven fabric samples strength. Strutex, TU Liberec, ISBN 978-80-7372-271-5
- Kovar, R. (2003). *Structure and properties of flat textiles* (in Czech). TU of Liberec, ISBN 80-7083-676-8, Liberec, CZ, 142 pages
- Lo, M. W. & Hu, J. L. (2002). Shear Properties of Woven Fabrics in Various Directions, *Textile Res. J.* 72 (5), 383-390
- Lomov, S. V. et al, (2007) Model of internal geometry of textile fabrics: Data structure and virtual reality implementation. *J. Text. Inst.*, Vol. 98, No. 1 pp. 1-13
- Pan, N. & Yoon, M. Y. (1996). Structural Anisotropy, Failure Criterion, and Shear Strength of Woven Fabrics. *Textile Res. J.* 66 (4), 238-244
- Pan, N. & Yoon, M. Y. (1993). Behavior of Yarn Pullout from Woven Fabrics: Theoretical and Experimental. *Textile Res. J.* 63 (1), 629-637
- Pan, N. (1996 b). Analysis of Woven Fabric Strength: Prediction of Fabric Strength Under Uniaxial and Biaxial Extension, *Composites Science and Technology* 56 311-327
- Peng, X. Q. and Cao, J. (2004). A continuum mechanics-based non-orthogonal constitutive model for woven composite fabrics. *Composites: Part A* 36 (2005) 859-874

- Postle, R.; Carnaby, G. A. & de Jong, S. (1988). *The Mechanics of Wool Structures*. Ellis Horwood Limited Publishers, Chichester. ISBN 0-7458-0322-9
- Sun, H. & Pan, N. (2005 a). Shear deformation analysis for woven fabrics. *Composite Structures* 67, 317-322
- Sun, H. & Pan, N. (2005 b). On the Poisson's ratios of a woven fabric. University of California Postprints, Paper 662
- Zborilova, J. & Kovar, R. (2004). Uniaxial Woven Fabric Deformation. Conference STRUTEX, TU of Liberec, pp. 89-92, ISBN 80-7083-891-4
- Zheng, J. et al (2008). Measuring technology of the Anisotropy Tensile Properties of Woven Fabrics. *Textile Res. J.*, 78, (12), pp. 1116-1123
- Zouari, R., Amar, S. B. & Dogui, A. (2008). Experimental and numerical analyses of fabric off-axes tensile test. *JOTI*, Vol. 99, iFirst 2008, 1-11
- European standard EN ISO 13934-1. Determination of maximum force and elongation at maximum force using the strip method
- CSN standard 80 0810 Zistovanie trznej sily a taznosti pletenin (Recognition of breaking stress and strain of knitted fabrics)

Mechanical Properties of Fabrics from Cotton and Biodegradable Yarns Bamboo, SPF, PLA in Weft

Živa Zupin and Krste Dimitrovski
*University of Ljubljana, Faculty of Natural Sciences and Engineering,
Department of Textiles
Slovenia*

1. Introduction

Life standard is nowadays getting higher. The demands of people in all areas are increasing, as well as the requirements regarding new textile materials with new or improved properties which are important for the required higher comfort or industrial use. The environmental requirements when developing new fibres are nowadays higher than before and the classical petroleum-based synthetic fibres do not meet the criteria, since they are ecologically unfriendly. Even petroleum as the primary resource material is not in abundance. The classical artificial fibres, e.g. polypropylene, polyacrylic, polyester etc, are hazardous to the environment. The main problems with synthetic polymers are that they are non-degradable and non-renewable. Since their invention, the use of these synthetic fibres has increased oil consumption significantly, and continues even today. It is evidenced that polyester is nowadays most frequently used among all fibres, taking over from cotton. Oil and petroleum are non-renewable (non-sustainable) resources and at the current rate of consumption, these fossil fuels are only expected to last for another 50–60 years; the current petroleum consumption rate is estimated to be 100,000 times the natural generation rate (Blackburn, 2005).

Environmental trends are more inclined to the development of biodegradable fibres, which are environment-friendly. A material is defined as biodegradable if it can be broken into simpler substances (elements and compounds) by naturally occurring decomposers – essentially, anything that can be ingested by an organism without harming the organism. It is also necessary that it is non-toxic and decomposable in a relatively short period on a human time scale (Blackburn, 2005). The biodegradability of fibres also depends on their chemical structure, molecular weight and super-molecular structure.

Biodegradable polymers can be classified into three main groups, i.e.:

- natural polysaccharides and biopolymers (cellulose, alginates, wool, silk, chitin, soya bean protein),
- synthetic polymers, esp. aliphatic polyesters (poly (lactic acid), poly (ϵ -caprolactone)), and
- polyesters produced by microorganisms (poly (hydroxyalkanoate)s) (Blackburn, 2005).

All known natural fibres are biodegradable; however, they have some disadvantages in the growing up and production processes. At growing cotton and other vegetable fibres, large amounts of pesticides are used which has a negative influence on the environment.

In the research, three biodegradable fibres, i.e. bamboo fibres, fibres from polylactic acid (PLA) and soybean protein fibres (SPF) were used for which the industrial procedures already exist. At the same time, there are enough natural resources for the latter and they are environment-friendly. The physical-mechanical properties of fabrics with biodegradable yarns in weft and cotton yarns in warp were researched. We would like to determine whether and to what extent physical and mechanical properties change and whether they are acceptable in terms of today's criteria.

The researchers have been investigating and researching the production of biodegradable fibres and their properties. This research focuses on the mechanical properties of yarns made from biodegradable fibres and first of all, on the mechanical properties of woven fabrics made from biodegradable yarns in weft and cotton yarns in warp. The latter is the most common way of producing woven fabrics, since the warp threads do not need to be changed.

2. Properties of bamboo, PLA and SPF fibres

New trends are being sought for naturally renewable resources in order to protect the nature. With the help of chemical processes, new biodegradable materials can be produced. Such materials can successfully replace or improve the existing artificial or natural materials. Many different sources can be used to produce biodegradable materials. Fibres from naturally renewable resources are made chemically as fibres from polylactic acid (PLA fibres) or as a secondary product of other technologies. Such products are soybean fibres, which are made from soy proteins after the extraction of oil from soybean. New, natural resources are also used for fibre-making purposes, e.g. bamboo tree for bamboo fibres. These are by far not the only existing fibres from renewable resources; nevertheless, in our research, these three types of yarns are used. All presented fibres have compatible properties with classical natural fibres and some additional properties with a good influence on the comfort of clothing to the human body.

2.1 Bamboo fibres

Bamboo is considered by many to be the ultimate green material (Netravali, 2005). Since it is a fast growing plant, it can be harvested in as little as six weeks, although more typically in three to five years. Bamboo reproduces through its extensive system of rhizomes. As such, there is a continuous supply of bamboo, which meets the definition of a renewable resource. And, of course, it is also a sustainable material, capable of sustaining itself with minimal impact to the environment.

Bamboo can thrive naturally without using any pesticide. It is seldom eaten by pests or infected by pathogen.

The bamboo fibre is a kind of regenerated cellulose fibre, which is produced from raw materials of bamboo pulp refined from bamboo through the process of hydrolysis-alkalization and multi-phase bleaching, then processed and pulp is turned into bamboo fibres.

The properties of bamboo fibre are:

- strong durability, stability and tenacity,
- thinness and whiteness degree similar to the classically bleached viscose,
- antibacterial and deodorizing in nature (even after being washed fifty times),
- incredibly hydroscopic (absorbing more water than other conventional fibres, e.g. cotton),

- fabric garments make people feel extremely cool and comfortable in hot conditions,
- fabric is exceptionally soft and light, almost silky in feel, and
- fabric has a high level of breathability, for the cross-section of bamboo fibres is filled with various micro-gaps and -holes (Das, 2010).

2.2 Polylactide fibres (PLA)

Poly(lactic acid) is a natural, biodegradable organic substance, which is harboured in the bodies of animals, plants and microbes. The poly(lactic acid) as such cannot be found in the nature but needs to be industrially prepared with the lactic acid polymerisation.

The lactic acid used for the synthesis of poly(lactic acid) is derived from genetically altered corn grains (Rijavec, Bukošek, 2009).

Unlike other synthetic fibre materials with vegetable resources (e.g. cellulose), PLA is well suited for melt spinning into fibres. Compared to the solvent-spinning process required for the synthetic cellulose fibres, melt spinning allows PLA fibres to be made with both lower financial and environmental cost, and enables the production of fibres with a wider range of properties (Dugan, 2000). The polymerisation occurs with the condensation of acid with alcohol, forming polyester. The misguidance in this observation is to assume that since PLA is polyester, it will behave in many ways similarly to PES or PA 6 fibres (Rekha et al., 2004).

The fundamental polymer chemistry of PLA allows control of certain fibre properties and makes the fibre suitable for a wide range of technical textile applications and special apparel (Farrington et al, 2005).

The properties of PLA fibre are:

- low moisture absorption,
- good natural regulation of the body temperature through moisture absorption,
- low flammability,
- high resistance to UV and a low index of refraction, and
- excellent mechanical properties and module of elasticity (Lou et al., 2008).

2.3 Soybean fibres

Soy protein fibre (SPF) is the only plant protein fibre (Rijavec, Bukošek, 2009). It is a liquefied soy protein that is extruded from soybean after the extraction of oil, and processed mechanically to produce fibres by using new bioengineering technology. Fibres are produced by wet spinning, stabilized by acetylating, and finally cut into short staples after curling and thermoforming.

A soybean protein fibre has not only the superiorities of natural fibres but also the physical properties of synthetic ones.

The properties of SPF fibres are:

- noble appearance and similar look as silk fibres, however, they are considerably cheaper (Yi-you, 2004),
- very comfortable to wear, soft, smooth, with soft handle,
- fabric has the same moisture absorption as cotton fibres (Brooks, 2005),
- better moisture transmission than a cotton fabric, which makes it comfortable and sanitary,
- higher tensile strength than wool, cotton, and silk, however, lower than polyester fibres,
- does not shrink when washed in boiling water,
- outstanding anti-crease, easy-wash and fast-dry properties,

- antibacterial properties, and
- high UV resistance.

In the table below, the physical and mechanical properties of fibres, e.g. length, fineness, dry tenacity, wet tenacity, dry breaking extension and physical density are shown.

Properties	Bamboo	Cotton	Viscose	PLA	PES	PA	SPF	Silk	Wool
Length (mm)	38–76	25–45	30–180		32–150		38–76	$3.5 \cdot 10^6$ – $9 \cdot 10^6$	50–200
Fineness (dtex)	1.3–5.6	1.2–2.8	1.3–25		1.3–22		0.9–3	1–3.5	4–20
Dry tenacity (cN/dtex)	2.33	1.9–3.1	1.5–3.0	3.2–5.5	3–7	3–6.8	3.8–4.0	2.4–5.1	1.1–1.4
Wet tenacity (cN/dtex)	1.37	2.2–3.1	0.7–1.11		2.4–7	2.5–6.1	2.5–3.0	1.9–2.5	1.0
Dry breaking extension (%)	23.8	7–10	8–24	20–35	20–50	26–40	18–21	10–25	20–40
Moisture regain (%)	13.3	8.5	12.5–13.5	0.4–0.6	0.4	4.5	8.6	11.0	14.5
Density (g/cm ³)	0.8–1.32	1.5–1.54	1.46–1.54	1.25–1.27	1.36–1.41	1.15–1.20	1.29–1.31	1.34–1.38	1.32

Table 1. Comparison of physical and mechanical properties of bamboo fibres, PLA, SPF, cotton, viscose, wool and PES

3. Mechanical properties of woven fabrics

With mechanical properties, the phenomenon on textile material is described which is a result of the material resistance on the activity of external forces causing the change of shape. The response of the textile material depends on the material properties, the way of load and its tension. With regard to the direction of the applied force, deformations at stretch and compression are known. To the mechanical properties of fabrics uniaxial or biaxial tensile properties, compression, shearing properties, bending rigidity, bursting and tear resistance can be listed.

Numerous parameters influence the mechanical properties of woven fabrics. Firstly, there are fibre properties, and their molecular properties and structure. The mechanical properties of fibres depend on their molecular structure, where macromolecules can be arranged in crystalline (unique arrangements of molecules) or amorphous (coincidental arrangements of molecules) structure. The macromolecules are orientated mostly along the fibre axis and are connected to each other with intermolecular bonds. When a force is applied, the supramolecular structure starts changing (Geršak, 2006).

The fibre properties and the type of spinning influence the yarn properties, while the fabric properties are also influenced by warp and weft density of the woven fabrics, and weave. The mechanical properties are also influenced by the weaving conditions, e.g. speed of weaving, warp insertion rate, weft beat-up force, the way of shed opening, warp preparation for weaving, warp and weft tension, number of threads in reed dent etc.

The properties of raw fabrics consequently depend on the construction and technological parameters. For the final use, raw fabrics have to be post-treated to add different functional properties. In most cases, these post-treatments worsen some mechanical properties, while again some other mechanical properties improve. In Figure 1, the procedure from fibres to the end of woven-fabric production is presented.

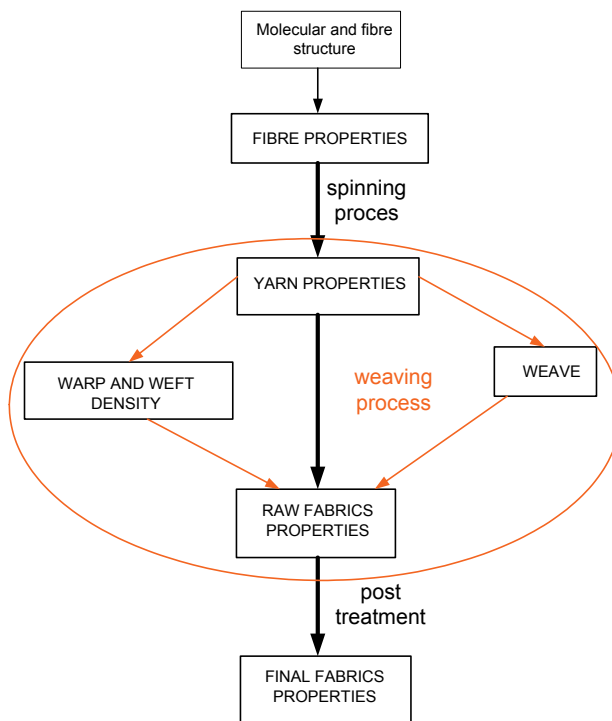


Fig. 1. Interrelation of fibre, yarn and fabric structure and properties

A lot of researches have been investigating the mechanical and tensile properties of fabrics. The approaches to the problem have included geometric, mechanical, energy and statistical models (Realf et al, 1997). The first geometric model of fabrics was presented by Pierce (Pierce, 1937), who presumed that yarn has an ideal circular cross section, which is rigid and inextensible. His work was continued by Womersley (Womersley, 1937), who presented a mathematical model of deformation of fabrics if exposed to a load. Similarly, other researchers have taken Pierce's work as a fundament. Kemp (Kemp, 1958) improved Pierce's model with the introduction of ecliptic shape of yarn. With the help of Pierce's and Kemp's geometry, Olofsson (Olofsson, 1965) presented a mechanical model of fabrics under uniaxial loading. His work was continued by Grosberg with co-authors (Grosberg et al, 1966), who were investigating tensile, bending, bulking and shearing properties, and fabrics and forces acting at counted properties on a fabric and yarn in the fabric. Kawabata approached the geometry of the interlacing point. He set the interlacing point in space, presented it as a space curve, and researched how the fabric behaves when forces act upon it and what deformations occur (Kawabata, 1989). Apart from the geometric and mechanical models, the researchers have also developed energy, statistical and numerical models of woven fabrics. In more recently, many researches are still based on the already known models, trying to improve or reform the already existed models. A lot of researchers have performed work based on real woven fabrics, studying their physical and mechanical properties. They have been investigating the influence of differently used yarn (material or different technique of spinning), the influence of different density of warp and weft threads, and weave.

Our research is also based on the investigation of the physical and mechanical properties of woven fabrics with different yarns used in weft.

3.1 Tensile properties of fabrics

For designing apparel as well as for other uses, the knowledge about the tensile properties of woven fabrics is important. Strength and elongation are the most important performance properties of fabrics governing the fabric performance in use. Their study involves many difficulties due to a great degree of bulkiness in the fabric structure and strain variation during deformation. Each woven fabric consists of a large amount of constituent fibres and yarns and hence, any slight deformation of the fabric will subsequently give rise to a chain of complex movements of the latter. This is very complicated, since both fibres and yarns behave in a non-Hookean way during deformation (Hu, 2004)

At the beginning of loading, extension occurs in amorphous parts, where primary and secondary bonds are extending and are shear loaded. If in this stage, an external force stops acting, most of the achieved extension will recover and the material shows elastic properties. If the loading continuous, a plastic deformation of the material occurs. Long chains of molecules are reciprocally re-arranged as a consequence of the disconnection of secondary bonds. The re-arrangements of the reciprocal position of molecules give material better possibility to resist additional loading. If the loading continuous, a final break will occur (Saville, 2002).

The stress-strain curve has three parts as it is shown in Figure 2. A higher initial module at a tensile test occurs, due to the resistance against friction and bending of fabrics. In the tested direction, in the direction of force, crimp yarns are straightened. When the yarns are straightened, the force in the fabrics increases quickly and fibres and yarns begin to extend, as it is shown in Figure 2b. The tensile properties of fabrics mostly depend on the tensile properties of yarns (Grosberg, 1969)

In the region of elasticity, where Hook's law exists, tenacity (σ) is given with Equation 1.

$$\sigma = E \cdot \varepsilon \quad (1)$$

Where:

σ - tenacity (N/mm²),

E - elastic or Young's module (N/mm²),

ε - extension - deformation (%).

A major difference between the shapes of the curves above occurs in the first part of the curve, i.e. in the Hook's zone (I - zone). This is influenced by a crimp of warp or weft yarns, when they begin to straighten. The elongation of the fabric is already increasing under a low force (still before the zone in which Young's modulus is calculated). Here, the crimp is interchanged between the threads of the two systems. The crimp decreases in the direction investigated, however, it increases in the perpendicular direction. Consequently, the tension of the threads of the system, which is perpendicular to the direction investigated, increases. When a tensile force acts on the threads of one system, the threads of both systems undergo extension. Due to the crimp interchange, the maximum possible elongation of perpendicular threads depends on the fabric geometry (Saville, 2002, Gabrijelčič et al, 2008).

The elastic or Young's module provides resistance against the deformation of the material (fabric). Lower the value of Young's module, the more deformable (extensible) is material. The Young's module in the diagram stress-strain represents the tangents of the inclination angle α . The more resistant the material, the higher the angle of inclination α .

$$E = \operatorname{tg}\alpha = \frac{\sigma}{\varepsilon} \quad (2)$$

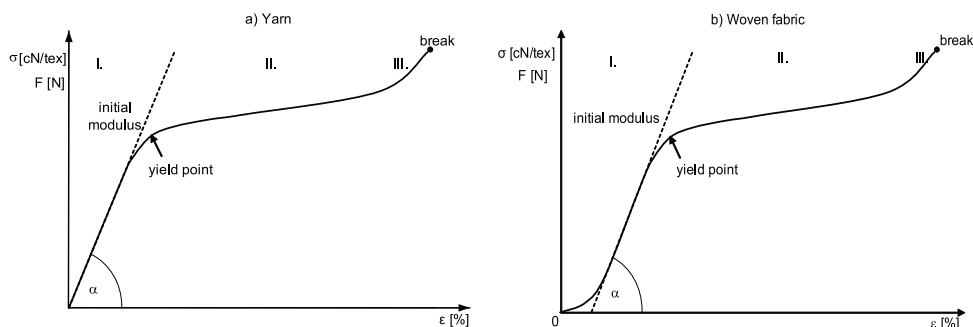


Fig. 2. Stress-strain curve of yarn and fabrics

As it can be seen in Figure 2, the load-extension curve is divided into three zones:

- the zone of elastic deformation or Hook's zone (zone I) of both yarn and fabric: If the extension occurs inside the Hook's zone, the material recovers to its initial length after the relaxation. This zone is also called the zone of linear proportionality or linear elasticity.
- the zone of viscoelastic deformation (zone II): After the loading, the material recovers to its initial length after a certain time of relaxation. The relationship between the stress and deformation is not linear. The limit between the elastic and plastic deformation is the yield point, on the stress-strain curve seen as a turn of curve.
- the zone of permanent deformations (zone III): The material does not recover after the relaxation (Geršak, 2006, Reallf et al, 1991)

3.2 Mechanical properties measured with KES evaluation system

Measuring other physical and mechanical properties and not only tensile properties is of great help in controlling and in the quality processes during the manufacture and post-treatment of textiles. Many researchers have been trying to develop a system for measuring the mechanical properties of textiles. The Kawabata Evaluation System (KES) is the first system for testing fabric mechanical properties. And it is also the system which evaluates fabric handle. This system has four different machines, and 16 parameters in warp and weft direction can be obtained, covering almost all aspects of physical properties of fabrics measured at small load. Tensile, bending, shearing, compressional and surface properties can be measured. From these measurements, properties such as stiffness, softness, extensibility, flexibility, smoothness and roughness can be inferred.

Tensile property

The tensile behavior of fabrics is closely related to the inter-fiber friction effect, the ease of crimp removal and load-extension properties of the yarn themselves as it was discussed before. Four tensile parameters can be determined through the KES instruments LT, WT, RT and EMT. LT represents the linearity of the stress-strain curve. A higher value of LT is supposed to be better. EMT reflects fabric extensibility, a measure of fabric ability to be

stretched under a tensile load. The larger the EMT, the more extensible is the fabric (Chan et al, 2006). A proper amount of extensibility is desirable, while both excessive and insufficient extensibility will cause problems for the production. LT represents the linearity of the stress-strain curve. A higher value of LT is supposed to be better. WT denotes the tensile energy per unit area, taking care of the effect of both EM and LT. Thus, the conclusion about WT can be deduced from the comparison of EM and LT. RT (tensile resiliency) measures the recovery from tensile deformation. A tight fabric structure contributes to a better recovery.

Property	Symbol	Parameter measured	Unit
Tensile	LT	Linearity of load extension curve	/
	WT	Tensile energy	cN cm/cm ²
	RT	Tensile resiliency	%
	EMT	Extensibility, strain at 500 cN/cm	%
Shear	G	Shear rigidity	cN/cm degree
	2HG	Hysteresis of shear force at 0.5°	cN/cm
	2HG5	Hysteresis of shear force at 5°	cN/cm
Bending	B	Bending rigidity	cN cm ² /cm
	2HB	Bending hysteresis	cN cm/cm
Compression	LC	Linearity of compression thickness curve	/
	WC	Compressional energy	cN cm/cm ²
	RC	Compressional resiliency	%
Surface	MIU	Coefficient of fabric surface friction	/
	MMD	Mean deviation of MIU	/
	SMD	Geometric roughness	μm
Thickness	T	Fabric thickness at 50 N/m ²	mm
Weight	W	Fabric weight per unit area	mg/cm ²

Table 2. Parameters measured on KES system

Shear property

Whenever bending occurs in more than one direction, so that the fabric is subjected to double curvature, shear deformations of the fabric are involved. As revealed by its definition, shear property is highly related to the fabric bending property. The shear property in conjunction with the bending property is thus a good indicator of the ability of a fabric to drape. A shear deformation is very common during the wearing process, since the fabric needs to be stretched or sheared to conform to the new gesture of a body movement. During the making-up of a garment, the shear deformation is also indispensable for an intended garment shape. Shear rigidity G provides a measure of the resistance to the rotational movement of the warp and weft threads within a fabric when subjected to low levels of shear deformation. The lower the value of G , the more readily the fabric will conform to three-dimensional curvatures. If the shear rigidity is not enough, a fabric distortion will easily occur. So does the skewing or bowing during handling, laying up, and sewing. On the other hand, too high shear rigidity might also present a problem to form, mould, or shape, especially at the sleeve head. 2HG and 2HG5, the hysteresis of shear force at 0.5° and 5°, are two other measures of the shear property of a fabric. Like 2HB, the lower the 2HG and 2HG5, the better the recovery from shear deformation.

Bending property

The fabric bending property is apparently a function of the bending property of its constituent yarns. Two parameters can be used to measure this property, i.e. B and $2HB$. B is bending rigidity, a measure of a fabric ability to resist to a bending deformation. In other words, it reflects the difficulty with which a fabric can be deformed by bending. This parameter is particularly critical in the tailoring of lightweight fabrics. The higher the bending rigidity, the higher the fabric ability to resist when it is bent by an external force, i.e. during fabric manipulation in spreading and sewing. Apart from for the bending rigidity of the constituent yarns and fibers, the mobility of the warp/weft within the fabric also comes into play in this aspect. In addition, the effect of density and fabric thickness are also very profound for this property. $2HB$ represents the hysteresis of the bending moment. It is a measure of recovery from bending deformations. A lower value of $2HB$ is supposed to be better.

Compression

Fabric compression is one of the most important factors when assessing fabric mechanical properties, since it is highly related to the fabric handle, i.e. fabric softness and fullness, and fabric surface smoothness. Especially, this property might even influence the thermal property of a fabric. For example, when a fabric is compressed, a subsequent drop in its thermal insulation will be found as well due to the loss of still air entrapped in the fabric. The compressional property can be influenced in many ways. Generally speaking, this property can reflect the integrated effect of a fabric structure like yarn crimp level and thickness, the constituent fiber and/or yarn surface property, and lateral compressional property. LC , the linearity of compression–thickness curve, WC , the compressional energy per unit area, and the last one RC , the compressional resilience, reflect the ability of a fabric to recover from a compressional deformation.

Surface property

Apparently, the fabric handle bears a close relationship with the surface property of a fabric. Three parameters are used as indices of fabric surface property, i.e. MIU , the coefficient of friction, MMD , a measure of the variation of the MIU , and SMD , a measure of geometric roughness. MIU is mainly governed by the contact area and type of weave. The greater the contact area, the higher the MIU value. Generally, a plain weave exhibits a higher geometric roughness in comparison with twill weave due to its shorter floats. [5, 6]

4. Experimental

The research was focused on the mechanical properties of fabrics with cotton warp and biodegradable yarns (bamboo, PLA and SPF) as well as cotton in weft. Pure cotton fabrics were made for the comparison with other fabrics with biodegradable yarns in weft.

Fabrics were made in four most commonly used weaves (i.e. plain weave, basket weave, twill 1/3 and twill 2/2). All fabrics were made on the same loom with the same density for all fabrics, 30 threads/cm in warp and 28 threads/cm in weft. Fabrics were washed after desizing.

For all fabrics, the physical characteristic warp and weft crimp, mass per square meter, thickness of fabrics, as well as tensile properties of used yarns and tensile properties of fabrics in warp and weft direction were measured in compliance with the SIST EN ISO 13934 standard. For a better comparison between the fabrics with different materials in weft,

breaking tenacity was calculated as well and presents how much force can yarn hold per linear density.

Moreover, other mechanical properties were measured on the KES system, e.g. bending, tensile properties at small load, shearing and compression. The measurements were statistically estimated and analyzed with multivariate statistical methods.

	Weave	Warp	Weft	Warp crimp	Weft crimp	Mass	Thickness
		Tt ₁ (tex)	Tt ₂ (tex)	C ₁ (%)	C ₂ (%)	(g/m ²)	(mm)
1	Plain	Cotton 28 tex	Bamboo 21 tex	9.24	13.32	170.83	0.163
2	Basket			2.94	5.44	164.30	0.241
3	1/3 Twill			2.72	15.08	168.21	0.266
4	2/2 Twill			3.28	13.06	167.44	0.247
5	Plain		PLA 20 tex	8.86	17.74	174.42	0.203
6	Basket			3.58	19.44	168.66	0.264
7	1/3 Twill			4.16	20.06	169.09	0.279
8	2/2 Twill			3.94	21.52	169.35	0.269
9	Plain		SPF 15 tex	8.04	23.32	156.93	0.162
10	Basket			2.54	21.80	153.97	0.234
11	1/3 Twill			2.84	25.62	159.32	0.247
12	2/2 Twill			3.16	22.98	152.35	0.244
13	Plain		Cotton 19 tex	11.06	14.86	164.40	0.201
14	Basket			2.34	13.46	158.58	0.281
15	1/3 Twill			3.36	14.70	161.61	0.283
16	2/2 Twill			3.76	15.86	161.80	0.278

Table 3. Construction parameters of fabrics and measured physical parameters of fabrics



Plain weave (PL)



Basket weave (BW)



Twill 1/3 (T 1/3)



Twill 2/2 (T 2/2)

Fig. 3. Used weaves in fabrics

5. Results

5.1 Tensile properties of yarns

As said before, the strength of a fabric depends not only on the strength of the constituent yarn, but also on the yarn structure, yarn bending behaviour, fabric geometry, thus tensile properties (i.e. tensile force and tensile elongation) of all used yarns were measured and for a better comparison, breaking tenacity of yarns was calculated. It was established that SPF yarn is the strongest and can withstand the most stress per linear density. Warp and weft cotton yarns have almost the same breaking tenacity (i.e. around 16 cN/tex). The breaking tenacity of PLA yarn is around 12.5 cN/tex and the lowest is for bamboo yarns.

Furthermore, the tenacity-extension curves were elaborated for each yarn, where the stress-strain behaviour of the used materials can be observed. In Figure 2, it can be seen that

biodegradable yarns differ from cotton yarns especially at tensile elongation, which is approximately two times (bamboo yarn), three times (SPF) and five times (PLA) higher than at cotton weft yarns. On the other hand, the tensile strength of weft cotton yarns is comparable with the tensile strength of bamboo and PLA, while the SPF yarn has a considerably higher tenacity.

	COTTON - WARP	BAMBOO	PLA	SPF	COTTON - WEFT
F (cN)	444.38	218.84	249.77	287.22	258.49
CV	8.44	12.32	8.03	8.39	9.21
E (%)	4.18	8.52	27.52	13.72	4.45
CV	9.39	12.34	8.27	6.41	11.24
σ (cN/tex)	16.35	10.42	12.49	19.17	16.88

Table 4. Tensile properties (breaking force, breaking elongation and breaking tenacity) of yarns used in fabrics

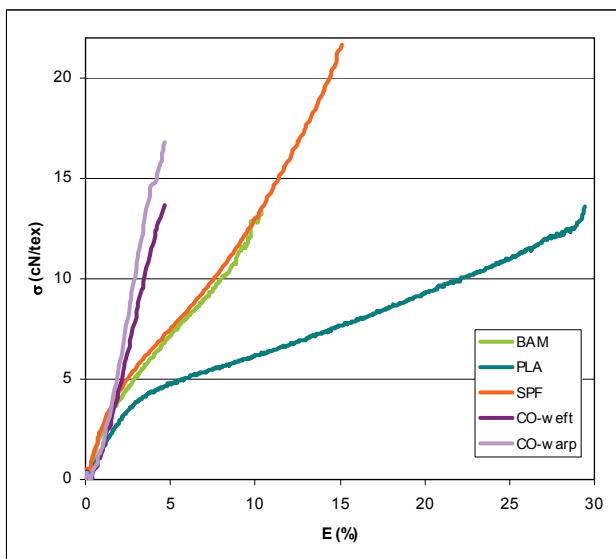


Fig. 4. Tenacity-extension curve for bamboo, PLA, SPF and cotton yarns

5.2 Tensile properties of fabrics

Tensile properties of all 16 fabrics were measured. The results of all measurements (breaking force and breaking elongation) are shown in Table 4. Moreover, the breaking tenacity of one yarn in weft direction of the fabric was calculated for a better comparison of yarns with different linear densities.

Firstly, it was established that the type of weave has a greater influence on the breaking force of fabrics in warp direction than different types of yarns. With a multivariate statistical analysis, it was proved that weave is a 5-time more important factor than different material

in weft. The highest tensile force is, as it was expected, in plain weave, due to the maximum number of interlacing points resulting in higher friction between yarns and consequently also higher tensile strength in warp direction. Twill 2/2, twill 1/3 and basket weaves follow with lower values, which are presented in Figure 5. The differences in the same weave depend considerably on the material used in weft. It was found out that the extensibility of yarns in weft direction influences the breaking force in warp direction. The highest breaking force in warp direction is shown at fabrics with PLA and SPF yarn in weft and the lowest tensile force at pure cotton fabrics, since cotton yarn has the lowest elongation.

No			WARP				WEFT				
			F (N)	CV	E (%)	CV	F (N)	CV	σ (cN/tex)	E (%)	CV
1	PL	Bamboo	903.75	1.24	13.95	2.06	322.13	3.3	54.78	19.58	4.26
2	BW		779.27	2.39	7.48	2.53	334.68	4.31	55.34	19.18	4.4
3	T1/3		815.44	3.18	7.98	3.44	326.05	3.63	54.29	21.69	3.12
4	T2/2		812.6	4.43	7.83	2.68	350.98	2.42	59.69	21.99	2.74
5	PL	PLA	907.77	3.44	15.82	2.51	376.91	3.91	63.67	44.14	4.36
6	BW		796.93	3.13	7.58	2.79	370.18	1.44	65.17	44.29	2.92
7	T1/3		806.68	2.92	7.93	1.7	360.12	1.46	64.31	46.6	2.04
8	T2/2		845.43	4.97	8.08	2.62	352.82	4.02	61.68	48.75	2.53
9	PL	SPF	965.67	3.99	14.06	3.99	351.04	2.68	82.11	32.34	2.53
10	BW		779.76	1.74	6.22	3.43	347.26	7.24	80.38	30.87	6.1
11	T1/3		788.65	3.53	7.23	2.91	332.87	2.74	78.14	30.53	1.24
12	T2/2		817.92	1.8	6.98	2.97	340.38	4.88	78.79	33.19	4.93
13	PL	Cotton	857.76	5.39	15.16	2.52	474.14	2.64	85.76	16.16	1.77
14	BW		766.48	4.11	7.13	4.04	424.42	5.75	79.49	16.82	16.86
15	T1/3		730.2	2.86	7.93	3.64	433.9	1.42	81.56	15.62	3.5
16	T2/2		771.94	4.8	7.58	2.77	451.16	2.1	84.20	19.18	12.73

Table 5. Tensile properties (breaking force, breaking elongation in warp direction and breaking force, breaking elongation and breaking tenacity in weft direction) of fabrics

Among the fabrics woven in plain weave, the fabric with SPF yarn in weft is distinguished with the highest breaking force (965.67 N), followed by the fabrics with PLA (907.77) and bamboo (903.75) yarn in weft. The lowest tensile strength belongs to the fabric with cotton yarn also in weft (857.76 N). In the case of basket weave, the difference between the highest value (fabric with PLA yarn in weft - 796.93 N) and the lowest value (fabric with cotton yarn in weft - 766.48 N) is small. Among the fabrics woven in twill 1/3, the highest breaking force is observed in the fabric with bamboo yarn in weft (815.44 N), and the lowest tensile strength again in the fabric with cotton also in warp (730.2 N). Among the fabrics woven in 2/2 twill, the fabric with PLA yarn in weft has the highest value of tensile strength (845.43 N); the lowest tensile strength is observed, as in previous weaves, in the fabric with cotton weft (771.94 N).

The tensile force in weft direction influences mostly the material used in weft, while the weave has practically no influence. For a better comparison and understanding how different weft yarns influence tensile properties, esp. breaking force, the breaking tenacity of fabrics in weft direction was calculated and is presented in Figure 7.

From Figure 6, it can be seen that the highest breaking force characterises pure cotton fabrics, since weft cotton yarn has also high breaking tenacity of yarns, however, not the

highest one. SPF yarns have the highest breaking tenacity (19.17 cN/tex); nevertheless, the fabrics have lower breaking force and also lower breaking tenacity calculated on one thread than pure cotton fabrics (83 cN/tex). The breaking tenacity of SPF yarns in fabrics is approximately 80 cN/tex. The reason could be that SPF yarns are much smoother than cotton yarns and less friction occurs between warp and weft yarns. The second highest breaking force in weft direction is typical of fabrics with PLA yarn in weft, although the breaking tenacity of PLA yarn (12.49 cN/tex) and the breaking tenacity calculated on one thread in fabrics are lower than for cotton and SPF. The average breaking tenacity of all fabrics with PLA in weft is approximately 64 cN/tex. It can be expected that the SPF fabrics with the same linear density of weft yarn will have higher tensile strength than the fabrics with PLA yarn in weft. The lowest breaking force in weft direction characterises the fabrics with bamboo yarn in weft. Bamboo yarn has the lowest tenacity (10.42 cN/tex) and in fabrics, the breaking tenacity is approximately 56 cN/tex.

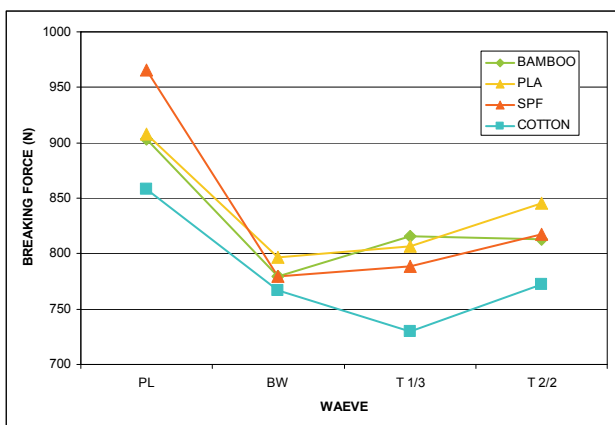


Fig. 5. Breaking force of fabrics in warp direction

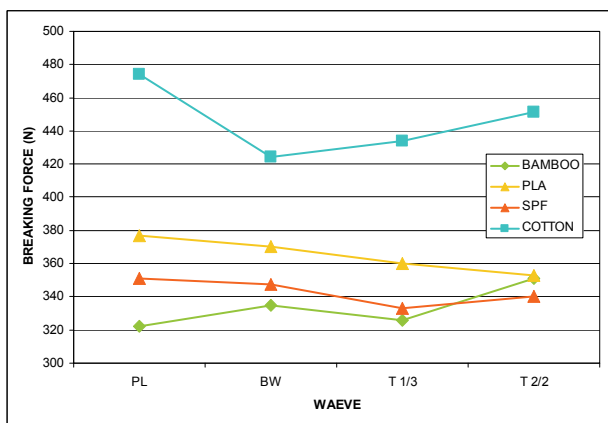


Fig. 6. Breaking force of fabrics in weft direction

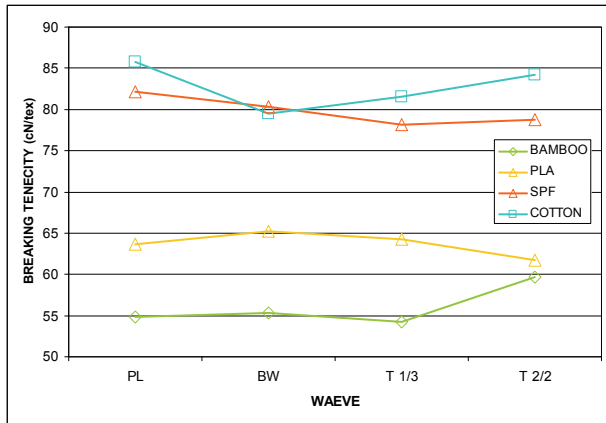


Fig. 7. Breaking tenacity of fabrics in weft direction

It was also found out that different properties of yarns have almost no influence on the tensile elongation of fabrics in warp direction, while mostly the weave type influences the tensile elongation in warp direction. The weave type is statistically 50 times more important than different materials used in weft. Figure 8 shows that fabrics in plain weave have the highest tensile elongation, which is approximately 15%, whereas the tensile elongation of all other fabrics, as can be seen in the diagram, is about 7%. Plain weave has the maximum number of interlacing points, which is twice as high as that of other weaves and, as a result, tensile elongation is higher. Also, warp crimp is the highest in plain weave, which influences tensile elongation as it was said before. The lowest tensile elongation is typical of the fabrics woven in basket weave.

Both the weave type and the material in weft influence the tensile elongation in weft direction, but the material used in weft is statistically 90 times more important. The highest tensile elongation is at fabrics with PLA yarns in weft, which are also the most extensible yarns. Then there are fabrics with SPF yarn, followed by fabrics with bamboo yarn and the lowest tensile elongation is at pure cotton fabrics, since cotton yarns have the lowest extensibility.

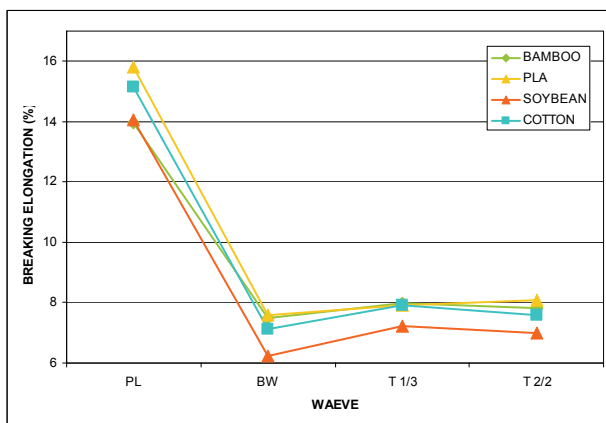


Fig. 8. Breaking elongation of fabrics in warp direction

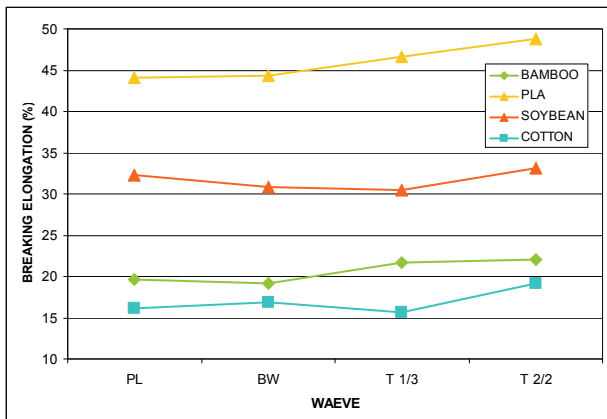


Fig. 9. Breaking elongation of fabrics in weft direction

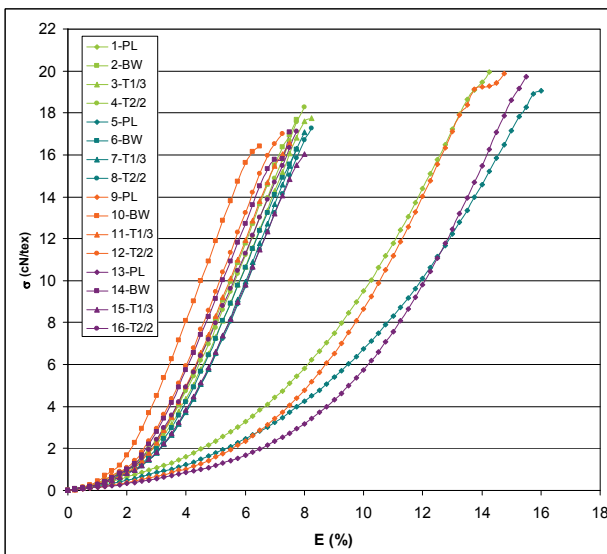


Fig. 10. Tenacity - extension curves for fabrics in warp direction

The fabrics with PLA yarn have the highest tensile elongation, for PLA yarn itself already has the highest tensile elongation (27.52%) and is the most extensible yarn. All these fabrics have tensile elongation about 45%. It is evident in Figure 9 that the fabrics in twill 1/3 and twill 2/2 have higher tensile elongation than plain and basket weave. The fabrics with SPF yarn in weft come in the second place. The tensile elongation of SPF yarn (13.72%) is ranked second. Figure 8 also shows that tensile elongation of these fabrics is ca 32%. The highest tensile elongation belongs to plain weave and twill 2/2 weave. Next to them, there are the fabrics with bamboo yarn with mean tensile elongation at about 20%. The tensile elongation of bamboo yarn is 8.52%. It is noticed again that twill 1/3 and twill 2/2 weaves have higher

tensile elongation than the plain and basket weave. Cotton fabrics have the lowest tensile elongation, since the cotton yarn itself also has the lowest tensile elongation of only 4.45%. The tensile elongation of cotton fabrics is 16%. The highest elongation is observed in the fabric in twill 2/2 weave.

For all fabrics in warp and weft direction, tenacity-extension curves were made to compare different behaviour at the tensile test.

The tenacity-extension curves in Figure 10 show that it is the weave, which has the highest influence on the shape of curves in warp direction. The curves of plain weave have almost the same shape, whereas the shapes of other weaves have very similar shapes. All curves for each group of materials are arranged in a defined order, i.e. twill 1/3, twill 2/2 and basket. Plain weave has a completely different shape of the curve due to a more frequent interlacing of threads in the weave, which results in a higher shrinkage of the fabric and, consequently, higher elongation.

The shapes of the curves for weft show that it is solely the material, which influences the shape of the curve. The weave has practically no influence, which has already been proved by previous results. Each group of materials has its own specific shape of the curve. The fabrics with cotton weft have the most vertical shape of the curve, for they have the lowest tensile elongation. The fabrics with PLA yarn in weft have a very specific shape of the curve. If the tenacity-extension of yarns (cf. Figure 5) is compared with the tenacity-extension curve of fabrics, some similarities can be detected. However, if the curves are compared with the shapes of the curves of standard materials, i.e. cotton, cellulose, PES or PA, and silk, it can be stated that the curve with bamboo yarn in weft has the same shape of the curve as cellulose fibres. The shape of the curve with SPF yarn in weft is similar to the shape of the curve of silk. Cotton fabrics have the same shape of the curves as cotton fibres.

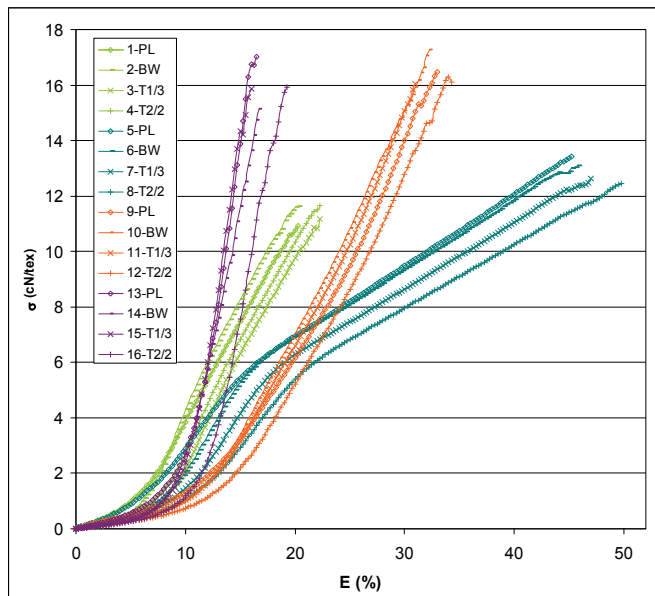


Fig. 11. Tenacity - extension curves for fabrics in weft direction

5.3 Other mechanical properties measured with KES evaluation system

The measurements on the KES system show which of the investigated fabrics is the most suitable for the clothing industry and what kind of behaviour can be expected. From the results, it can be seen that fabrics with SPF yarn in weft are very extensible and flexible. Cotton fabrics are the softest and fabrics with bamboo weft have very similar properties as cotton fabrics.

As it was discussed above, the measurements of tensile properties on the KES system confirmed as well that the tensile behavior of fabrics is closely related to the inter-fiber friction effect, the ease of crimp removal and load-extension properties of the yarn themselves. The measurements of extensibility (EMT) of fabrics and tensile work (WT) show that as at tensile test, the weave mostly influences the tensile properties in warp, and the material used in weft the tensile properties in weft. At EMT, it can be seen that the highest extensibility characterizes the fabric with the SPF yarn in weft direction; however, the SPF yarn is not the most extensible material (13.72%) but the fabric with the highest weft crimp, which has the highest influence on EMT. The fabrics in plain weave usually demonstrate a higher tensile work (WT), as it is also seen at our fabrics. It is also demonstrated that the fabrics wit SPF yarn in weft have the highest WT.

Shear rigidity G provides a measure for the resistance to the rotational movement of warp and weft threads within a fabric when subjected to low levels of shear deformation. The lower the value of G , the more readily the fabric will conform to three-dimensional curvatures. If the shear rigidity is not enough, a fabric distortion will easily occur. Shear properties are most commonly influenced by weave, while the material used in weft has practically no influence.

The KES system tensile properties influence both the type of weave and the material used in weft. It was also established that some properties measured on the KES system have very good correlation with each other (e.g. thickness, and compressional properties, bending and shearing properties) and some properties inversely proportional (e.g. tensile energy and tensile resilience, bending and shearing properties, and compressional properties). If it is known which properties correlate with each other, it is easier to predict what kind of properties the fabric will fabrics.

	LT	WT	RT	EMT	G	2HG	2HG5	B	2HB	LC	WC	RC	TO	TM	THIC
LT	1														
WT	0.588	1													
RT	-0.696	-0.819	1												
EMT	0.202	0.906	-0.623	1											
G	0.745	0.223	-0.449	-0.147	1										
2HG	0.702	0.159	-0.367	-0.201	0.992	1									
2HG5	0.770	0.181	-0.411	-0.204	0.983	0.974	1								
B	0.600	0.315	-0.298	0.060	0.648	0.631	0.691	1							
2HB	0.652	0.114	-0.213	-0.211	0.842	0.855	0.868	0.893	1						
LC	0.302	0.018	-0.084	-0.146	0.527	0.531	0.528	0.069	0.207	1					
WC	-0.128	-0.287	0.314	-0.311	0.272	0.325	0.199	-0.247	0.027	0.422	1				
RC	-0.180	0.003	0.136	0.127	-0.363	-0.368	-0.299	-0.167	-0.301	-0.064	-0.402	1			
TO	-0.683	-0.312	0.543	0.007	-0.820	-0.794	-0.821	-0.684	-0.742	-0.476	0.189	0.266	1		
TM	-0.670	-0.268	0.572	0.072	-0.799	-0.753	-0.784	-0.541	-0.658	-0.232	-0.019	0.582	0.801	1	
THIC	-0.794	-0.415	0.640	-0.057	-0.805	-0.756	-0.811	-0.701	-0.729	-0.238	0.132	0.470	0.840	0.942	1

Table 6. Correlation table of measured data on KES system

The principal components analysis (PCA) enables the visualization of linear correlations between the measured data on the KES system. PCA transforms multivariate data into a

lower-dimensional space where trends and patterns in the data can be detected. It extracts a set of new variables - the so-called principal components (PCs) - that are linear combinations of the original variables. The number of PCs equals the number of variables, however, generally, the first few (two or three) PCs already account for most of the variability in the data. By plotting two PCs, the relationships among the samples as well as among the studied variables can be visualized (Zupin et al, 2009).

From the correlation Table 6 and Figure 12 below, it can be seen that between the mechanical properties measured on the KES system, positive and negative correlations exist. The surface properties (MIU, MMD and SMD) and mass per square meter are not included into the PCA analysis. The surface properties are mostly influenced by weave, which makes the structure and surface of fabrics. Mass per square metre is almost the same at all fabrics, since the set density is the same at all fabrics.

From the correlation Table 6 and Figure 12 where close proximity, clustering, of points suggests that a high degree of positive correlation exists among the linearity of tensile load-extension curve (LT) and shear properties of fabrics (G, 2GH, 2GH5); tensile energy per unit area (WT) and extensibility (EMT); shear rigidity (G) and shear hysteresis (2HG, 2HG5) and bending properties (B, 2HB). This result was expected, for the shear and bending properties are highly related, both influenced by construction parameters of fabrics, esp. yarn properties and weave. Bending and shear properties are the most important properties for explaining the fabric stiffness, hardness and tailorability (Lam, Postle, 2006). It is also known that tensile work and extensibility correlate with each other.

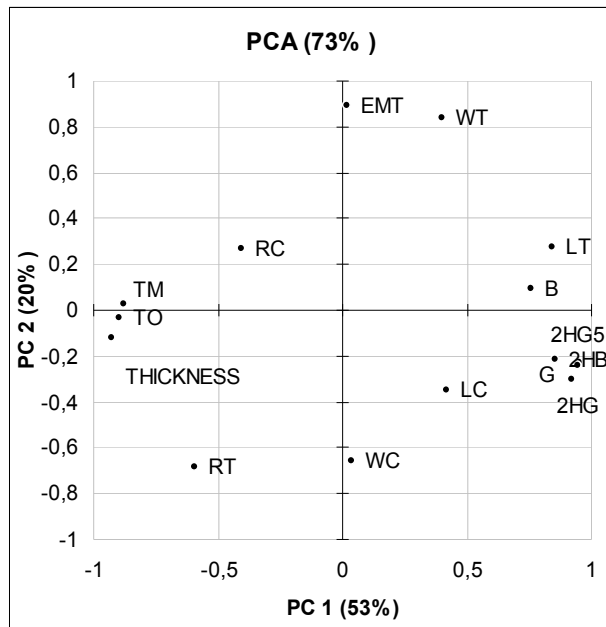


Fig. 12. Plot of original variables in PC1-PC2 coordinate system made with multivariate statistical method PCA, which presents correlations between mechanical properties measured on KES evaluation system

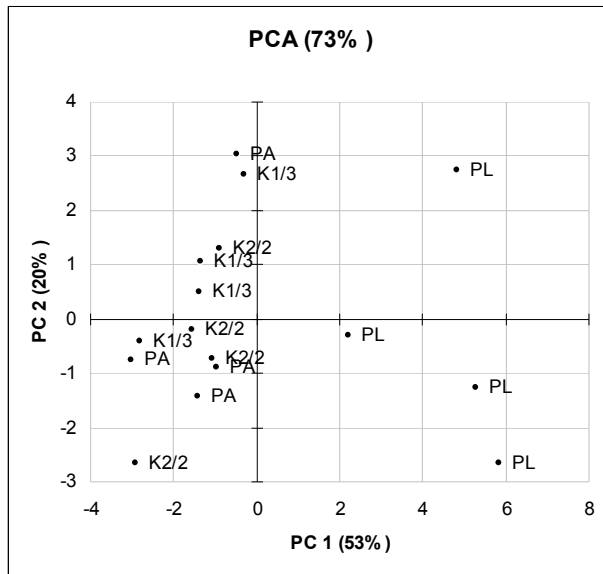


Fig. 13. Plot of 16 fabrics samples in PC1-PC2 coordinate system, each data label representing particular weave type

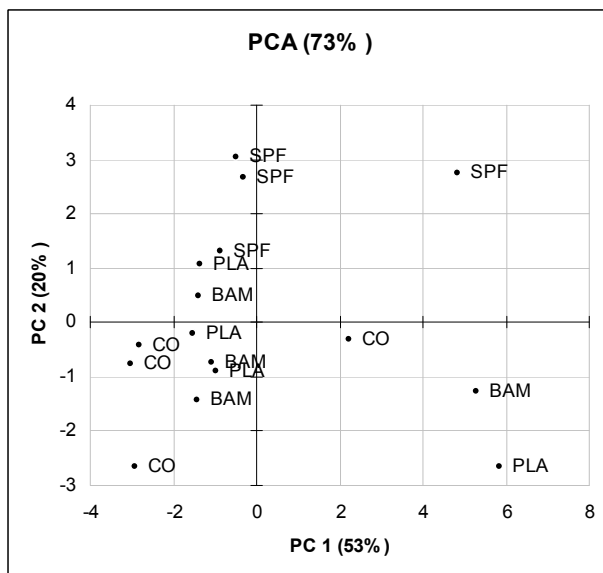


Fig. 14. Plot of 16 fabrics samples in PC1-PC2 coordinate system, each data label representing particular material used in weft

A strong negative correlation is observed where the points are opposite each other. A high degree of negative correlation exists among the linearity of tensile load-extension curve (LT) and thickness of fabrics; tensile energy per unit area (WT) and tensile resilience (RT); thickness of fabrics and shear (G, 2GH, 2GH5) and bending (B, 2HB) properties. These findings are expected, since the higher the fabric thickness, the harder it is to bend and shear the material. A negative correlation is also expected between WT and RT, for the more the fabric extends, the more energy is required to extend the fabrics to the final extension percentage. In Figure 13, it can be seen that the fabrics made in plain wave (PL) have different properties than all other fabrics, as has already been discussed. And Figure 14 shows that fabrics are clustered according to different material used in weft.

6. Conclusion

From the research results, it can be seen how different materials used in weft influence the mechanical properties of fabrics. The highest breaking force in warp direction is exhibited in the fabrics with the highest tensile elongation: SPF, PLA and bamboo yarn, followed by the fabrics with cotton yarn in weft. The material used in weft has almost no influence on the breaking elongation in warp direction; it is influenced almost only by weave. In weft direction, cotton fabrics have the highest tensile force, whereas lower tensile strength is observed in the fabrics with PLA, SPF and bamboo wefts. The materials also have the highest influence on the tensile elongation of fabrics in weft direction. Each yarn selected in weft has its own specific properties, which is reflected in the fabric.

It was established that all fabrics in weft direction have elongation from 20 to 45%, which is completely suitable to use as a fabric with increased elasticity.

It can also be seen that different weave types also influence fabric properties; however, their influence is lower.

The research of other mechanical properties measured with the KES system shows that fabrics with SPF yarn in weft are the most extensible and flexible, while the fabrics with cotton and bamboo in weft have higher tensile resilience than the fabrics with PLA and SPF in weft. Fabrics with PLA in weft are the stiffest and the most rigid, while the cotton fabrics are the softest.

In general, it can be claimed that fabrics with PLA, SPF and bamboo yarn in weft have a lower tensile force in comparison with pure cotton fabrics but higher tensile elongation in comparison with pure cotton fabrics. The tensile elongation or extensibility of fabrics is an important property for comfortable feeling when wearing clothes.

With the help of multivariate statistical analysis, the correlation between the measured mechanical properties on the KES system was established. Good positive correlation can be seen between shear and bending properties, and between tensile work and extensibility, while good negative correlation is seen between thickness and shear, and bending properties.

In the future researches, apart from the mechanical properties, we would like to research permeability properties of fabrics made with biodegradable material in weft and cotton in warp, *inter alia* air permeability, water vapour permeability, thermal resistance of fabrics and permeability of UV rays.

Moreover, we would like to test the mechanical and permeability properties of woven fabrics made from 100% biodegradable fibres (bamboo, PLA or SPF) and compare the properties with presented samples. Nevertheless, for a successful weaving of biodegradable

yarns in warp, it would be necessary to determine the behaviour of warp yarns in the weaving process, since, as it can be seen from the research, these yarns have high extensibility, i.e. from 8.5 to 27.5%, and not very high strength in comparison with cotton yarns.

It would also be interesting to test how the biodegradable materials act in other application as knittings and nonwovens.

For a more frequent use of biodegradable materials, various constructions, woven and knitted fabrics, and nonwovens should be tested and fabric properties and behaviour after the wearing, usages and after caring, e.g. washing and ironing, should be determined.

7. Acknowledgements

I would like to thank Prof. Dr. Manuela Neves from the University of Minho, Portugal, for providing us with the yarns and woven samples used in this research.

8. References

- Rijavec, T., Bukošek, V. (2009). Novel Fibres for the 21st Century. *Tekstilec*, Vol. 52, No.10-12/2009, 312-327, ISSN 0351-3386
- Blackburn, R. S. (2005). *Biodegradable and sustainable fibres*, Woodhead Publishing, ISBN 1-85573-916-x, Cambridge England
- Brooks, M. M. (2005). Soya bean fibres – past, present and future, In: *Biodegradable and sustainable fibres*, Blackburn, R. S. (Ed.), 389-440, Woodhead Publishing, ISBN 1-85573-916-x, Cambridge England
- Farrington, D. W., Lunt, J., Davies, S., Blackburn, R. S. (2005). Poly(lactic acid) fibres, In: *Biodegradable and sustainable fibres*, Blackburn, R. S. (Ed.), 389-440, Woodhead Publishing, ISBN 1-85573-916-x, Cambridge England
- Dugan, J.S. (2000). Novel properties of PLA fibres Vice President. Research Fiber Innovation Technology. Inc. Available on-line: <http://www.fitfibers.com/files/PLA%20Fibers.doc>
- Das, S. (2010). Properties of bamboo fibres. [cited 25.3.2010]. Available on -line: <http://www.fibre2fashion.com/industry-article/textile-industry-articles/properties-of-bamboo-fibre/properties-of-bamboo-fibre1.asp>
- Netravali, A.N. (2005). Biodegradable natural fiber composites, In: *Biodegradable and sustainable fibres*, Blackburn, R. S. (Ed.), 389-440, Woodhead Publishing, ISBN 1-85573-916-x, Cambridge England
- Rekha, R., Purnima, D. C. (2004). Biodegradable Polylactic Acid Polymers for Textile Applications. *Man-made Textiles in India*. February 2004, 42-44, ISSN:0377-7535
- Lou, C.W. et al (2008). Manufacturing and Properties of PLA Absorbable Surgical Suture. *Textile Research Journal*, Vol. 78, No.11, 958-965, ISSN 0040-5175
- Yi-you, L. (2004) The soybean protein fibre – A healthy & comfortable fibre for 21st century. *Fibres & Textile in Eastern Europe*. Vol. 12, No. 2 (46), 8-9, ISSN 1230-3666
- Realf, M.L., Boyce, M.C, in Backer, S. (1997) A Micromechanical Model of the Tensile Behavior of Woven Fabric. *Textile Research Journal*, Vol. 67, No. 6, 445-459, ISSN 0040-5175
- Grosberg, P. (1969). The tensile properties of woven fabrics. In: *Structural Mechanics of Fibres, Yarns and Fabrics. Volume 1*. ,John Wiley&Sons, 339-354, ISBN 471-36669-2

- Saville, B. (2002). *Physical testing of textiles*. Woodhead Publishing and CRC Press, ISBN 1-85573-367-6, Cambridge
- Gabrijelčič, H., Černoša, E. in Dimitrovski, K. (2008). Influence of weave and weft characteristics on tensile properties of fabrics. *Fibres & textiles in Eastern Europe*, Vol. 16, No. 2 (67), 45-51, ISSN 1230-3666
- Geršak, J. (2006). *Mehanske in fizikalne lastnosti tekstilnih materialov*. Fakulteta za strojništvo, Laboratorij za oblačilno inženirstvo ter fiziologijo in konstrukcijo, ISBN 86-435-0754-7, Maribor
- Hu, J. (2004). *Structure and mechanics of woven fabrics*. Woodhead Pub., ISBN 0-8493-2826-8, Cambridge
- Realf, M. L., Seo, M. H., Boyce, M. C., Schwartz, P., and Backer, S. (1991). Mechanical properties of fabric woven from yarns produced by different spinning technologies : yarn failure as a function of gauge length. *Textile Research Journal*, Vol. 61, No. 9, 517-530, ISSN 0040-5175
- Brooks, M. M. (2005). Soya bean fibres - past, present and future, In: *Biodegradable and sustainable fibres*, Blackburn, R. S. (Ed.), 389-440, Woodhead Publishing, ISBN 1-85573-916-x, Cambridge England
- Kawabata, S. (1989). Nonlinear mechanics of woven and knitted materials, *Textile Structural Composites*, Chou, T. W. and Ko, F. K. (Ed.), Elsevier Science Publisher, 67-116, ISBN 0-444-42992-1, Amsterdam
- Zupin, Ž., Dimitrovski, K. (2008). Tensile properties of fabrics made from new biodegradable materials (PLA, soybean, bamboo fibres). *Proceedings of Magic world of textiles*, pp. 185-190, ISBN 978-953-7105-26-6, Dubrovnik, Croatia, October, 2008, Faculty of Textile Technology, University of Zagreb, Zagreb
- Pierce, F.T. (1937). The geometry of cloth structure. *The Journal of the Textile Institute*, Vol. 28, No. 3, T45-T96, ISSN 0368-4474
- Womersley, J.R. (1937). The application of differential geometry to the study of the deformation of cloth under stress. *The Journal of the Textile Institute*, Vol. 28, No. 3, T97-T112, ISSN 0368-4474
- Zupin, Ž., Dimitrovski, K., Hladnik, A. (2009). Determination of woven fabrics influential parameters using multivariate statistics. *Proceedings of the 9th Autex Conference*, pp. 585-590, ISBN 978-975-483-787-2, Izmir, Turkey, May, 2009, Ege University, Engineering Faculty, Department of Textile Engineering, Izmir
- Lam, J.K.C., Postle, R. (2006). Multivariate Studies of Mechanical Properties for Wool and Cotton Fabrics. *Textile Research Journal*, Vol. 76, No. 5, 414-425, ISSN 0040-5175
- Chan, C.K. et al (2006). Evaluation of mechanical properties of uniform fabrics in garment manufacturing. *Journal of Materials Processing Technology*, Vol. 174, 183-189, ISSN 0924-0136
- Kemp, A. (1958). An extension of Peirce's cloth geometry to the treatment of non-circular threads. *The Journal of the Textile Institute*, Vol. 49, No. 1, T44-T48, ISSN 0368-4474
- Olofsson, B. (1965). A general model of a fabrics as a geometric-mechanical structure. *The Journal of the Textile Institute*, Vol. 55, No. 11, T541-T557, ISSN 0368-4474

Wing Tear: Identification of Stages of Static Process

Beata Witkowska¹ and Iwona Frydrych²

¹*Textile Research Institute,*

²*Technical University of Lodz,
Poland*

1. Introduction

In 1945 Krook and Fox (Krook & Fox 1945) analyzing photos of torn tongue shape samples distinguished and described the fabric tearing zone, i.e., the zone, which appears between both thread systems of torn fabric sample. The fabric tearing zone is limited by two threads of stretched thread system arising from the cut strips of torn sample, and the torn thread system being in the position "just before the breakage". Krook's and Fox's research was an inspiration for the next researchers, who were interested in the fabric tearing. They have very often based their considerations on Krook's and Fox's conclusions.

The research was continued by Teixeira et al. in 1955 (Teixeira et al., 1955). They developed Krook's and Fox's (Krook & Fox, 1945) observations, and also formulated the theoretical equation, which described the tearing phenomenon.

In 1959 Taylor (Taylor, 1959) elaborated the mathematical relationship, which on the basis of fabric and thread structure parameters enables to predict the tear strength. He analyzed the geometry of tearing zone in the aspect of friction forces of stretched thread system (not torn) along the threads of perpendicular system (torn). Taylor didn't analyze the phenomena taking place in perpendicular (torn) threads.

Research on the tearing process of trapezoidal samples was carried out by Hager, Gagliardi and Steele (Hager et al., 1947). They (as Taylor) did not take into consideration the influence of the perpendicular thread (torn) system and occurring friction forces in the torn system. Moreover, they assumed the linear relationship between the load and strain of stretched thread system.

Hamkins and Backer (Hamkins & Backer, 1980) presented their results concerning the tearing mechanics on the basis of two quite different in their structure fabrics: made from a glass yarn of „loose” weave and a big possibility of threads to be moved as well as from an elastomeric yarn of small possibility of threads to be moved. The application of previous models was not fully satisfactory for different variants of fabric structure.

Then the problem was analyzed by Seo (Scelzo et al., 1994a), who broaden the Taylor's (Taylor, 1959); (Letters to the Editor, 1974) model by the proposed by him parameters of the tearing zone geometry. The common feature of both models was an existence of such parameters as: the friction coefficient (thread by thread in a fabric), mean thread breaking force, distance between the axes of neighbor threads.

Scelzo, Backer and Boyce (Scelzo et al., 1994a); (Scelzo et al., 1994b) proposed the description of phenomenon taking place in the cotton fabric during the tearing basing on the tearing zone shape analysis and adapting the rheological model consisted of spring arrangement for a description of tearing process.

Now, the resistance on the static tearing is one of the most important assessment criteria of strength parameters of fabrics destined for the work and protective clothing, high-tech textiles, technical and interior textiles, upholstery and daily used clothing. In experiments the different specimen shapes are used, a choice of which can be found in the appropriate standards (Witkowska & Frydrych, 2004) (Witkowska & Frydrych, 2005).

In the chapter, there are presented the theory verified experimentally concerning the stages of the cotton fabric static tearing with taking into consideration the fabric tearing zone assessment, i.e., its length, depth and the thread number in the tearing zone. The analysis was carried out for the wing shape specimen described in the standard PN-EN ISO 13937-3:2002. An observation of tearing stages required the application of appropriate measurement system, which enabled the registration of changes taking place during the tearing process; and next, an analysis of obtained images. Such an opportunity was guaranteed by a specially elaborated for this purpose software working in the Windows environment. The whole software enables the observation of the video image on the computer screen, an image registration on CD with the given speed and image analysis. The special stand for the on-line tearing phenomenon registration was designed and built. Experiment was done for the model cotton fabrics of such a structure, which enables the observation of changes of tearing zone parameters dependably on the fabric weave at the assumption that the parameters of torn and stretched thread systems are unchanged.

1.1 Methods used for determination of static tear strength

In the whole period of fabric static tear resistance research, which has been estimated for over 95 years (Harrison, 1960), i.e., from 1915 up till now, there were proposed ca. ten different specimen shapes. Dependably on the assumed specimen shape, the particular investigators proposed their own specimen sizes and a measurement methodology, and also their own way of assessment of fabric tearing strength as well as own expression of results. The fabric tear strength (resistance) is a property determining the fabric strength on the static tearing action (static tearing), kinetic energy (dynamic tearing) and tearing on the "nail" of appropriate prepared specimen.

Different ways of tearing were reflected in the measurement methodology. The methods were diversified by the shape and size of specimen, a length of torn fabric distance, and also a way of tear force determination. The most popular methods were standardized. Now, in the all methods the parameter, which characterizes the fabric tear strength, is the tear force. In the static tearing methods as well as in the dynamic one the tearing process is a continuation of tearing started by an appropriate cutting the specimen before the measurement.

In Fig. 1, there are presented the specimen shapes, which are now used in the laboratory measurements of static tear strength; whereas in Table 1, there are presented the important data concerning the applied specimen shapes and dealt with them a measurement methodology.

Similarly as shapes and sizes of specimens also a way of tear force calculation has been changed since 95 years. This process was finished by a standardization, which unified a way of calculation of the static tear strength result. The result of static tearing can be read:

- directly from the measurement device;
- from the tearing chart dependably on the assumed measurement methodology.

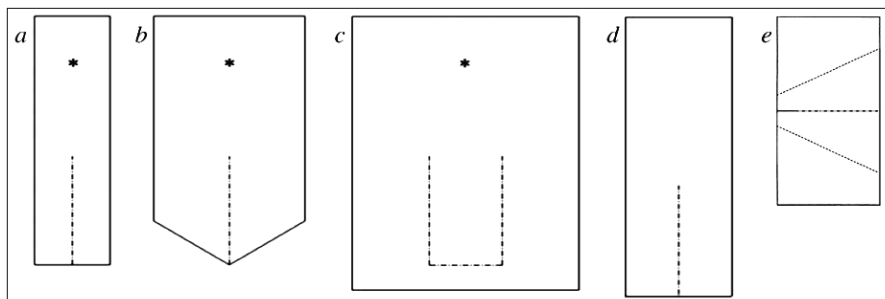


Fig. 1. The actual used shapes of specimens; a) trousers according to PN-EN ISO 13937-2 and PN-EN-ISO 4674-1-method B (for rubber or plastic-coated fabrics); b) wing according to PN-EN ISO 13937-3; c) tongue with double tearing according to PN-EN ISO 13937-4 and PN-EN ISO 4674-1-method A (for rubber or plastic-coated fabrics); d) tongue with single tearing according to ISO 4674:1977-method A1; e) trapezoidal shape according to PN-EN ISO 9073-4 (for nonwoven) and PN-EN 1875-3 (for rubber or plastic-coated fabrics)

A source: Own on the basis of present-day standards concerning the static tearing

Fig. 1a single tearing	Fig. 1b single tearing	Fig. 1c double tearing	Fig. 1d single tearing	Fig. 1e single tearing
Tearing direction to the acting force				
	⊥			⊥
Tearing distance, mm				
75	75	75	145	210
Measurement rate, mm/min				
100	100	100	100	100
Distance between jaws, mm				
100	100	100	75	25
Specimen dimension,mm; length, depth				
200; 50	200; 100	220, 150	225; 75	150; 75
Length of cut, mm				
100	100 ; angle 55°	100	80	15

Table 1. The description of static tearing methods

A source: Own on the basis of present-day standards concerning the static tearing

Now reading the tear forces from the tearing chart is possible for all used measurement methods of static tearing, i.e., for specimens of tongue shape with a single (trousers) and double tearing, for the wing and trapezoidal shape. As the tearing chart the curve, which occurs as a result of sample tearing on the tearing distance, is assumed. The initial point of tearing curve is a peak registered in the moment of breakage of the first thread (or thread group) being on the tearing distance, and the end of tearing curve is a breakage of the last thread (or thread group) on the given distance.

According to the standardized measurement procedure the following methods are used now:

- the method described in the standard series PN-EN ISO 13937 part 2 (trousers), part 3 (wind) and part 4: tongue - double tearing (Witkowska & Frydrych, 2004). The tearing graph is divided onto four equal parts starting from the first and finishing on the last peak on the tearing distance. The first part of graph is neglected in calculations. From the rest three parts of graph six the highest and lowest peaks are chosen (by the manual method) or all the peaks on 3/4 of tearing distance are calculated (by the electronic method). As a result an arithmetic mean of tear forces is given.
- the method A1 described in ISO 4674:1997, which is in agreement with the *American Federal Specifications* (Harrison, 1960), was elaborated in 1951. It relies on a median determination from five tear force values represented by maximum peaks for the medium graph distance creating 50% of tearing distance (Witkowska & Frydrych, 2004).
- the method described in PN-EN ISO 9073-4 for nonwovens and according to the PN-EN 1875-3 for rubber and plastic-coated fabrics - relies on the calculation of arithmetic mean from the registered maximum peaks on the assumed tearing distance.

1.2 Tear force as the criterion of fabric assessment

Analysis of fabric strength parameters showed that the tear strength is one of the important criteria of fabric assessment destined for the protective and work clothing; high-tech and technical textiles, interior textiles, upholstery and daily clothing.

There are many possibilities of fabric destruction by tearing. To the most characteristic cases of tearing belong:

- fabric tearing by nail or the other sharp tool;
- tearing in the places, where textile elements are joined together (in the utility or decorative purpose) by the elements of the high strength, for example rivets. In these places there can be often observed the characteristic tearing of its element from the fabric and the hole appearance;
- the hole occurrence (random) in the fabric by, for example, cigarette or spark. If this place is stressed, for example, during the utility, the local area decrement causes the increase of stresses on the hole circumference and the fabric is torn;
- fabric cutting on the same distance and next, its stretching. Such a situation is observed during the utility process, for example, cutting on the pocket can cause the clothing destruction, if these places are not protected at the ends.

The diversity of fabric tearing processes as well as the existence of many measurement methods often cause the problems dealt with a choice of the appropriate measurement method for the given fabric assortment. The selection of tearing strength measurement method for the given fabric should follow the analysis of criteria of such fabric assessment. These criteria are described in:

- harmonized standards (concerning the protective clothing);
- other standards (national, European, international);
- in so-called a list of technological and utilization indices (old Polish national standard introduced before 2000 year);
- contracts between textile producers and their customers.

Below, in Table 2, there is presented a division of static tear methods dependably on the chosen fabric assortment.

The other aspect is an application possibility of the admitted tearing method for the given fabric structure. It often happens that, for example, for a high tear strength fabric, i.e., of tear

force above 100 N or for fabric destined for the protective and work clothing (often cotton or cotton similar) of diversified tear strength dependably on the thread direction (warp-weft) and for fabric of weaves with long floating threads there is possible the application (undependably on the mentioned above rules) of only one tearing method, i.e., according to PN-EN ISO 13937 Part 3 (Fig. 1c). It is caused by the fact that the sample shape in this method and a way of mounting it in the tensile tester jaws enables the obtaining the better its clamping in the tensile tester jaws. Thanks to it the sample is not broken in the jaws and the measurement can be performed.

Textiles - rubber or plastic-coated fabric	
PN-EN 1875	Technical textiles
ISO 4674:1977	Method A1: protective clothing (high-visibility warning for professional use; protection against rain), Method A2: textiles for tarpaulin
PN-EN ISO 4647-1	Method A: Protective clothing (protection against cold), Method B: protective clothing (for firefighters for firefighting)
Textiles - non-coated	
PN-EN ISO 13937-2	protective clothing (for firefighters in action), work clothing (overalls, shirts, trousers), mattress – woven, daily textiles, textiles for flags, banners
PN-EN ISO 13937-3	upholstery (furniture) textiles, bed clothing, textiles for beach chairs, technical textiles (roller bind)
PN-EN ISO 13937-4	work clothing (changeable with PN-EN ISO 13937-2)

Table 2. The division of static tear methods dependably on the chosen fabric assortment
A source: Own on the basis of present-day standards concerning the static tearing

Summing up, the significance of static tear force measurement increased in the last years. Laboratory practice showed that this parameter has the same importance for the fabric assessment as a tensile strength. The main reason of such situation is the growing significance of safe fabric utility, first of all destined for the protective clothing.

It should be pointed out that the fabric producers taking into consideration the significance of strength parameters in the complex fabric assessment apply modern raw materials of better quality, for example, PES, PA, PI, AR and their blends with natural fibers, which guarantee the obtaining the required level of these parameters.

The fabric tear strength is the complex problem, character of which is still not fully explained. The big number of tearing methods and not useful models with parameters, which are not available in the laboratory practice make difficult the prognosing the tear strength; therefore, the experimental research in this field has been necessary.

2. Analysis of stages of cotton fabric static tearing process for the wing shape specimen

The tearing process of cotton fabric sample of the wing shape (according to PN-EN ISO 13937-3) started by loading the specimen by the tensile force was divided into three stages, which were presented schematically in Fig. 2.

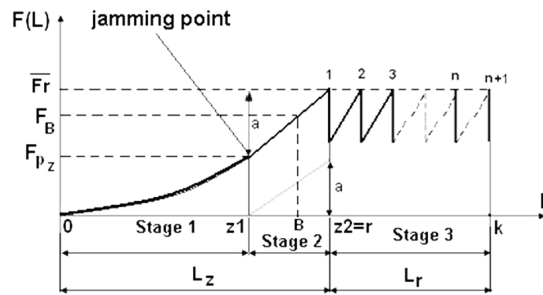


Fig. 2. The graph of tear force of specimen in the function of tensile tester clamp displacement, i.e., the tearing process graph. Stages of tearing process of cotton fabric for the wing shape specimen

Source: own

In Fig. 2 the following designations were assumed:

point 0 - start of sample tearing process, i.e., start of movement of tensile tester clamp. *Point 0* means also the beginning of stage of both thread system displacement;

point z1 - the end of stage of thread displacement and the beginning of stretching the torn thread system;

point z2 - the end of stretching stage and the beginning of thread breakage - *point r*;

point k - the end of specimen tearing process, i.e., the end of measurement;

point B - any point on the distance $z1-z2$;

distance a - the value of breaking force, i.e., the value, which is „added” to the value of displacement in the moment of achieving the jamming point;

L - the way of movement of the tensile tester clamp;

L_z - the way of the movement of the tensile tester clamp up to the first thread breakage on the distance L_r ;

L_r - tearing distance, i.e., the distance of displacement of tensile tester clamp since the moment of first thread breakage up to the breakage of the last thread on the marked tearing distance;

$F(L)$ - the stretching force acting on the torn sample on the distance of displacement of tensile tester clamp;

\bar{F}_r - the mean value of tearing force calculated as an arithmetic mean of local tear forces represented by peaks 1, 2, 3 ... n, n+1 on the tearing distance L_r , (for ideal conditions $F_{r1}=F_{r2}=F_{r3}=F_{rn}=F_{rn+1}$);

F_B - the value of tensile force in any point B;

Line z1 - the end of distance *a* - the relationship between the breaking force and strain for the single thread, i.e., $W_z = f(\epsilon_z)$;

Curve 0 - jamming point - the relationship between the distance, on which the clamp of tensile tester is moving and the force causing the displacement of both thread systems of torn specimen up to achieving the thread jamming point;

Curve 0-1 - the relationship between the distance, on which the clamp of tensile tester is moving and the stretching force up to the first thread breakage on the tearing distance.

Curve 0-1 on the distance $z1-z2$ is the value of *line z1* - the end of a distance - moved about a displacement force value in the jamming point.

The analysis of tearing stages is presented assuming that the process of forming the fabric tearing zone on the assumed tearing distance has been started since the moment that the tensile tester clamp has started to move. In the tearing zone dependably on the stage of tearing the following areas can be distinguished: displacement, stretching and breaking (Witkowska, 2008).

Stage 1. Mutual displacement of both specimen system threads. The appearance of the *displacement area in the tearing zone*. The phenomena taking place in this stage are initiated in the moment of starting the movement of tensile tester clamp. The clamp movement on the *distance 0-z1* (Fig. 2) causes the displacement of both thread systems of torn fabric specimen, i.e., threads of stretching system - mounted in the clamps and threads of torn system - perpendicular to the thread system mounted in the clamps. It was assumed that in this stage the threads of torn system are not deformed.

Stage 2. Stretching the threads of torn system. It is done due to the further increase of loading the threads of stretched system, but without the mutual displacement of both thread systems of torn fabric sample. In this stage there are *two areas of tearing zone: displacement and stretching*. Continued in this stage the movement of tensile tester clamp on the *distance z1-z2* (Fig. 2) causes that due to a lack of possibility of further mutual displacement of both fabric system threads the first thread of torn system (being in the displacement area) goes into the stretching area and started to elongate up to the achievement of critical value of elongation, i.e., the value of elongation at the given thread breaking force. Therefore, it was assumed that in the successive tearing process moments in the stretching area there was only one thread of torn system, for which the relationship between the load and strain was linear.

Stage 3. The breakage of torn system thread on the assumed tearing distance. In this stage of tearing process the tearing zone is *built from three areas: displacement, stretching and breaking*. The further movement of tensile tester clamp on the *distance r-k* (Fig. 2) causes the breakage of successive threads of torn system on the tearing distance up to finishing the tearing process (*point k*, Fig. 2).

Between stages 1 and 2 there is so-called the *jamming point* (Fig. 2), i.e., the point, in which fabric parameters and values of friction force between both system threads make impossible the further mutual displacement of both thread systems. Therefore, the achievement of jamming point finishes the stage 1, and the breakage of the first thread on the given tearing distance finishes the stage 2.

Since the moment of the first thread breakage on the tearing distance, the phenomena described in *stages 1, 2 and 3* have been taking place simultaneously up to the moment of breakage of the last thread of torn system on the tearing distance.

The characteristics of tearing process stages have some features similar to the description of this phenomenon for the wing shape specimen presented by the previous researchers of tearing process, i.e.:

1. Distinguishing in the torn fabric sample two thread systems, i.e., the stretched thread system - mounted in the tensile tester clamps; and the torn thread system, which is perpendicular to the stretched one (Krook & Fox, 1945); (Scelzo et al., 1994a); (Scelzo et al., 1994b); (Teixeira et al., 1955); (Taylor, 1959). Both systems can be called also un-torn and torn.
2. Distinguishing the fabric tearing zone (Krook & Fox, 1945); (Scelzo et al., 1994a); (Scelzo et al., 1994b); (Teixeira et al., 1955); (Taylor, 1959) in the torn wing shape specimen.
3. Stating that in the torn fabric sample there are simultaneously the displacement and stretching of both system threads, displacement of stretched system of threads (Taylor, 1959), displacement of both thread systems (Teixeira et al., 1955).

4. Limiting the fabric tearing process to three components represented by threads being in the tearing zone (Scelzo et al., 1994a) (Scelzo et al., 1994b) (Teixeira et al., 1955): the first component - torn system thread in the position "just before the breakage", second and third components - "at the border of tearing zone" threads of stretched system (threads on the inner edge of cut sample elements).

To the most important differences between the descriptions of fabric tearing process presented in this paper and done by the previous Authors belong:

1. Division of fabric tearing zone onto the following areas: the displacement, stretching and breaking.
2. Distinguishing the jamming point of both thread systems of torn sample.
3. Stating that the both thread system displacement (*stage 1*) phenomenon and stretching (*stage 2*) of torn thread system are not taking place at the same time. This statement is true at the assumption that it is possible to find such a point, in which the first thread of torn system being in the displacement area cannot be further displaced. This thread goes into the stretching area and starts to elongate up to achieving the critical value of elongation and the thread breakage.
4. Stating that the tear force is a sum of vector forces, i.e., the force, which causes the displacement without both system thread deformation up to achieving the so-called jamming point; and the force, which causes the elongation of torn system thread up to achieving the critical value of elongation and thread breakage.

Consideration that assumptions for elaboration of the theoretical model of cotton fabric tearing for the wing shape sample are proceeded by the separation of three tearing stages in the fabric tearing zone, i.e., displacement of both system threads to achieve the thread jamming point, stretching and breaking the threads of torn system. Next, there was stated that from the moment of the first thread breakage on the tearing distance the phenomena described in the mentioned above stages have a place simultaneously up to the breakage of the last thread of torn system. The force put to the torn specimen in the function of displacement of tensile tester clamp, i.e., $F=f(L)$ was described as follows:

$$F=f(L)=F_p(L)+Fw_z(L) \quad (1)$$

where:

$F_p(L)$ - force F in the function of displacement of tensile tester moving clamp during the displacement of both system threads of torn sample;

$Fw_z(L)$ - force F in the function of displacement of tensile tester moving clamp during the stretching one thread of torn system, which is in the tearing zone at this moment. It was assumed that the relationship $Fw_z(L)$ is described by the Hookean law.

According to the proposed stages of tearing process the relationship (1) takes the form:

$$\text{stage 1: } F=f(L)=F_p(L) \quad (2)$$

$$\text{stage 2 and stage 3: } F=f(L)=F_p(L)+Fw_z(L) \quad (3)$$

and the thread breakage in the tearing zone:

$$F=f(L)=F_r \quad (4)$$

where:

F_r - local value of breaking force.

The value of fabric breaking force in the moment of the first thread breakage on the given tearing distance on the border of stretching and breaking of tearing zone is described by the relationship (5) (general model of fabric tearing):

$$F_r = F_p(z_1) + F_{w_z}(r) = F_{pz1} + F_w \quad (5)$$

where:

r - the end of stages of stretching of torn thread system and the beginning of thread breaking stage;

F_{pz1} - the value of displacement force in the jamming point of both thread systems of torn fabric sample;

F_{w_z} - the value of breaking force of torn thread system.

3. Experiment

3.1 The stand for image analysis

The stand for image analysis was built from the following elements: the tensile tester Zwick model 1120 (1), jaws of tensile tester (2), computer with the software *test-Xpert* (3) for textile static tearing, color camera TV (5) (zoom 3.5 to 8.0 mm), computer with the software *Microstudio* (4) or image analysis, tripod camera (6) (Witkowska & Frydrych, 2008); (Witkowska, 2008). In order to observe the cotton fabric tearing stages and tearing zone the video system was used (Fig. 3 and Fig. 4).

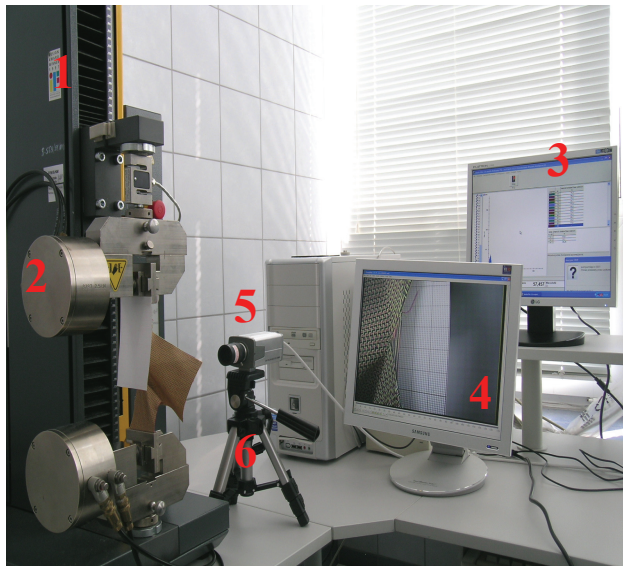


Fig. 3. Stand for the registration of tearing process and computer analysis of images of tearing zone

Source: own

The system enables also to archive and analyze the static images. To obtain a dynamic image the stand assured the registration of 25 images per second. For the image acquisition there was used the digital camera CCD CP-720 with a special optical system enabling the analysis of moving images, choosing the observed area and obtaining the clear (sharp) images of analyzed objects. In order to archive and analyze the static images the *MicroStudio Video* software was applied. From the video images showing the fabric tearing there were chosen

the static images representing the fabric in the exactly the same measurement points. On the basis of static images there were determined the length of tearing zone (l_{Δ}), depth of tearing zone (d_{Δ}), and the thread number in the tearing zone ($L_{n-\Delta}$) for each marked measurement point. An analysis of static images representing tearing zones enables to state that the tearing zone in many cases is not symmetrical according to $x-x$ axis going through the point determining the depth of tearing zone. Therefore, the length of distance from the $x-x$ axis to the end of marked tearing zone is (l_{Δ}), the length (l_{Δ}) and depth (d_{Δ}) of tearing zone were assumed in the agreement with Teixeira's (Teixeira et al., 1955) model of tearing zone. From the static images the following values were read: the total tearing zone length (l_{Δ}), length (l_{Δ}) and depth (d_{Δ}) of tearing zone in pixels; and next, these values were recalculated into millimeters.

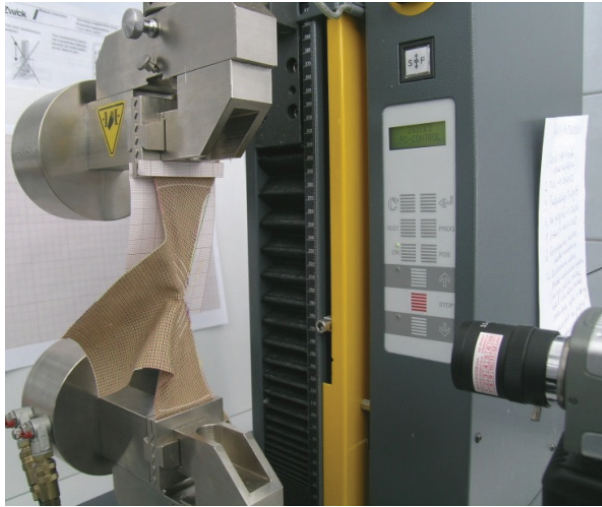


Fig. 4. The way of sample mounting in the tensile machine jaws for the tearing zone registration
Source: own

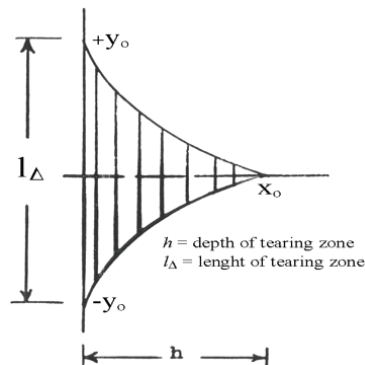


Fig. 5. Teixeira's model of fabric tearing zone (Teixeira et al., 1955)

Successive operations at registration of tearing process of cotton fabrics:

1. Mounting the marked specimen of wing shape in the tensile machine jaws.
2. Setting the video camera in such a position to have on the screen of computer with *MicroStudio Video* software the specimen with the marked measurement points and appropriate scale (millimeter paper).
3. Simultaneous starting of tensile machine and software *MicroStudio Video* registering the video camera image.
4. Finishing the movement registration and the specimen tearing process after the third measurement point.
5. Repeating the points 1 to 4 for each prepared specimen.

3.2 Testing materials

100% cotton woven fabrics of characteristics presented below from woven color threads were design and manufactured for the need of experiment. An application of color threads facilitated the observation of video images of the fabric tearing process.

Fabric characteristics (Witkowska, 2008):

- weaves: plain, twill 3/1 Z, satin 7/1 (5), and broken twill 2/2 V4;
- warp and weft thread linear density: 25 tex x 2;
- the mean number of threads per 1 dm: warp - 188, weft - 174.

From the each fabric three specimens in each direction (warp/weft) were cut. On the right side of fabric starting from the cut edge three points were marked every 5 mm representing three measurement distances, i.e., 5 mm, 10 mm and 15 mm (Fig. 6). The speed of testing was 75 mm/min.

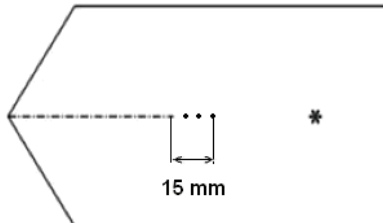


Fig. 6. The way of sample marking for the measurement

Source: own

The static tear resistance of analyzed fabrics was determined according to PN-EN ISO 13937-3:2002. From each fabric 10 specimens in the warp and weft directions were measured; and next, the tear force values using the tensile tester Zwick 1120 controlled by the software *test-Xpert version 4.12* were determined. The measurement was carried out with the speed 100 mm/min. From charts the tear force (F_T) for the whole tearing distance, i.e., from the first to the last peak registered on the assumed tearing distance were read. The obtained values of force of 10 specimens were statistically assessed; the mean value and variation coefficient were determined.

3.3 Results

The set of mean values of cotton fabric tear forces dependably on the weave of analyzed fabrics are presented in Table 3. The data of obtained parameters of tearing zone

dependably on the fabric weave, length of tearing distance are presented in Tables 4-7; whereas the chosen static images of cotton fabrics tearing zones of registered in the measurements point 15 mm (specimen 1) for the wing shape specimens in plain and satin weave variants are presented in Fig. 7 and 8.

Parameter/fabric	Fabric weave							
	plain		twill 3/1 Z		satin 7/1 (5)		broken twill 2/2 V4	
	warp	weft	warp	weft	warp	weft	warp	weft
Mean tear force, N	19.7	19.8	23.9	23.0	63.2	52.2	26.5	21.0
Variation coefficient, %	3.6	3.7	3.8	3.7	4.4	5.4	1.4	5.1

Table 3. The set of tear force results for cotton fabrics dependably on the weave

Specimen	Plain warp - measurement point											
	5 mm				10 mm				15 mm			
	l_A	$l_{A\uparrow}$	d_A	L_{n-A}	l_A	$l_{A\uparrow}$	d_A	L_{n-A}	l_A	$l_{A\uparrow}$	d_A	L_{n-A}
1	7.0	3.5	0.7	1	4.5	2.1	0.7	2	5.7	2.8	0.7	2
2	7.2	3.6	0.7	2	4.8	2.3	0.8	1	6.3	3.1	0.7	2
3	7.7	3.9	1.0	2	5.0	2.4	0.8	2	6.5	3.3	1.0	2
Specimen	Plain weft - measurement point											
	5 mm				10 mm				15 mm			
	l_A	$l_{A\uparrow}$	d_A	L_{n-A}	l_A	$l_{A\uparrow}$	d_A	L_{n-A}	l_A	$l_{A\uparrow}$	d_A	L_{n-A}
1	5.2	2.6	0.5	1	4.6	2.3	1.0	1	5.2	2.6	1.0	1
2	5.5	2.7	1.0	1	4.7	2.3	0.9	2	5.1	2.5	0.8	1
3	5.1	2.5	0.8	1	5.6	2.8	1.0	1	5.2	2.6	0.9	1

Table 4. Parameters of tearing zone and the thread number in the tearing zone for the model plain cotton fabrics

Specimen	Twill 3/1(Z) warp - measurement point											
	5 mm				10 mm				15 mm			
	l_A	$l_{A\uparrow}$	d_A	L_{n-A}	l_A	$l_{A\uparrow}$	d_A	L_{n-A}	l_A	$l_{A\uparrow}$	d_A	L_{n-A}
1	18.7	9.3	2.5	5	24.7	12.3	3.6	5	31.9	15.4	4.8	6
2	18.7	9.4	2.6	4	28.3	14.2	4.1	5	36.5	18.6	5.3	7
3	18.7	9.4	2.6	5	26.1	13.0	3.2	5	35.0	15.6	5.0	7
Specimen	Twill 3/1(Z) weft - measurement point											
	5 mm				10 mm				15 mm			
	l_A	$l_{A\uparrow}$	d_A	L_{n-A}	l_A	$l_{A\uparrow}$	d_A	L_{n-A}	l_A	$l_{A\uparrow}$	d_A	L_{n-A}
1	13.1	6.3	2.1	5	25.9	13.0	3.6	6	32.9	14.7	5.2	8
2	12.2	5.9	2.1	4	25.8	12.8	3.8	5	31.1	14.9	5.4	8
3	13.1	6.6	2.4	3	24.3	12.2	4.1	5	34.3	16.4	5.2	7

Table 5. Parameters of tearing zone and the thread number in the tearing zone for the model twill 3/1 Z cotton fabrics

Specimen	Satin 7/1 (5) warp - measurement point											
	5 mm				10 mm				15 mm			
	l_A	$l_{A\uparrow}$	d_A	L_{n-A}	l_A	$l_{A\uparrow}$	d_A	L_{n-A}	l_A	$l_{A\uparrow}$	d_A	L_{n-A}
1	12.1	6.0	2.9	7	22.3	11.1	4.1	10	41.5	21.2	5.6	14
2	13.7	7.7	2.9	7	24.9	12.2	3.5	9	39.8	18.2	5.7	12
3	13.6	6.9	3.0	5	24.4	14.2	3.6	8	40.3	24.0	5.2	11
Specimen	Satin 7/1 (5) weft - measurement point											
	5 mm				10 mm				15 mm			
	l_A	$l_{A\uparrow}$	d_A	L_{n-A}	l_A	$l_{A\uparrow}$	d_A	L_{n-A}	l_A	$l_{A\uparrow}$	d_A	L_{n-A}
1	13.1	7.1	2.5	6	24.5	12.1	3.1	9	34.5	13.5	4.6	14
2	14.0	7.0	2.4	7	25.0	12.4	3.8	10	34.4	15.1	4.6	15
3	12.7	6.2	2.3	6	26.1	13.1	3.8	13	34.0	17.2	4.9	17

Table 6. Parameters of tearing zone and the thread number in the tearing zone for the model satin 7/1(5) cotton fabrics

Specimen	Broken twill 2/2 V4 warp - measurement point											
	5 mm				10 mm				15 mm			
	l_A	$l_{A\uparrow}$	d_A	L_{n-A}	l_A	$l_{A\uparrow}$	d_A	L_{n-A}	l_A	$l_{A\uparrow}$	d_A	L_{n-A}
1	14.5	7.2	2.3	5	23.9	12.0	4.2	7	34.3	15.9	5.1	10
2	15.7	7.8	2.2	5	24.1	9.0	3.6	6	35.5	12.7	5.5	9
3	16.0	7.0	2.4	4	25.4	12.6	4.0	7	38.5	18.6	5.6	10
Specimen	Broken twill 2/2 V4 weft - measurement point											
	5 mm				10 mm				15 mm			
	l_A	$l_{A\uparrow}$	d_A	L_{n-A}	l_A	$l_{A\uparrow}$	d_A	L_{n-A}	l_A	$l_{A\uparrow}$	d_A	L_{n-A}
1	14.8	7.5	2.0	4	22.8	11.5	3.6	7	34.3	17.2	4.3	10
2	14.3	7.1	1.6	4	23.9	12.0	3.7	9	35.2	16.7	5.0	13
3	13.4	6.8	2.0	4	24.9	12.5	3.3	7	34.4	16.7	4.9	11

Table 7. Parameters of tearing zone and the thread number in the tearing zone for the model broken twill 2/2 V4 cotton fabrics

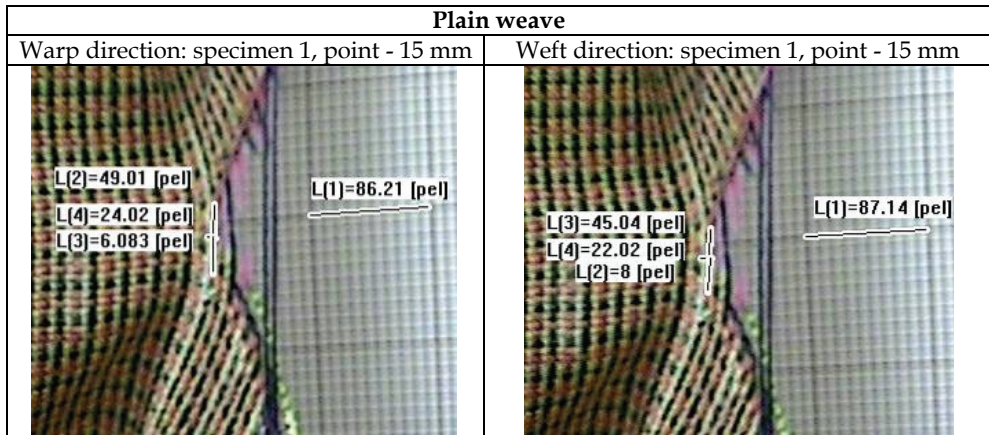


Fig. 7. The fabric images of tearing zone registered in the measurement point 15 mm for the wing shape specimen for plain weave

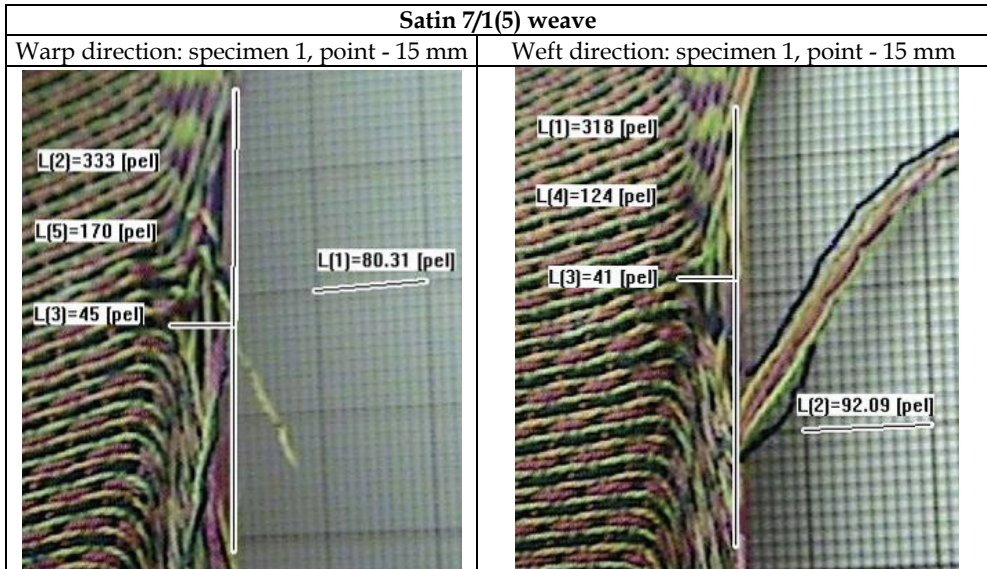


Fig. 8. The fabric images of tearing zone registered in the measurement point 15 mm for the wing shape specimen for satin 7/1(5) weave

4. Analysis and modelling the fabric tearing zone geometry

4.1 Analysis of fabric tearing zone geometry parameters

The graphic presentation of obtained results of the thread number in the tearing zone as well as the mean values of length and depth of zone dependably on the fabric weave, the torn arrangement (warp/weft) and tearing distance are shown in Fig. 9, 10 and 11.

The analysis of presented photos allows drawing out the following conclusions:

1. The smallest changes and at the same time the lowest values of length and depth of tearing zone as well as the thread number in the tearing zone dependably on the tearing distance were observed for zones registered for plain fabrics. The torn thread system (warp/weft) does not influence significantly the changes of mentioned parameters. An analysis of movies presenting the plain fabric tearing showed that in the assumed in measurements the maximum specimen length distance 15 mm there are many zones, in which there are the most often one thread. When it is broken, the next tearing zone is started to create. The threads in the plain fabric are displaced insignificantly. It is worth to remind (Tab. 3) that the obtained mean values of tear forces for plain cotton fabrics are on the lowest level in the comparison to the rest fabrics of different weaves.

The obtained values of plain cotton fabric tear resistance and carried out observations of tearing zones confirmed the Teixeira's et al. (Teixeira et al., 1955), Hamkins's and Backer's (Hamkins & Backer, 1980) also Scelzo, Backer's, Boyce's (Scelzo et al., 1994b) conclusions that for fabrics of higher number of interlacements (on the assumed tearing distance) the value of tear force and also of tearing zone parameters are the lowest ones.

In Fig. 12, there are shown the torn (on the distance of 15 mm) plain cotton fabric specimens. In the place of tearing the sample deformation is not observed, the successive threads on the tearing distance are broken.

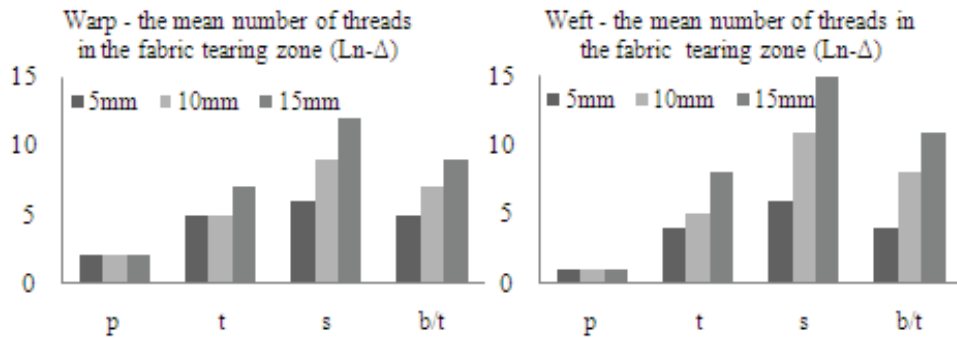


Fig. 9. The mean number of threads in the cotton fabric tearing zone ($L_{n-\Delta}$) dependably on the weave, torn thread system (warp/weft) and the tearing distance

where: p, t, s, b/t are symbols of cotton fabric: plain, twill 3/1 (Z), satin 7/1 (5), broken twill 2/2 V4;

$L_{n-\Delta}$ is the mean thread number in the fabric tearing zone;

5, 10, 15 are symbols of specimen measurement points successively on 5-th, 10-th and 15-th millimeter of tearing distance.

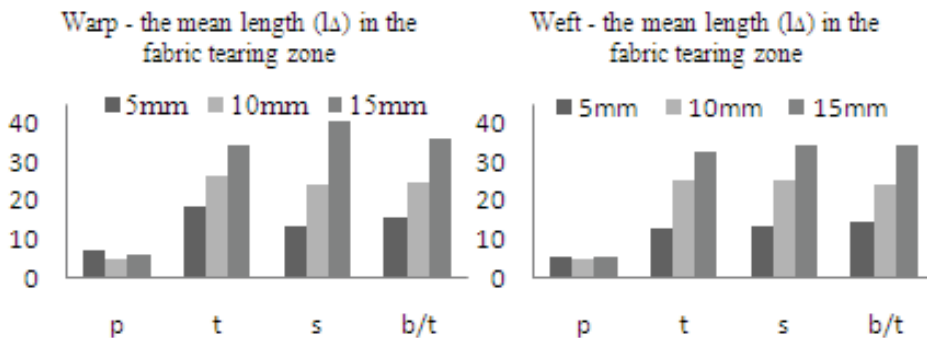


Fig. 10. The mean length (l_{Δ}) of tearing zone dependably on the fabric weave, torn thread system (warp/weft) and the length of tearing distance

where: p, t, s, b/t are symbols of cotton fabric: plain, twill 3/1 (Z), satin 7/1 (5), broken twill 2/2 V4,

l_{Δ} is the mean length of tearing zone, in mm,

5, 10, 15 are symbols of specimen measurement points successively on 5-th, 10-th and 15-th millimeter of tearing distance.

2. Mean values of length and depth of tearing zones registered for twill 3/1 Z, satin 7/1 (5) and broken twill 2/2 V4 fabrics increase in the torn thread system with the increase of tearing distance. But in the area of given measurement points (5, 10, 15 mm) these lengths are smaller dependably on the weave change and these changes concern the mean tearing zone length. The observation of images of specimen tearing allow stating that the increase of

length and depth of tearing zone of mentioned weaves is caused by the graduated process of zone formation, i.e., in the last measurement point (15 mm). Such a way of tearing zone formation results from the bigger possibility of thread displacement in fabrics of weaves with the smaller number of interlacements (Fig. 10 and 11) than the plain weave has.

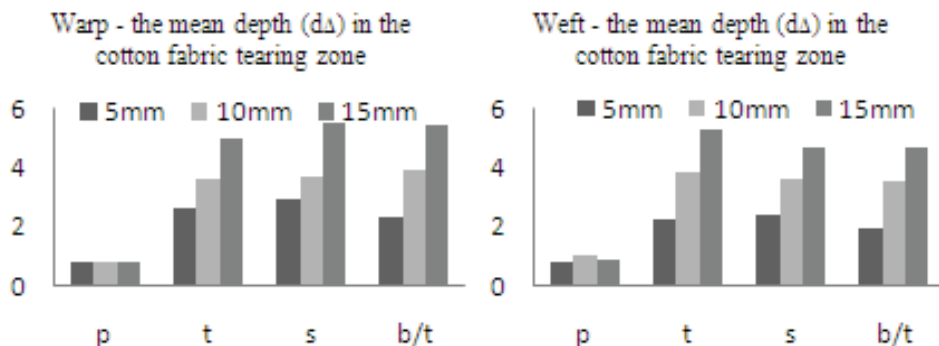


Fig. 11. The mean depth (d_{Δ}) of tearing zone dependably on the fabric weave, torn thread system (warp/weft) and the length of tearing distance

where: *p*, *t*, *s*, *b/t* are symbols of cotton fabric: plain, twill 3/1 (Z), satin 7/1 (5), broken twill 2/2 V4,

d_{Δ} is the mean of depth of tearing zone, in mm,

5, 10, 15 are symbols of specimen measurement points successively on 5-th, 10-th and 15-th millimeter of tearing distance.

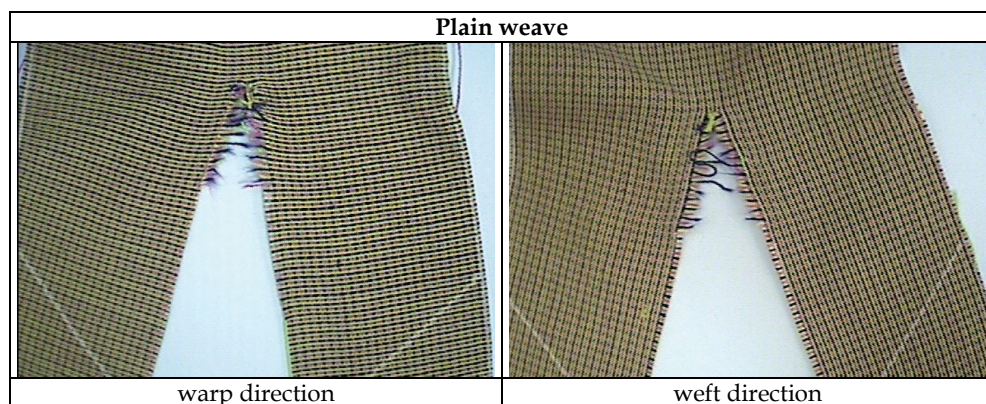


Fig. 12. The wing shape specimens of plain fabrics torn on the measurement distance 15 mm
Source: own

3. The analysis of results of mean tear force of fabrics of proposed weaves showed that in the warp as well as weft direction the highest mean values of tear resistance were obtained for fabric of satin 7/1 (5) weave. But the mean values of length and depth of tearing zone for fabric samples of this weave in the given measurement point only in two cases, i.e., warp system - measurement point 15 mm, and weft system - measurement point 10 mm (Fig. 10

and 11) are a little higher than analogous values for twill and broken twill samples. It can be explain in the following way:

3.1 Observation of graphs $F_r=f(L_r)$ (Fig. 13).

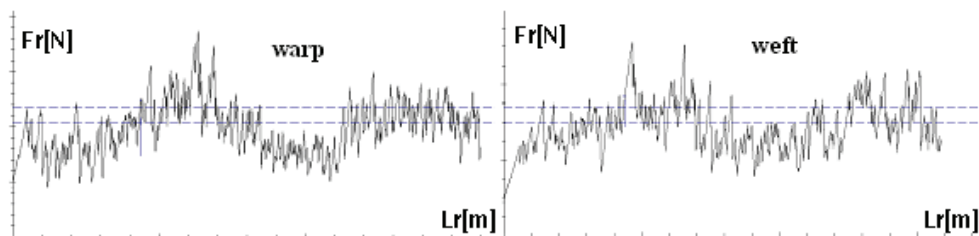


Fig. 13. The example of cotton fabric of satin 7/1 (5) weave tearing process graphs

Source: own

The local values of tear forces (F_r) of satin 7/1 (5) fabric registered on the tear distance (L_r), are characterized by a big variability. Moreover, the highest values of local tear forces are observed the most often from the tearing distance about $\frac{1}{4}$ of chart, i.e., about 40 mm. Therefore, the highest local values of tear forces, and at the same time - the highest values of length and depth of tearing zone are observed in the assumed observation points (5, 10, 15 mm).

3.2 Observation of torn fabric samples of the following weaves: twill 3/1 Z, satin 7/1 (5) and broken twill 2/2 V4 (Fig. 14).

Analyzing the obtained images it can be noticed a strong deformation of torn fabric specimens of mentioned weaves - the bigger than in the case of deformation of plain fabric sample. Particularly visible it is for satin fabric samples 7/1(5). The successive threads on the tearing distance are not broken, they are only „pulled out” from the fabric sample (from many of them totally). It is caused by a fact that threads of fabric of this weave have a big possibility of displacement and it is difficult to achieve the so called „jamming point” (the point, in which fabric parameters and values of friction forces between threads of both systems enable the further mutual thread displacement in the torn samples. The force, which is necessary to pull out the single thread and in the further part of specimen the group of threads, is higher than the force necessary for breaking threads. From one side it explains very high tear resistance values for satin fabrics; and from the second one - it explains the variability of local tear forces on the tearing distance. The variability of local values of tear forces results from the variable number of pulled out threads from the fabric on the tearing distance. At the beginning of tearing process the number of pulled out threads increases, what causes the growth of local values of tear forces. If the tearing is continued, the first thread or a few first threads being on the tearing distance are pulled out from the fabric and the local values of tear forces will be lower. Next, on the tearing distance there are appeared the successive threads, which gradually are pulled out from the fabric and the local values of tear forces again start to rise. This process is repeated up to the end of tearing distance.

The described sample deformation during the tearing process is also observed, but in the lower extent in the twill and broken twill fabric samples. In the torn samples of mentioned weaves on the tearing distance there are visible the broken as well as „pulled out” from the fabric threads.

4. The highest number of threads in the tearing zone in the each measurement point as well as in the torn thread system (warp/weft) were observed for satin 7/1 (5) (Fig. 9).

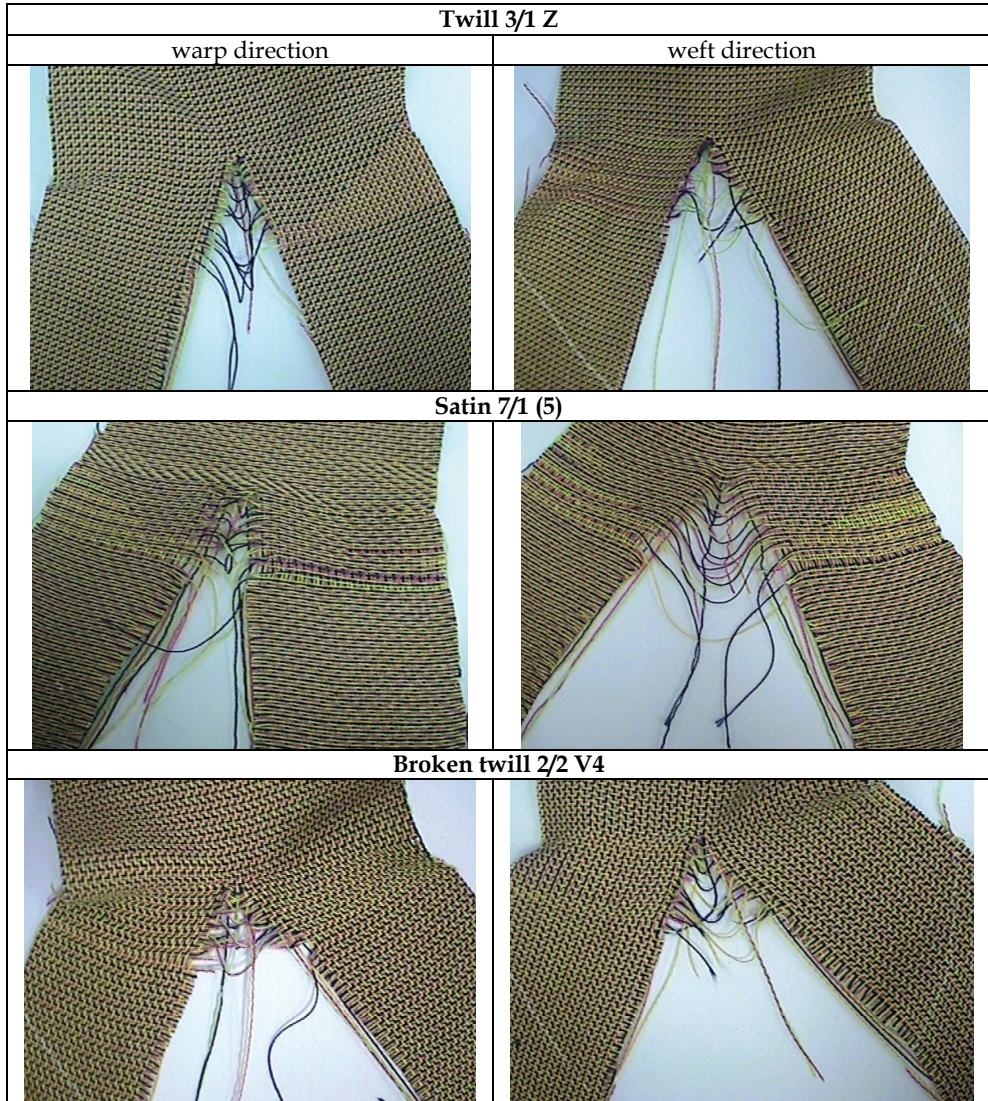


Fig. 14. The wing shape specimens of twill 3/1 Z, satin 7/1(5) and broken twill 2/2 V4 fabrics torn on the measurement distance 15 mm

Source: own

4.2 Modelling the shape of „arms” of tearing zone

In this chapter the process of modelling the shape of tearing zone was divided into two stages. In the first one in order to make a better visualization of sizes and to compare the

tearing zones of samples of four weaves in Fig. 15, there were set in the same scale the obtained values of parameter of fabric tearing zone for all the registered zones. The marked on the axes points, i.e., the depth of tearing zone d_A , length of tearing zone $l_{A\uparrow}$ [length $l_{A\uparrow}$ is the length measured from the abscissa $x-x$ (axis going through the point determining the depth of tearing zone) up to the end of the marked length of tearing zone $l_{A\cdot}$] and the length difference $l_{A\cdot} - l_{A\uparrow}$ were connected by the straight lines.

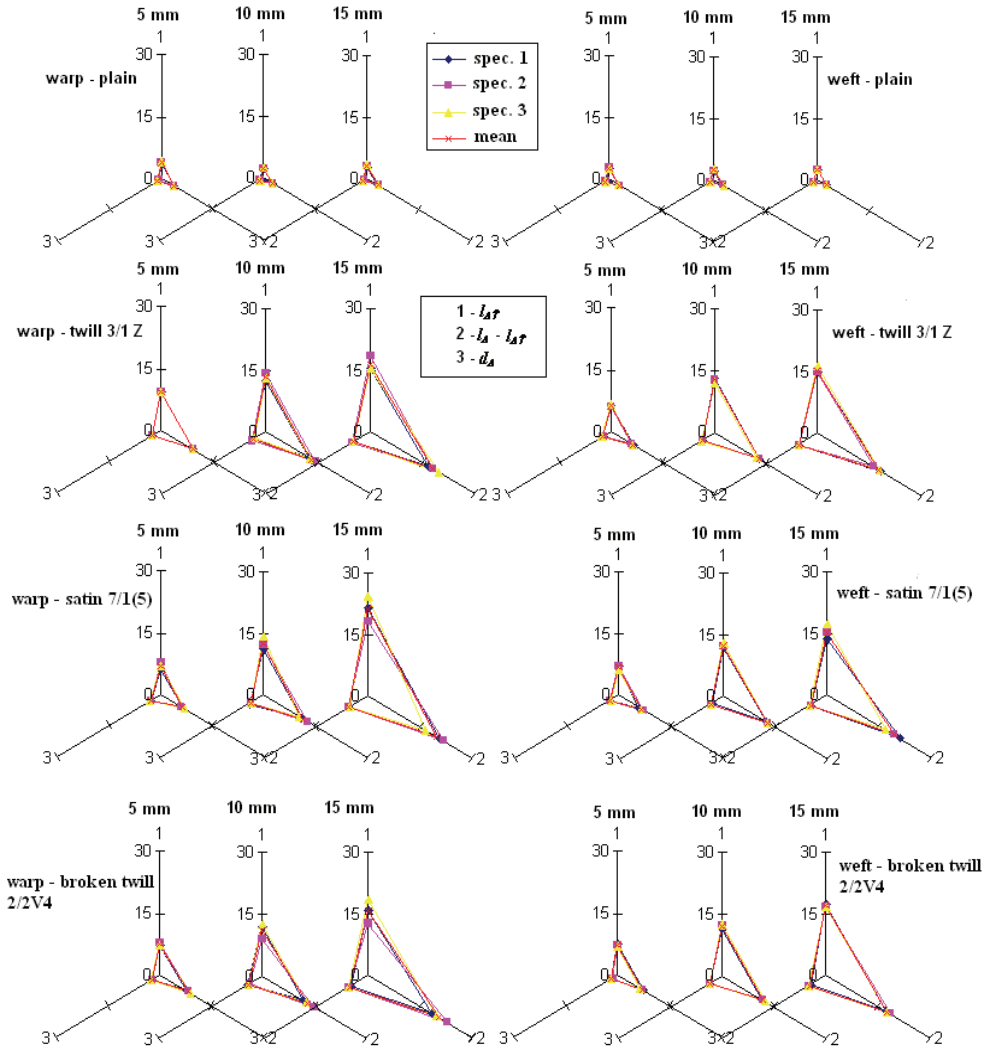


Fig. 15. The size of fabric tearing zone dependably on the fabric weave, torn thread system (warp/weft) and measurement point

The schematic presentation of fabric tearing zones enabled to notice the following observation:

- disproportions between the size of tearing zones dependably on the torn fabric weave;
- insignificant differences between the sizes of tearing zones in the given weave dependably on the given thread system (warp/weft);
- small variability of obtained length and depth for three specimens measured in the thread system (warp/weft);
- symmetry of tearing zone ($l_{\Delta} - l_{\Delta\uparrow} = \frac{1}{2} l_{\Delta}$) according to abscissa $x-x$ going through the point determining the zone depth for torn fabric specimens of the following weaves:
 - plain in the all measurement points for the thread system (warp/weft);
 - twill 3/1 Z for the measurement points (5 and 10 mm) for the thread system (warp/weft);
 - broken twill 2/2 V4 for the measurement point 5 mm for the weft direction;
- a lack of symmetry of tearing zone ($l_{\Delta} - l_{\Delta\uparrow} \neq \frac{1}{2} l_{\Delta}$) in the relation to the abscissa $x-x$ for the rest variants of torn specimens. The biggest differences between the values $l_{\Delta\uparrow}$ and $\frac{1}{2} l_{\Delta}$, i.e., differences ≥ 1 mm were calculated for the tearing zones of fabrics of the following weave:
 - satin 7/1 (5): warp thread system – measurement point (10 and 15 mm), weft thread system – measurement point 15 mm;
 - broken twill 2/2 V4: warp thread system – measurement point (10 and 15 mm).

In the second stage of modelling process of the shape of fabric tearing zone, speaking more precisely the shape of zone “arms” there was assumed the following procedure:

1. In the theoretical considerations carried out (Witkowska, 2008) it was shown that the shape of tearing zone, which was formed in the both system threads the jamming point can be described by an exponential function. Therefore, the shape of “arms” of tearing zone observed on the static images presenting the tearing zones in three measurements points were also described by the exponential function:

$$y = A \exp(-Bx) + C \quad (6)$$

where: A , B and C are the constant of exponential function;

y is a value of half length of fabric tearing zone;

x is a value of depth of fabric tearing zone.

2. Modelling the shape of tearing zone „arms” was carried out for the described weaves for zones registered in the measurement point 15 mm and for the given thread system (warp/weft) for specimen No. 3. On the basis of analysis of static images of tearing zones it was assumed that the constant $C=0$.

3. In each weave variant and torn thread system (warp/weft) for calculating the constant values A and B two pairs of points (x, y) were used, i.e.:

$$(x_1, y_1) = G(0, 0, l_{\Delta\uparrow}) \quad (7)$$

$$(x_2, y_2) = E(\frac{1}{2}d_{\Delta}, l_{\Delta\uparrow e}) \quad (8)$$

where:

$l_{\Delta\uparrow}$, d_{Δ} , $l_{\Delta\uparrow e}$ are the values of tearing zone parameters read out from the static images shown in the Fig. 16.

4. The appropriate modelled curves describing the tearing zone „arms” should go through the point:

$$(x_3, y_3) = D(d_{\Delta}, 0, 0) \quad (9)$$

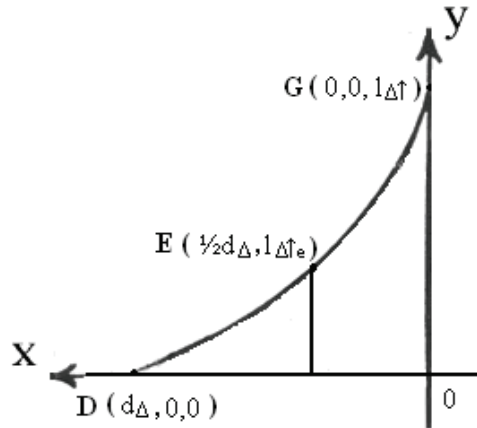


Fig. 16. The way of reading out the measurement points for modelling the fabric tearing zone „arms”

Source: own

Example:

The tearing zone “arm” shape was described for sample No. 3 made of twill 3/1Z for the warp thread system (the measurement point 15 mm).

Data: $l_{\Delta} = 6.5$ mm, $l_{\Delta \uparrow} = 3.3$ mm, $d_{\Delta} = 1.0$ mm.

$(x_1, y_1) = G(0.0, 3.3)$; $(x_2, y_2) = E(0.5, 0.2)$

Introducing the values x_1, y_1 into the equation 6 the value of constant A was calculated:

$$3.3 = A \exp(-B \cdot 0) \rightarrow A = 3.3 \quad (10)$$

Introducing the values x_2, y_2 and the value of constant A into the equation 6 the value of constant B was calculated:

$$0.5 = 3.3 \exp(-B \cdot 0.2) \rightarrow B = -5.61 \quad (11)$$

Introducing the values of constant A and B into the equation 6 the exponential equation for the following form was obtained:

$$y = 3.3 \exp(-5.61x) \quad (12)$$

Equation 12 describes the shape of tearing zone “arms” (in the first quarter of coordinate system x - y) for plain fabric in the case, when the warp was the torn thread system, and the observation point was on 15-th mm of tearing distance. The curve described by the equation 12 goes through the point $(x_3, y_3) = D(1, 0, 0)$ determining the depth of tearing zone (Fig. 17). Applying such a procedure the A and B constants of exponential functions describing the tearing zone „arm” shape for the rest fabric weaves were determined. In Table 8, there are set the values of point coordinates $(x_1, y_1, \text{ and } x_2, y_2)$ necessary for determination A and B constants of exponential functions and coordinate values (x_3, y_3) determining the depth of tearing zone. In Fig. 17, there are set the chosen curves describing the “arm” shape of tearing zone of examined fabrics and presented equations of the exponential functions describing these curves.

Weave / torn system / measurement point 15 mm, specimen No. 3								
Coordinates	plain		twill 3/1 Z		satin 7/1 (5)		broken twill 2/2 V4	
	warp	weft	warp	weft	warp	weft	warp	weft
(x ₁ , y ₁)	(0.0, 3.3)	(0.0, 2.6)	(0.0, 16.5)	(0.0, 16.4)	(0.0, 21.2)	(0.0, 17.2)	(0.0, 18.5)	(0.0, 16.7)
(x ₂ , y ₂)	(0.5, 0.2)	(0.5, 0.2)	(2.5, 1.4)	(2.6, 1.2)	(2.8, 1.8)	(2.4, 1.6)	(2.8, 1.6)	(2.5, 1.5)
(x ₃ , y ₃)	(1.0, 0.0)	(0.9, 0.0)	(5.0, 0.0)	(5.2, 0.0)	(5.5, 0.0)	(4.7, 0.0)	(5.6, 0.0)	(4.9, 0.0)

Table 8. The set of values of coordinates points necessary for calculation of A and B constants of exponential functions describing the shape of „arms” of fabric tearing zone

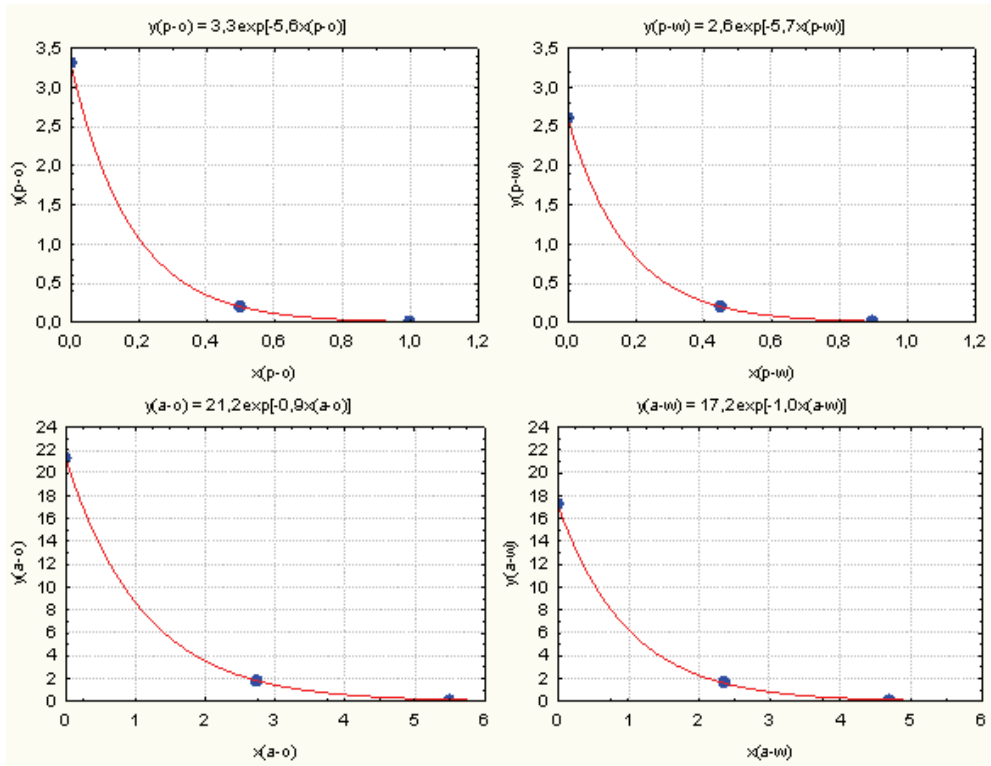


Fig. 17. Set of „arms” of fabric tearing zones of plain and satin 7/1 (5) weaves dependably on the torn thread system (warp/weft) for the measurement point 15 mm (specimen No. 3)

- where:
- $p-o$ - warp system of plain fabric,
 - $p-w$ - weft system of plain fabric,
 - $a-o$ - warp system of satin 7/1(5) fabric,
 - $a-w$ - weft system of satin 7/1(5) fabric,
 - y - $1/2$ of length of tearing zone (symbol l_A , Fig. 5),
 - x - depth of tearing zone (symbol d_A , Fig. 5),
 - exp i.e., an exponential function of basis e , of natural logarithm.

5. Summing up

5.1 The theoretical considerations on the static tearing process stages were confirmed by an experiment. It was enabled by the digital analysis of video images of fabric sample tearing. The image analysis was a very powerful measurement tool used for an identification purpose as well as for measurement of changes in the fabric structure in time due to the force acting.

5.2 The designed stand of computer image analysis, with the use of which the cotton fabric tearing was registered, aided the process of fabric phenomenon identification. The elaborated methodology enables the measurement of changes in the fabric structure in time. The additional advantage is its universality, i.e., the possibility of adapting its elements (video camera and *MicroStudio Video* software) for registration and analysis of the other phenomena. Additionally, *MicroStudio Video* software is a good tool for the result presentation. Moreover, the advantage of presented system for the computer image analysis is its multi-functionality. It can be also used for the reconstruction and measurements of changes during the other tensile destructive measurements like strength measurements and for the observation, for example, the flammability or wetting processes.

5.3 The registration of fabric tearing process and analysis of obtained static images helped to describe the parameters of fabric tearing zone such as: the length and depth of tearing zone and the number of threads in this zone.

5.4 The significant influence of fabric weave on the size of fabric tearing zone is observed. With the drop of interlacement number in the fabric, the increase of cotton fabric tear strength is observed. The lower number of interlacements causes the lower number of so called "pseudo-jammings" between the threads and in the same way, it enables the thread displacement and deformation. Simultaneously, the deformation of torn fabric specimens of weaves with the small number of interlacements is observed. Modelling the shape of "arms" of cotton fabric tearing zones showed that the "arm" shape can be described by an exponential function.

6. Acknowledgements

This work has been supported by: European Social Fund and Polish State in the frame of "Mechanism WIDDOK" programme (contract number Z/2.10/II/2.6/04/05/U/2/06); and the Polish Committee for Scientific Research, project no 3T08A 056 29.

7. References

- Harrison, P. (1960). The tearing strength of fabrics. Part I: A review of the literature, *Journal of Textile Institute* 51, T91-T131.
- Hamkins, Ch. P. & Backer, S. (1980). On the Mechanisms of Tearing in Woven Fabrics, *Textile Research Institute*, May, 323-327.
- Hager, O. B.; Galiardi, D. D. & Walker, H. B. (1947). Analysis of Tear Strength; *Textile Research Journal*; July, 376-381.
- Krook, C. M. & Fox, K. R. (1945). Study of the tongue tear test, *Textile Research Journal*, No. 11, 389-396.

- Scelzo, W. A.; Backer, S. & Boyce, C. (1994a). Mechanistic role of yarn and fabric structure in determining tear resistance of woven cloth - Part I: Understanding tongue tear, *Textile Research Journal*, Vol. 64, No. 5, 291-304.
- Scelzo, W. A.; Backer, S. & Boyce, C. (1994b). Mechanistic role of yarn and fabric structure in determining tear resistance of woven cloth. Part II: Modelling tongue tear, *Textile Research Journal*, Vol. 64, No. 6, 321-329.
- Teixeira, N. A.; Platt, M. M. & Hamburger, W. J. (1955). Mechanics of elastic performance of textile materials: Part XII: Relation of certain geometric factors to the tear strength of woven fabrics, *Textile Research Journal*, No. 10, 838-861.
- Taylor, H. M. (1959). Tensile and tearing strength of cotton cloths, *Journal Textile Research*, Vol. 50, T151-T181.
- Letters to the Editor (1974). Modified Tearing Model, *Journal of the Textile Institute* 65, No 10, 559-561.
- Witkowska, B. & Frydrych, I. (2004). A Comparative analysis of tear strength methods, *Fibres & Textiles in Eastern Europe*, Vol. 12, No 2(46), 42-47.
- Witkowska, B. & Frydrych, I. (2005). Protective clothing - test methods and criteria of tear resistance assessment, *International Journal of Clothing Science and Technology (IJCST)*, Vol. 17, No 3/4, 242-252.
- Witkowska, B. & Frydrych, I. (2008). Static tearing. Part II: Analysis of stages of static tearing in cotton fabrics for wing - shaped test specimens, *Textile Research Journal*, 78, 977 - 987.
- Witkowska, B. (2008). Modelling of the cotton fabric static tearing, Doctoral dissertation Technical University of Lodz, Poland.

Effects of Topographic Structure on Wettability of Woven Fabrics

Alfredo Calvimontes¹, M.M. Badrul Hasan² and Victoria Dutschk³

¹*Leibniz Institute of Polymer Research Dresden*

²*Institute of Textile Machinery and High Performance Material Technology, Dresden*

³*EFSM group, Faculty for Engineering Technology, University of Twente, Enschede*

^{1,2}*Germany*

³*The Netherlands*

1. Introduction

Each surface is characterised by its chemical composition, a certain surface geometry and roughness. The interaction of liquids with textile fabrics may involve one or several physical phenomena such as fibre wettability, depending on the intermolecular interaction between the liquid and fibre surface, their surface geometry, the capillary geometry of the fibrous assembly (Hasan et al., 2008), the amount and chemical nature of the liquid as well as on external forces. A rough textile surface possesses pores, crevices, capillaries or other typical structures with their own characteristic wetting and penetration properties. As a consequence, the apparent contact angle on these surfaces will be affected by thermodynamics and kinetics associated with such intrinsic structures.

Fabric texture affects the porosity and strongly influences the textile characteristics such as fabric mass, thickness, draping ability, stress-strain behaviour, or air permeability (Potluri et al., 2006; Milašius et al., 2003; Kumpikaitė, 2007). The surface topography of fabrics is responsible for their functionality - appearance and handle, wettability, soiling behavior and cleanability (Calvimontes et al., 2005), abrasion resistance and wear (Dutschk et al., 2007). However, there are very few systematic investigations of quantitative relations between construction parameters, topography of fabrics and their wettability.

One technique that has been extensively used for studying the wetting properties of solid surfaces, is dynamic wetting measurements. Calvimontes et al. (2005), demonstrated its utility in characterizing both textile materials and interactions between them and aqueous solutions of soil release polymers. Differences between the soiling behaviour and cleanability of three polyester textile materials with various topographical structures were determined despite the similarity of their chemical nature. In other studies (Calvimontes et al., 2005; Hasan et al., 2009), the usefulness of the application of a relatively new imaging technique based on the principle of chromatic aberration was shown in characterizing the surface of textile materials before and after impregnation with soil release polymers.

2. Textile topography

In almost all the studies cited above, a large number of roughness and waviness parameters were obtained that did not take into account the scales-morphologic periodicity of each

surface studied and its influence on the whole topography. All textile materials having periodic surfaces show some horizontal and vertical repeating units; therefore, different length scales have to be taken into account for a proper interpretation of the topographic data measured (Hasan et al., 2009; Calvimontes et al., 2009).

2.1 Topography measurements

Depending on fabric characteristics, and the structure and size of repeating units, several non-contact measurement methods such as chromatic with-light sensor (CWL) - also called chromatic confocal imaging-, high-resolution scandisk confocal microscopy (SDCM), scanning electron microscopy (SEM), confocal laser scanning microscopy (CSOM), conoscopic holography (CSL), etc. can be used.

In Calvimontes et al. (2009) CWL was used and recommended for the optical topographic analysis of textile materials. This instrument allows a lateral and a vertical measure range up to 100 mm and 380 μm , respectively, and a lateral and vertical resolution up to 1 μm and 3 nm, respectively. In Lukesch (2009) and Calvimontes (2009), the use of CWL to measure topography of textile surfaces was compared with the use of SDCM. According to these studies, wider cut-off lengths and larger z-ranges make CWL more appropriate than SDCM to measure topographic characteristics of polyester and cotton fabrics.

It is important to note, that the selection of a method due to its high resolution could be inadequate if the cut-off length available or z-range is too small. On the other hand, the use of a very high resolution and larger cut-off lengths (scan areas) results in data whose excessive size could demand extremely long calculation times and special or non-existent hardware and software.

2.2 Optimal sampling conditions

Cut-off length (L_m), defined as the length of one side of the square sampling area, and resolution (distance between measured points Δ_x , assuming that $\Delta_x = \Delta_y$) are the most important sampling parameters, which apart from particular instrumental dependent parameters, such as light intensity, measuring frequency, etc., have to be optimally defined before characterising topography.

Tsukada & Sasajima (1982) and Yim & Kim (1991), discussed the problem of an optimum sampling interval (L_m) by checking the variance of the root mean square roughness (R_q) for a surface under different sampling intervals. According to Stout et al. (1993), recommendation mentioned above for the choice of sampling interval is doubtful because of the fact that the optimum L_m seems to influence the amplitude parameters (wave height W_t and waviness W_z).

The use of tables that relate foreseen the mean rough height (R_z), root mean square roughness (R_q) and arithmetic mean roughness (R_a) with L_m is frequently recommended to set the optimal value of L_m for periodic as well as non-periodic surfaces. As optimal sampling conditions are strongly dependent on the type of material to be characterized, researcher experience is usually required. A systematic procedure to define optimal cut-off length and resolution values was proposed and probed in Calvimontes (2009).

2.3 Topographic characterization using different length scales concept

The use of a scale concept to characterize and study textile surfaces is a new skill that helps to correlate textile parameters, topography and topographical changes with interface

phenomena such as spreading, wetting, capillary penetration, and soil release (Calvimontes et al., 2007).

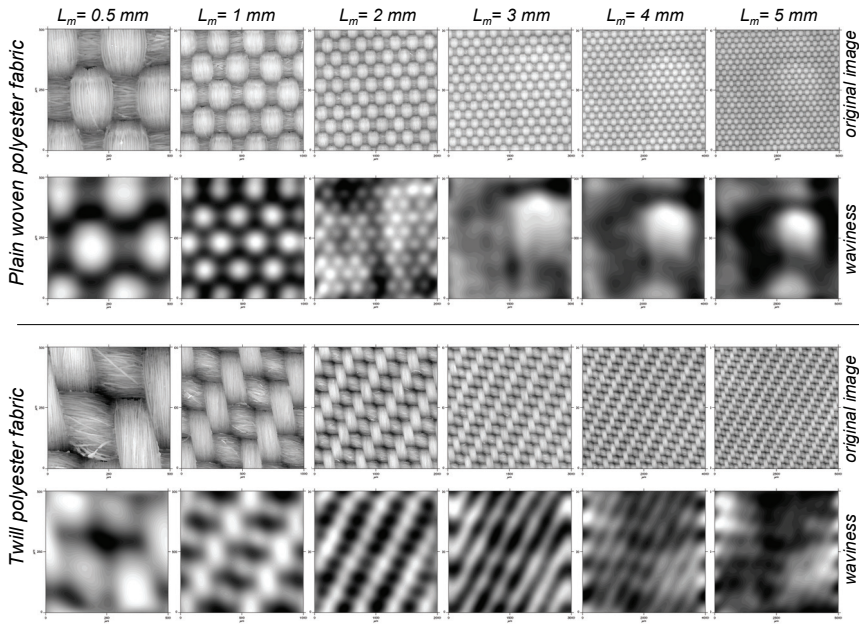


Fig. 1. Original and waviness images of polyester fabric surfaces as a function of L_m

As shown in Figure 1, waviness images obtained by Fast Fourier Transformation-filtering (FFT) (Raja & Radhakrishnan, 1979) provide different type of information depending on cut-off length used. Due to the structural diversity of textile materials, their classification by unit size and morphology on different length scales is necessary. A suggestion to find general range values of L_m in order to identify different measurable length scales is not reasonable. However, the specification of at least three different length scales (macro-, meso- and microscale) is absolutely necessary to describe morphologically homogeneous textile groups. From a conceptual point of view, each one of the length scales proposed for a textile structure has to provide specific information about the surface morphology and topometry of the materials.

Macro-morphological irregularities of textile surfaces such as folds and wrinkles can be studied using FFT-filtering of topographical data measured by large values of L_m . A cut-off length value larger than 3 mm was suggested by Calvimontes et al. (2009) to quantify plane irregularities (waves and wrinkles) of polyester fabrics.

Dimensional changes (relaxation/shrinkage) of fabrics at macro scale influence their meso- and micro-topography due to the modification of repeating unit dimensions and, therefore, distances between yarns, filaments and fibres.

In Figure 2 macro-waviness diagram alone for woven plain does not show any morphological influence of repetitive units (r.u.) morphology, in this case $r.u. > 13^2$. For macro-topographical characterization of twill and Panama types of weave, optimal L_m values have to be larger than 5 mm.

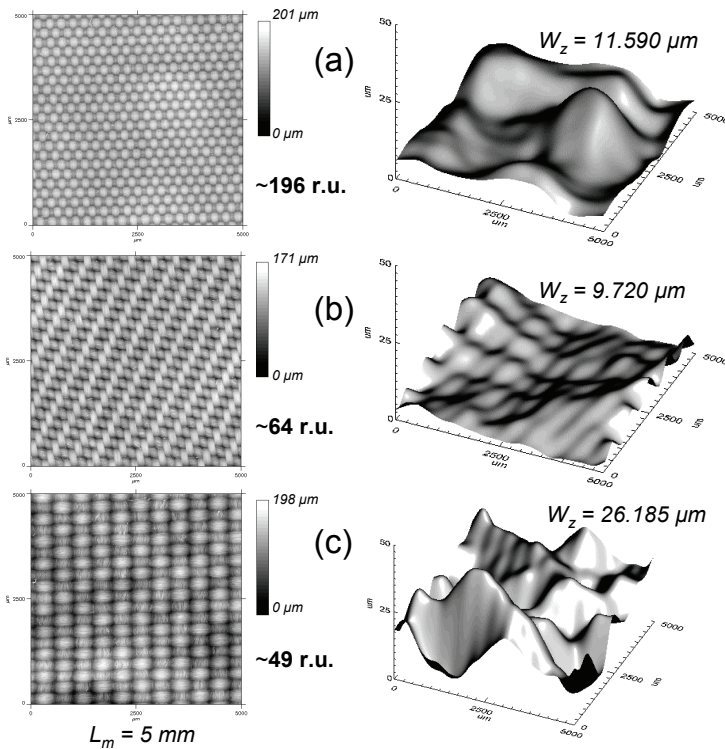


Fig. 2. 2D images (left) and 3D waviness diagrams (right) with W_z values for: (a) woven plain; (b) twill and (c) panama polyester fabrics.

Meso-scale of textile materials should be used to describe the surface topography produced by the type of weave and yarn used, without attending previous defined macro-topographic irregularities and details corresponding to fibres or filaments. A study of fabric surface topography at a mesoscopic scale using FFT-filtering starts with the selection of a new optimal L_m value, which basically depends on the size of fabric repeating unit. From a large amount of experimental data for polyester fabrics studied, it was revealed that a sample area ($L_m \times L_m$) has to cover about 8 repetitive units (Calvimontes et al. 2009).

Another way to construct meso-topographic diagrams is the use of digital surface filtering, which calculates the arithmetical mean of each data point with its neighbourhood (Stout et al., 1993). Filter density used depends on fabric characteristics and has to be able to produce a surface without topographical details of fibres or filaments. Figure 3 shows the construction of meso-topographic surfaces by using FFT-filtering and Smooth filtering. In order to compare morphologies and W_z values obtained, L_m and filtering method used should be remained the same during the characterisation process.

An application of the study on meso-scales claims to know relative z-distances between warps and wefts for woven fabrics and the amplitude of their wave (sinoidal) trace. As shown in Figure 3, wefts describe almost a linear trace (their amplitudes are small). As a consequence, the first contact of any solid with the fabric surface takes place by the warps (“hills”) and the final penetration of fluids into the fabric surface takes place principally on

wefts (“valleys”). This finding plays a crucial role in understanding the wetting behaviour of textile materials (Calvimontes et al. 2007).

Unlike macro- and meso-scales, characterisation at a micro-length scale reveals the influence of filaments and fibres characteristics on the resulting topography. Profile, fineness, as well as natural or machined texture of these elements or distances between them are only some of possible characteristics which define the resulting morphology and topometry at this length scale.

The selection of an optimal cut-off length in this case no longer depends on some statistical or mathematical criteria as seen at macro and meso length scales, rather on the size and location of the set of filaments or fibres by type and orientation.

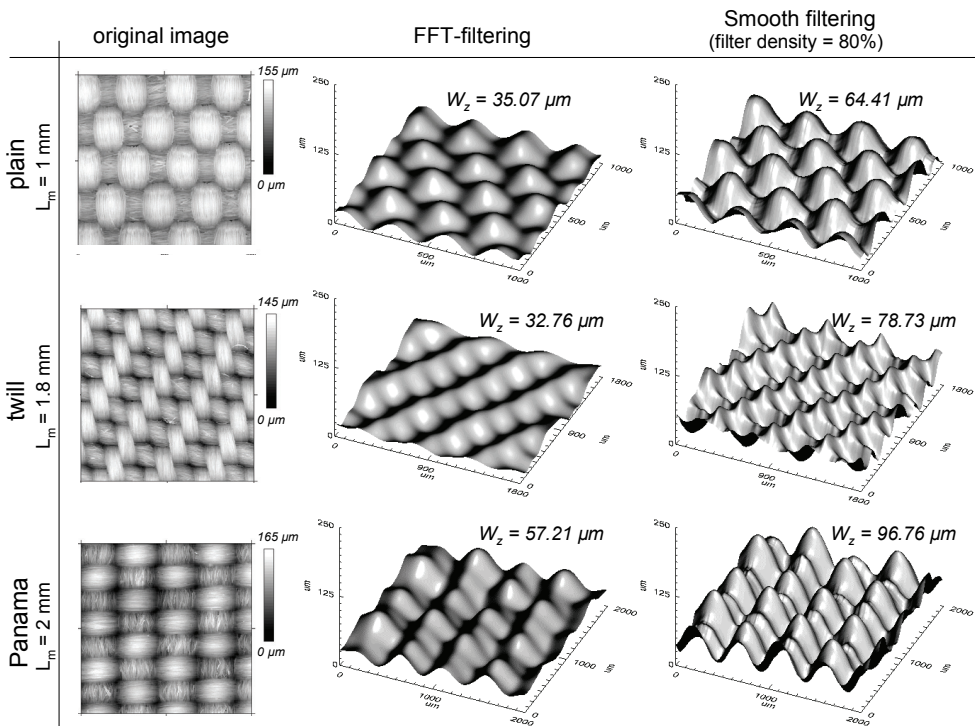


Fig. 3. Meso-topography of different polyester fabrics by FFT filtering and smooth filtering

To study the micro-topography of woven plain fabrics, warps and wefts should be zoomed separately. Optimal L_m values of warps and wefts depend on the type of weave and construction parameters such as yarn types, their diameters, warp densities, weft densities, etc. Depending on the textile structure, more than one L_m value could be necessary for a complete micro-topographical characterisation, as shown in Figure 4.

The number of sub-areas to be isolated depends on topographical parameters studied and on standard deviations of their mean values. Usually, five different zooms should be enough to characterise polyester monofilament fabrics. Depending on the characterization criteria, the elimination of micro-waviness, a consequence of yarn profile and fabric meso-topography, is possible by FFT-filtering, as shown in Figure 5.

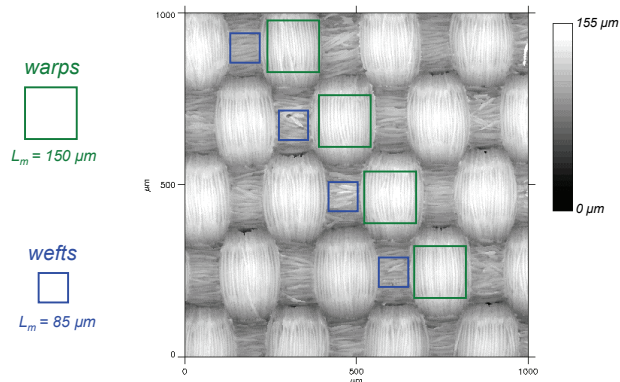


Fig. 4. Optimal L_m values for the characterisation of warps and wefts micro-topography separately at the surface of woven plain polyester fabric.

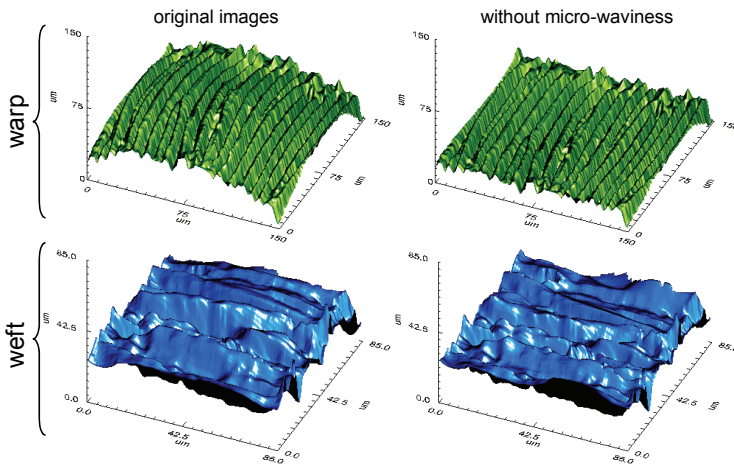


Fig. 5. Micro-topographical images of a warp and a weft. The elimination of micro-waviness was possible by FFT-filtering

Using the new topographical data generated, it is possible to calculate any micro-topographical parameter by profiling or by using the whole surface. The volumetrical characterization is a good tool to measure textile surfaces through evaluating of porosity or filling quantities at different deep heights. Fractal dimension or Wenzel roughness factor could be of interest to characterize micro-topographical modifications of natural fibres, e.g. changes caused by plasma or enzymatic action.

3. Influence of topography on wettability of textile structures

One technique that has found extensive use in studying the wetting properties of solid surfaces is dynamic wetting measurements. Seven different cases of connection between topography and wetting of textiles will be described in following pages. In all of them,

dynamic wetting measurements were carried out by a FibroDAT 1122 HS dynamic contact angle tester (Fibro System, Sweden). Some advantages of this equipment over other contact angle measuring systems as well as the measuring procedure have been detailed by Dutschk et al. (2003).

3.1 Type of weave and construction parameters



Hasan et al. (2008) studied the influence of the type of weave on topography and wettability of polyester fabrics produced using multi-microfilament yarn with different filament structures with filament diameter being between 6 and 7.5 μm . The characteristics of yarns used are summarised in Table 1. Two basic types of weaves - plain (1/1) and twill (2/2 Z) - were produced by variation yarn combinations and the weft density without changing the warp density. After the manufacturing, the fabrics were desized under laboratory conditions raising the primary fabric density. The composition of each sample are detailed in previous studies (Calvimontes et al., 2006).

Yarn	Number of filaments	Structure	Filament fineness, dtex ¹	Filament diameter, μm	Yarn fineness, dtex ¹
A	128	flat	0.78	6.0	9.9
B	128	textured, tangled	0.92	7.5 ²	11.5
C	256	false-twist textured	0.78	6.5 ²	16.3
D	384	textured, tangled	0.67	6.5 ²	24.6

¹ Measured according to DIN EN ISO 1973:1996; ² before texturing.

Table 1. Characteristics of the multi-microfilament yarns used by Hasan et al. (2008)

Relevant topographic characteristics obtained from the fabrics are given in Table 2. Comparing the macroscopic roughness parameters for different types of weave, it was ascertained that a decrease occurs for the plain weave and an increase for the twill weave if the weft density increases. Fabric density calculated according to Walz & Luibrand (1947), is inversely proportional to air permeability (for the same weft yarn) measured, as expected, and the results are summarized in Table 3. This nearly linear relationship is independent of the fabric texture, contrary to the macroscopic roughness parameters as shown in Figure 6. An increase in weft density smoothes the surface waviness independently of the type of weave, as illustrated in Figure 7. The values of waviness are higher for the twill weave than for the plain weave with the same weft density.

Type of weave		Yarn variations					
		A-B		A-C		A-D	
		weft/cm*		weft/cm*		weft/cm*	
Plain		39	40	32	36	26	29
		43	46	36	40	30	32
Twill		50	54	42	47	35	38
		56	57	45	53	39	44

* Weft density is given for each sample before (above) and after desizing (below), respectively.

Table 2. Composition of polyester fabrics woven varying construction parameters (68 warps (cm))

Type of weave	Yarn composition/ weft density	Sample specification	Root mean square roughness, R_{qz} , μm	Mean peak to valley height R_{z} , μm	Porosity, $\mu\text{m}^3/\mu\text{m}^2$	Waviness, μm
Plain 1/1	A-B / 39	pB39	9.7	95.5	1.189	48.7
	A-B / 40	pB40	9.5	90.1	0.942	47.5
	A-C / 32	pC32	10.9	115.8	2.528	52.8
	A-C / 36	pC36	9.7	87.3	1.325	50.3
	A-D / 26	pD26	11.1	93.7	1.574	67.9
	A-D / 29	pD29	10.6	83.7	0.760	60.2
Twill 2/2 Z	A-B / 50	tB50	9.4	48.8	0.552	47.5
	A-B / 54	tB54	9.3	88.5	0.916	40.5
	A-C / 42	tC42	9.4	70.9	0.583	59.8
	A-C / 47	tC47	9.8	79.6	0.628	48.9
	A-D / 35	tD35	11.2	111.6	1.221	76.8
	A-D / 38	tD38	11.6	114.9	1.438	65.3

Table 3. Topographic characteristics obtained by means of CWL (chromatic white light sensor)

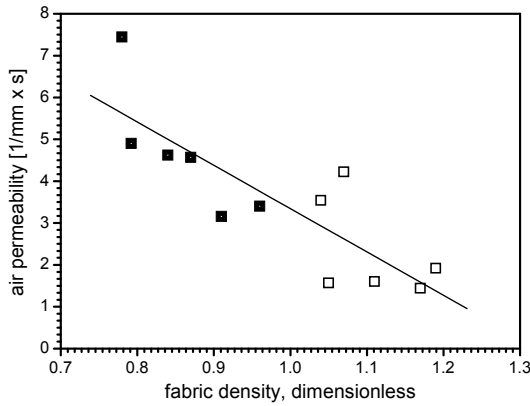


Fig. 6. Nearly linear relationship between fabric density calculated and air permeability measured: (□) plain and (■) twill weave

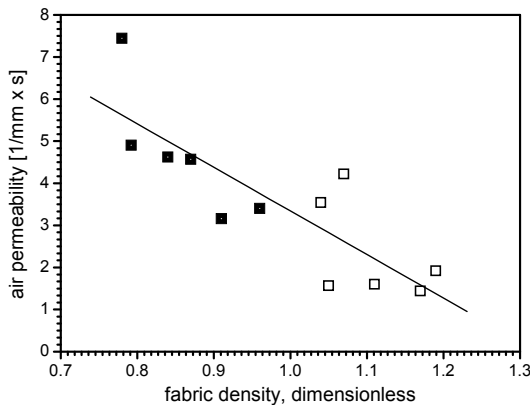


Fig. 7. Dependency of the waviness on the weft density for (□) plain and (■) twill weave

Variations in interlacing are also reflected in the fabric wettability considered in terms of the spreading rate as shown earlier (Calvimontes et al., 2006). The spreading rate decreased with increasing waviness for the plain weave, whereas it increased in the case of twill. It was concluded that the fabric wettability could be adjusted (in certain limits) by variation of density and interlacing, keeping in mind the same chemical nature of microfilaments.

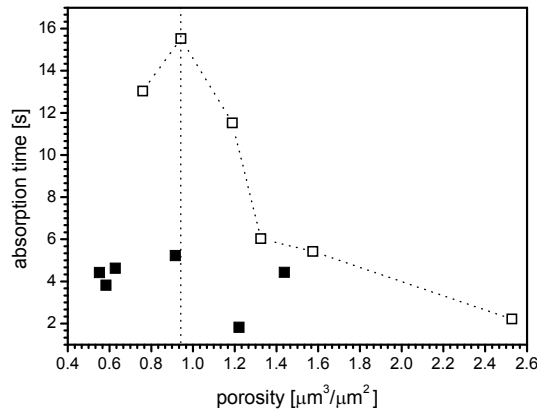


Fig. 8. Absorption time vs. surface porosity calculated as the ratio between the real pore volume and the corresponding geometric surface for (□) plain and (■) twill structures

Noticeable differences in the wetting behaviour of water were seen between the two types of weave, if changes in porosity are considered. In the case of the plain weave, higher weft density leads to lower porosity and, as a consequence, to higher water absorption time, as shown in Figure 8. Moreover, water penetration into the plain texture is slightly slowed down with increasing porosity, reaches a maximum value of the absorption time (about 16 s) in the porosity range of approximately $1 \mu\text{m}^3/\mu\text{m}^2$, and then accelerates towards the higher porosity values. It can be speculated about a “critical” value of the fabric’s porosity. Presumably, below this value water percolates with low velocity and above this with a high value. In contrast, the higher weft density of the twill weave results in higher porosity (cf. Table 2). The values of absorption time obtained for the twill texture are generally very low of about 2 – 5 s and are almost independent of the porosity, as illustrated in Figure 7.

The differences in the penetration behaviour of water observed on two predetermined patterns of interlacing are caused by the different topographical structure, since the chemical nature of filaments used was kept constant. It is noted, that the lateral distance between the threads is about 120 and 300 μm for the twill and plain weaves, respectively. The vertical dimension of the surface features is measured up to 20 μm for the plain topography and 40 μm for the twill topography. It is well known, that in the case of moderately hydrophobic surfaces the complex internal geometry of real porous systems could enhance liquid penetration (Bico et al., 2001). As reported earlier (Matsui, 1994), polyester is moderately hydrophobic with a water contact angle of 77° on its flat surface. The results obtained in the present study would suggest that water advanced in a stable flood (wicking regime) is observed (Kissa, 1996). The difference in the penetration behaviour (lower for the plain weave and faster for the twill weave) arises from the difference in the shape and size of the pores.

The same comments were applied in the relationship between air permeability and the absorption time in an earlier work (Calvimontes et al., 2006), where it was found that water penetration strongly depends on air permeability for the plain topography. It seems to be absolutely independent of this textile parameter for the twill structure, although no correlations between both characteristics air permeability and porosity were found.

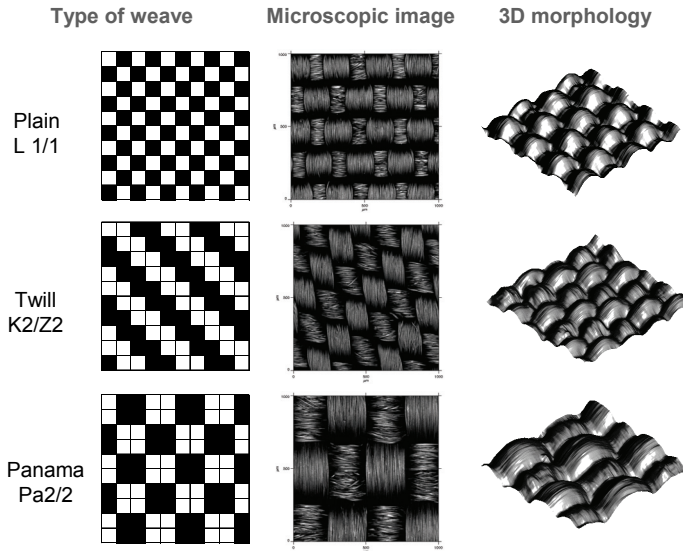


Fig. 9. Polyester fabrics used to study the influence of the type on weave on water spreading
 In essence, to achieve a more hydrophobic fabric texture, the technological parameters should be changed as follows: for both plain and twill structure, the weft density and filament fineness should be increased, and the yarn fineness should be reduced. In general, the plain weave with the yarn combination A-B and density of 46 wefts/cm (desized) shows the “best” wetting properties with the longest delay of penetration.

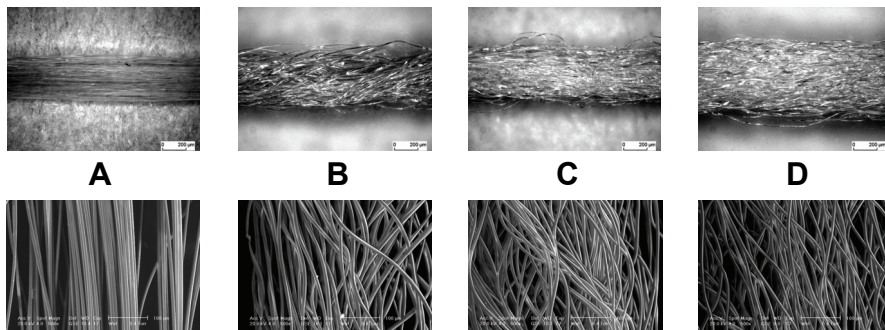


Fig. 10. Microscopic images of warp yarns (above) and filaments (below), according to parameters detailed in Table 1

Calvimontes et al. (2007) used 14 different polyester fabrics, having plain, twill and panama structures to show how the use of topographic characterisation at different scales can provide important information of the spreading behaviour.

Polyester fabrics of three different types of weave (Figure 9) were manufactured using filaments produced by spinning of the same polymer material (polyethylene terephthalate). Warp yarns were formed from flat filaments, while wefts were textured by three different processes (Table 1 and Figure 10).

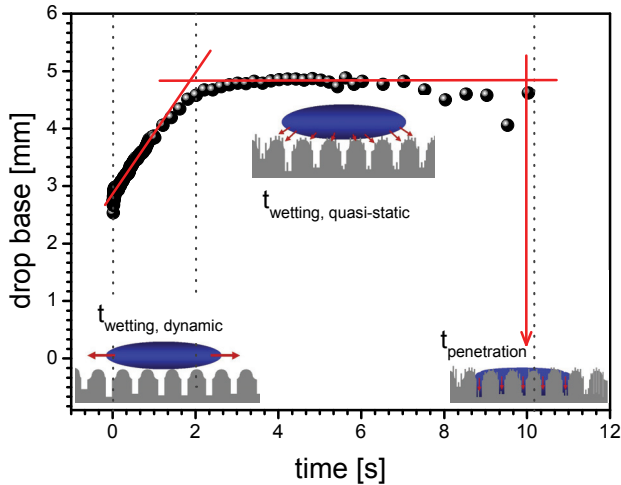


Fig. 11. Three different wetting regimes for a textile surface

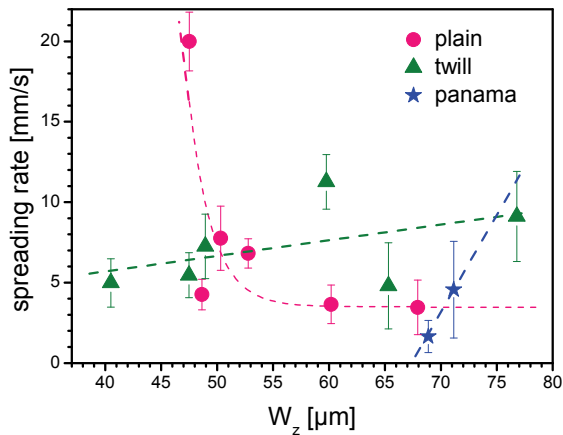


Fig. 12. Dynamic wetting: meso-morphology controls the spreading rate of a liquid drop on a textile structure

On the basis of macroscopic water drop base changes measured with a dynamic contact angle tester (Fibro DAT 1122, Fibro System, Sweden), the wetting behaviour of a water drop can be divided into three regimes (Figure 11): dynamic wetting, defined as growing of the drop diameter depending on time (also known as spreading), the quasi-static wetting, where the drop diameter remains approximately constant, and penetration, which is marked by liquid drop absorption into fabrics depending on time.

By using the waviness as a meso-topographical parameter, it is evident that the meso-topography of the fabrics controls the spreading rate of a liquid drop (Figure 12). For the plain weave, an increase of the waviness depth causes a decrease of the spreading rate; warp yarns (“hills”) slow down the liquid motion (Figure 13). For twill weave, an increase of the waviness depth causes formation of deep and long domains of weft yarns (“canals”) with small “islands”. As a consequence, an increase of the spreading rate is observed. Finally, for the panama weave, an increase of the waviness depth causes formation of long and quasi-endless (without “islands”) deep domains (“canals”). Consequently, the waviness depth and spreading rate are proportional to each other.

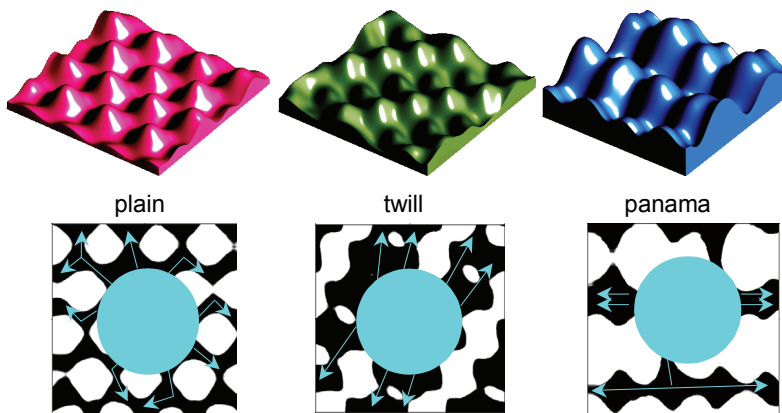


Fig. 13. Respective textile morphology at a meso-length scale controls the spreading rate. Above: morphology; below: spreading directions of a liquid drop

A thorough comparison between topographic parameters for 14 fabrics, having three different types of weaves, reveals that the respective morphology at meso length scale controls the spreading rate.

3.3 Yarns texture

By zooming of warps and wefts separately at a smaller scale, topography measurements and the characterisation concept at different length scales provide important information about changes in textile microstructures. Using this information, the behaviour of a liquid drop on fabrics, detailed in Tables 1 and 2, while wetting can be explained. On the basis of experimental results (Calvimontes, 2009), revealing differences for two basic types of woven fabrics - plain and twill - in respect to capillarity and water penetration (Figure 14), the concept of a novel wicking model was developed. This conceptual model was verified in respect to the cleanability behaviour of fabrics using paraffin oil and acetylene black soils.

Results illustrated in Figure 14 show: (i) warp yarns topography hardly affect the cleanability of fabrics; (ii) spaces between fibres make the plain weave surface oleophil (the larger they are, the more stain penetrate); (iii) spaces between fibres make the twill weave surface oleophob. The larger and deeper they are, the more stain penetrates and the worse their cleanability and (iv) the weft yarn roughness controls the hydrophobicity or hydrophilicity of fabrics and, as a consequence, their cleanability (cf. Figure 15).

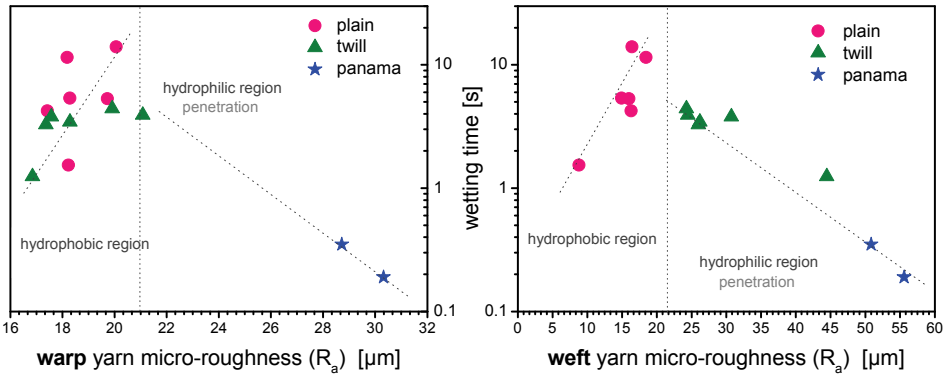


Fig. 14. Liquid flow in warp and weft directions occurs in two different regimes, depending on the micro-topography

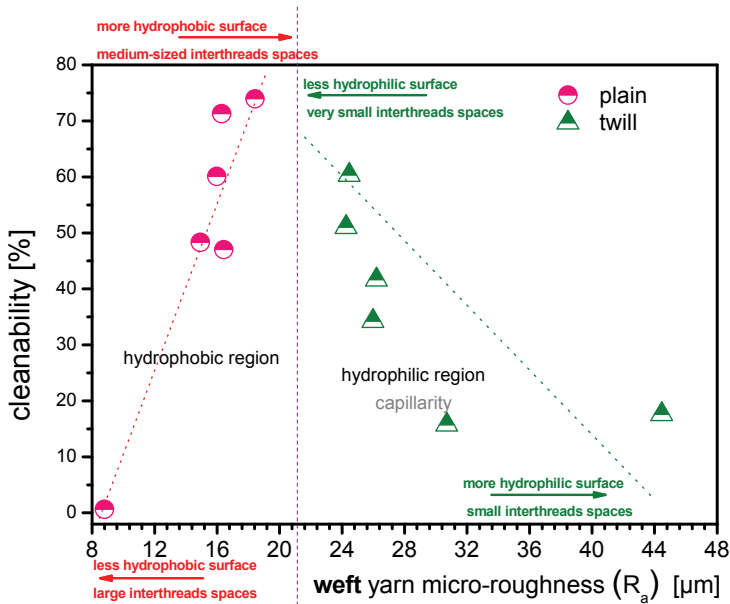


Fig. 15. The conceptual model proposed allows a better understanding of the cleanability phenomenon of polyester fabrics by using a different length scale concept for their characterisation. Soil material: paraffin oil and acetylene black in the ratio 97.98:2.02

3.4 Fibre cross sectional shape and the effect of heat-setting

Hasan et al. (2008), studied warp rib (2/2) fabrics (a derivative of the plain weave) produced using differently profiled polyester filaments – round and cruciform – in a melt-spinning process. The general manufacturing procedure is detailed by Hasan (2007).

Microscopic images of different cross sectional shapes of the fibre manufactured are shown in Figure 16. The fabrics were desized and treated by heat-setting at 190 °C for 10 s after being manufactured. Both modifications – desized with and without heat-setting – were discussed. Figure 17 illustrates different basic weaves used in this study.

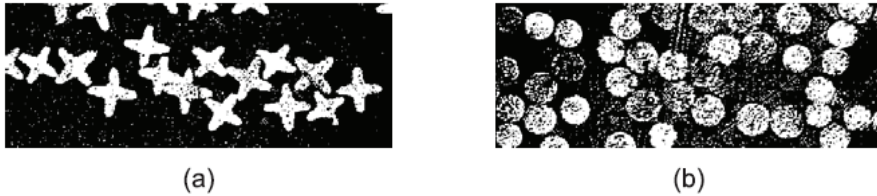


Fig. 16. Microscopic images showing different cross-sectional shapes of the polyester fiber manufactured: (a) cruciform; (b) circle-shaped

Geometric cover factor of the fabrics was calculated using their microscopic images as the ratio of the projected fabric surface area covered by yarns to the total fabric surface area given using the following equation (Sabit, A., 2001).

$$cf = c_w + c_f - c_w \cdot c_f$$

where c_w and c_f are the warp and weft cover factor, respectively. The warp cover factor is a product of the warp count and the diameter of warp yarn. Following the same logics, the weft cover factor is a product of the weft count and the diameter of weft yarn. In our calculations, the yarn diameter was replaced by the major axis length of yarn having an ellipsoid form. The relevant topographic characteristics obtained for the fabrics manufactured using differently profiled fibre as well as water contact angle for the fabrics are given in Table 4. For convenience, the fabrics analyzed are specified by identification codes, detailed in Table 5.

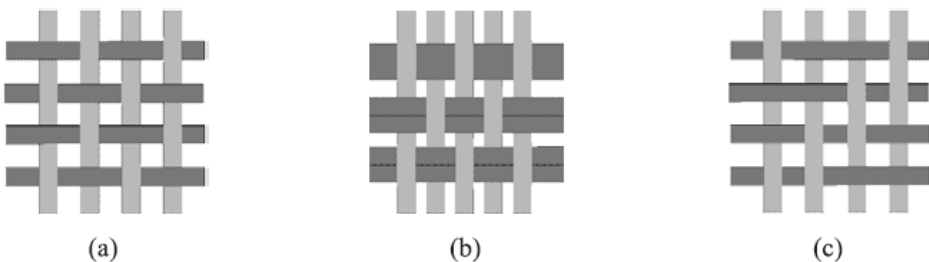


Fig. 17. Basic weaves used: (a) plain weave; (b) warp rib weave; (c) twill

Fabrics identification code	Cover factor	Water contact angle, deg
R-20-D	1.084	113 ± 5
R-30-D	1.017	106 ± 6
R-20-H	1.110	118 ± 6
R-30-H	1.029	117 ± 6
X-20-D	1.032	109 ± 5
X-30-D	0.974	114 ± 4
X-20-H	1.043	119 ± 5
X-30-H	0.998	124 ± 5

Table 4. Geometric factor and water contact angle data

Fibre cross-section	Weft density	Treatment	Fabrics identification code
Round	20/cm	desized	R-20-D
		heat-setted	R-20-H
	30/cm	desized	R-30-D
		heat-setted	R-30-H
Cruciform	20/cm	desized	X-20-D
		heat-setted	X-20-H
	30/cm	desized	X-30-D
		heat-setted	X-30-H

Table 5. Identification code of fabrics.

In contrast to wetting measurements on plain and twill fabrics, woven using commercial multi-microfilament yarn, water drops do not penetrate into the textile surface. No statistically significant changes were found in the wetting behaviour of the fabrics containing round and cruciform shaped fibres (Figure 18). The wettability of fabrics changes

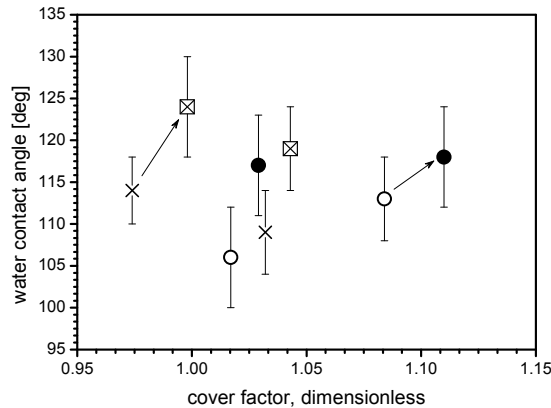


Fig. 18. Water contact angle as a function of the geometric cover factor: (O) round desized without heat-setting (●) round desized with heat-setting; (x) cruciform without heat-setting; (⊠) cruciform with heat-setting.

after their heat-setting. The largest water contact angle of 124° was observed for fabrics containing cruciform fibres with a cover factor that is smaller than that for fabrics with round fibres.

However, no relationship was found between the geometric cover factor and water contact angle. It therefore seems worth pointing out that the geometric cover factor is an idealized effective parameter, which cannot precisely describe the topography of fabrics. On the contrary, surface roughness and waviness can be used to understand the wetting behaviour of liquids on fabrics with a complex structure. A clear linear tendency was found for the water contact angle and surface roughness, as shown in Figure 19, independent of the modification applied.

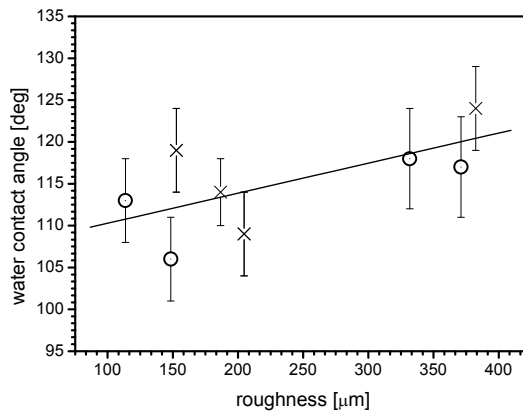


Fig. 19. Water contact angle as a function of roughness (O) round; (X) cruciform

The topography analysis allows filtering measured total profiles of a surface to split them into two analytical representations for displaying surface features: roughness and waviness. The first information represents the shorter spatial wavelengths, whereas the second one represents the longer wavelength features of the surface. Both filtered profiles as well as the schematic of a complex fabric structure are illustrated in Figure 20. Interestingly, surface waviness measured is a function of the geometric cover factor calculated, shown in Figure 21. The fabrics with cruciform fibres have smaller cover factors than those of round fibres. Generally, the maximum cover factor is 1, whereby idealised yarns touch each other. The factor can be larger than 1 if the yarns pile up on top of each other (Sabit, 2001). Real yarns, usually consisting of several single filaments, are flexible and can take different shapes from elliptic to round depending on warp and weft densities. By these means, the appearance of a minimum in the cover factor versus the porosity curve, as shown in Figure 22a, can be explained. A sketch in Figure 22b illustrates possible fabric structures depending on the warp and weft density.

Summarising, by the use of profiled fibres, e.g. the cruciform, the fabric manufacture could lead to a more hydrophobic fabric texture on the basis of different roughness length scales.

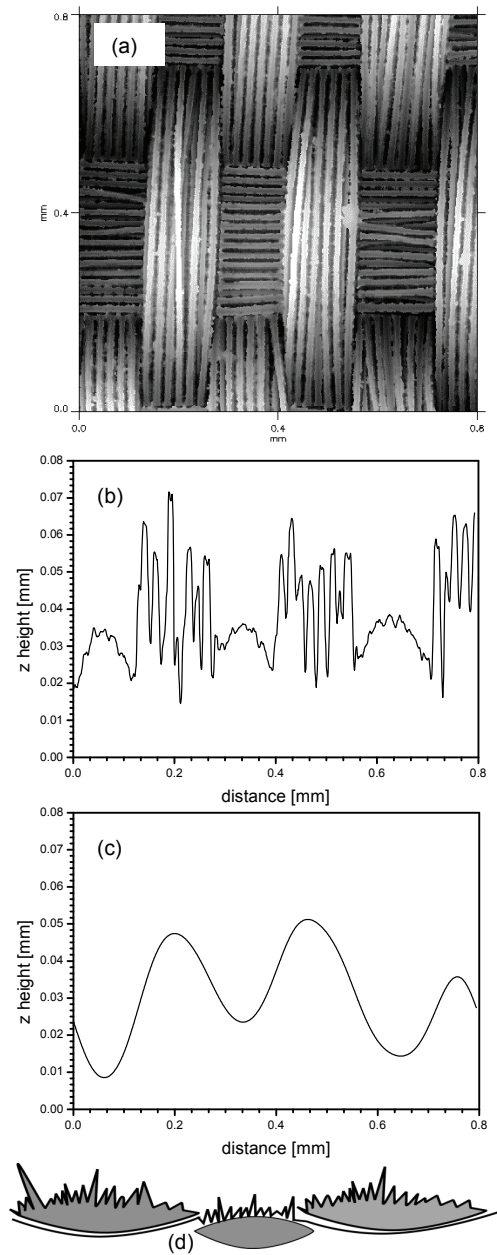


Fig. 20. (a) 2D image of a fabric scanned with chromatic confocal sensor; (b) filtered roughness profile of a plain fabric surface as an example; (c) filtered waviness profile of a plain fabric surface as an example; (d) schematic of a complex fabric structure: the total profile contains both roughness and waviness information

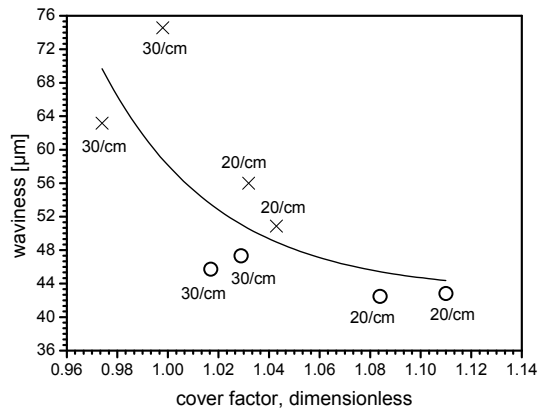
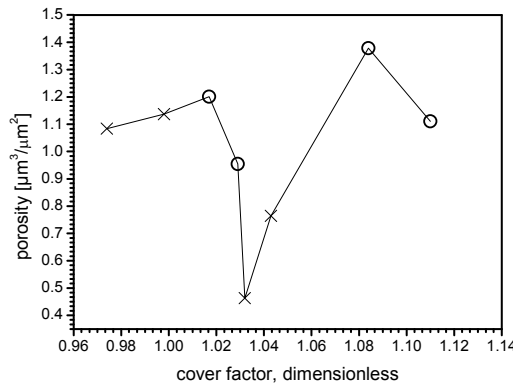
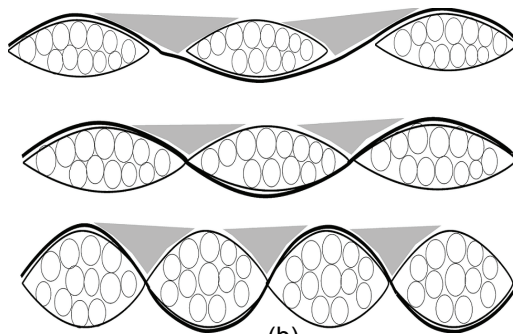


Fig. 21. Relationship between waviness measured and the cover factor calculated: (O) round; (X) cruciform



(a)



(b)

Fig. 22. (a) Fabric's surface porosity measured versus the cover factor calculated: (O) round; (X) cruciform; (b) schematic of differently shaped yarns within a fabric resulting in different surface porosity

Saha (2010) reported the effect of heat setting on the improvement of hydrophobicity of an hydrophobic polyester plain woven fabric, which was heat-setted at 170°C, 180°C, 190°C, 200°C, 210°C, 220°C and 240°C for 60 seconds. According to these results, the effect of thermosetting increased the water contact angle for fabrics thermofixed at 170°C from 113° up to 122° for the thermofixed ones at 200°C (Figure 23). Pilling factor, calculated using mean roughness variations according to Calvimontes (2009), shows a minimum value precisely at 200°C (Figure 24). At this temperature a relative maximum of micro-porosity of warps surface was also found (Figure 25a).

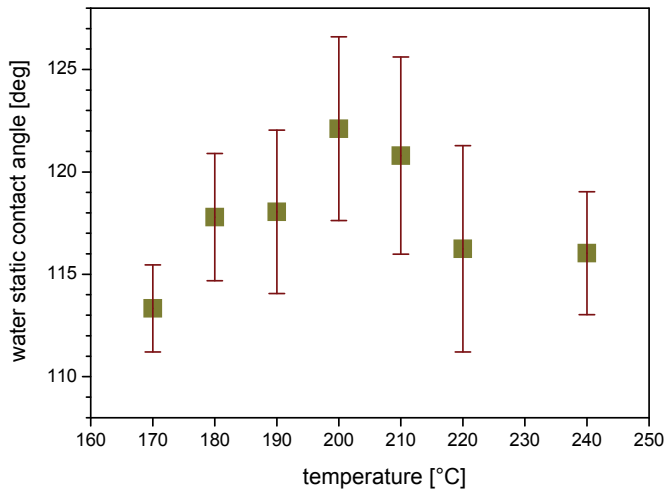


Fig. 23. Water contact angle on thermofixed polyester fabrics

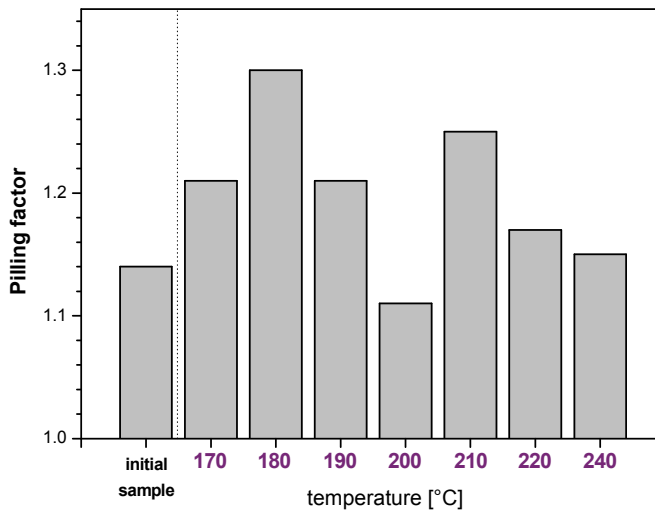


Fig. 24. Pilling factor for thermofixed polyester fabrics

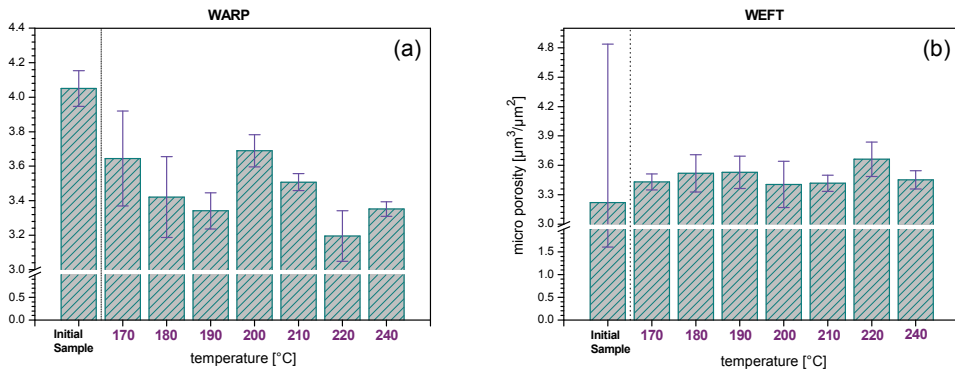


Fig. 25. Micro-porosity of thermofixed polyester fabrics: (a) warps; (b) wefts

On the contrary, the porosity of wefts surface is stabilized by thermosetting (Figure 25b). However, according to that explained previously (Section 2.3), the first contact of any liquid with the fabric surface takes place by the warps, because their higher wave amplitude.

This information allows to conclude that heat-setting smoothes the fabric surface on mesoscopic scale by decreasing pilling, but at the same time, it increases the spaces between warp filaments. The effect is a decrease of the solid fraction –contact area– between polyester fibres surface and water, which, according to Cassie & Baxter (1944), improves hydrophobicity of hydrophobic surfaces.

It was shown in this Chapter, that topographical characteristics of the fabrics strongly depend on their construction parameters such as the type and fineness of filaments, yarn fineness, yarn density, and the type of weave. This characteristics have strong influence on, and in many cases, control the wetting properties.

The topographical study of textile materials using a length scale concept allows to effectively characterize surfaces separately by considering and analyzing their specific morphologies caused by their construction parameters and to successfully find correlations between topography and wettability.

4. References

- Bico, J., Tordeux, C. & Quéré, D. (2001). Rough wetting. *Europhys. Lett.*, Vol. 55, 214-220
- Calvimontes, A., Dutschk, V., Breitzke, B., Offermann, P. & Voit, B. (2005). Soiling Degree and Cleanability of Differently Treated Polyester Textile Materials. *Tenside Surf. Det.*, Vol. 42, No. 1, 17-22
- Calvimontes, A., Dutschk, V., Koch, H. & Voit, B. (2005). New Detergency Aspects through Visualisation of Soil Release Polymer Films on Textile Surfaces. *Tenside Surf. Det.*, Vol. 42, No. 4, 209-216
- Calvimontes, A., Synytska, A., Dutschk, V., Bell, Ch. & Lehmann, B. (2006). Influence of polyester woven fabrics on their wettability. *Melliand English*, Vol. 1-2, E16-E18
- Calvimontes, A., Dutschk, V., Cheriff, Ch. & Heinrich, G. (2007). Ein neues Konzept zum besseren Verständnis der Penetration von Flüssigkeiten in textilien Oberflächenstrukturen, *Proceedings of 15. Neues Dresdner Vakuumtechnisches*

- Kolloquium: Beschichtung und Modifizierung von Kunststoffoberflächen*, pp.48-52, ISBN 973 3 00 022604 5, Dresden, Germany
- Calvimontes, A., Dutschk, V. & Stamm, M. (2009). Advances in Topographic Characterization of Textile Materials. *Textile Res. J.*, Vol. 80(11), 1004-1015, DOI: 10.1177/0040517509348331
- Calvimontes A. (2009). *Topographic Characterization of Polymer Materials at Different Length Scales and the Mechanistic Understanding of Wetting Phenomena*, PhD Thesis, Technische Universität Dresden, Germany
- Cassie, A.B.D. & Baxter, S. (1944). Wettability of porous surfaces. *Trans. Faraday Soc.*, Vol. 40, 546-551
- Dutschk, V., Sabbatovskiy, K.G., Stolz, M. Grundke, K., Rudoy, V.M. (2003). Unusual wetting dynamics of aqueous surfactant solutions on polymer surfaces. *J. Colloid Interf. Sci.*, Vol. 267, 456-462
- Dutschk, V., Myat, S., Märtin, J., Stolz, M., Breitzke, B., Cheriff, Ch. & Heinrich, G. (2007). A Comparative Analysis between Different Ether Carboxylic Acids with Respect to Wettability and Surface Topography of Abrasively Treated Polyester Fabrics. *Tenside Surf. Det.*, Vol. 44, No. 6, 348-354
- Hasan, M.M.B. (2007). *Untersuchungen der Oberflächeneigenschaften von gewebten Textilmaterialien aus Polyesterfasern verschiedener Geometrie*, Master Thesis, Technische Universität Dresden, Germany
- Hasan, M.M.B., Dutschk, V., Calvimontes, A., Hoffmann, G., Heinrich, G. & Cheriff, Ch. (2008). Influence of the Cross-sectional Geometry on Wettability and Cleanability of Polyester Woven Fabrics. *Tenside Surf. Det.*, Vol. 45, No. 5, 274-279
- Hasan, M.M.B., Calvimontes, A., Dutschk, V. (2008). Effects of Topographic Structure on Wettability of Differently Woven Fabrics. *Textile Res. J.*, Vol. 78, No. 11, 996-1003
- Hasan, M.M.B., Calvimontes, A. & Dutschk, V. (2009). Correlation Between Wettability and Cleanability of Polyester Fabrics Modified by a Soil Release Polymer and Their Topographic Structure. *J. Surfact. Deterg.*, Vol. 12, 285-294
- Kissa, E. (1996). Wetting and wicking. *Textile Res. J.*, Vol. 66, 660-668
- Kumpikaitė, E. (2007). Analysis of Dependencies of Woven Fabric's Breaking Force and Elongation at Break on its Structure Parameters. *Fibres Text. East. Eur.*, Vol. 15, No. 1, 35-38
- Lukesch, M. (2009). *Vergleichende Untersuchungen mit modernen optischen Messmethoden zur Bestimmung der Mikrotopographie von Oberflächen*, Praxissemesterarbeit, Hochschule Zittau/Görlitz (FH) - University of Applied Sciences, Germany
- Matsui, M. (1994). *Advanced Fiber Spinning Technology*, Nakajima, T. (ed.), Woodhead Publishing Ltd, p. 115, ISBN 1 85573 182 7, Cambridge
- Milašius, V., Milašius, R., Kumpikaitė, E. & Olauškine, A. (2003). Influence of Fabric Structure on Some Technological and End-use Properties. *Fibres Text. East. Eur.*, Vol. 11, 48-51
- Potluri, P. Parlak, I., Ramgulam, R. & Sagar, T.V. (2006). Analysis of tow deformations in textile performs subjected to forming forces. *Comp. Sci. Technol.*, Vol. 66, 297-305
- Raja, J. & Radhakrishnan, V. (1979). Filtering of Surface Profiles using Fast Fourier Transform. *Int. J. Mach.Tool. Des. Res.*, Vol. 19, 133-141
- Sabit, A. (2001). *Handbook of Weaving*, Technomic Publ. P. 362, ISBN 9 7815871 60134 , Lancaster

- Saha, R. (2010). *Roughness-induced capillary uptake of liquids into textile structures*, Master Thesis, Institute of Textile Machinery and High Performance Material Technology, Technische Universität Dresden, Germany
- Stout, K. J., Sullivan, P.J., Dong, W.P., Mainsah, E., Luo, N., Mathia, T. & Zahouani, H. (1993). *The Development of Methods for the Characterisation of Roughness in Three Dimensions*, Commission of the European Communities, ISBN 1 8571 8023 2, Brussels-Luxembourg
- Trukada, T. & Sasajima, K. (1982). *An Optimum Sampling Interval of Digitizing Surface Asperity Profiles*. *Wear*, Vol. 83, 119-128
- Walz, F. & Luibrand, J. (1947). Die Gewebedichte. *Textil Praxis*, Vol. 11-12, 330-336

Importance of the Cloth Fell Position and Its Specification Methods

Elham Vatankhah
Isfahan University of Technology
Iran

1. Introduction

The warp and weft densities are important parameters having significant effect on the visual, physical and mechanical properties of the fabrics. So, to have a fabric with desirable properties, these two parameters play the key role. Density has affected by many factors which appreciating them is crucial in controlling the evenness of fabric. Although, most of the warp regularity is the result of the appropriate weaving preparation, weft evenness is obtained by correct weaving process.

Therefore, pick density or pickspacing is one of the most important parameters that should be controlled continuously during weaving process to prevent any variations. pickspacing itself is influenced by different causes. Some studies have been done to investigate the effect of these factors on pickspacing.

According to previous studies, position of the cloth fell and the cloth fell distance (c.f.d.) are the effective elements on the pickspacin, the variations of which result in unevenness pickspacing.

As weaving is started, the cloth fell gradually finds its correct position by action of the take-up motion. When a low-pick density fabric is woven, the cloth fell lies on the front position of the reed; however in fabrics with more pick density, the cloth fell tends to move towards the warp direction and the distance of this position of the cloth fell from the front position of the reed is referred to as the cloth fell distance (c.f.d.). This position is maintained as long as the loom runs satisfactorily.

There are, however, many occasions when the correct cloth fell position is temporarily lost. The weft may break and the loom turn over for one or two revolutions without inserting weft; a fault may necessitate unweaving; more frequently still, the loom may be stopped for the night or for a meal break and the cloth fell may creep away from its correct position. In all these cases the weaver has to restore the cloth fell to its correct position. In addition, during weaving, the warp tension undergoes a cyclic change which is due to shedding and this, in turn, causes a cyclic variation in the position of the cloth fell (Greenwood & Cowhig, 1956).

The importance of the cloth fell position is recognized and commented on by many researchers, especially from the point of view of the effecting parameters on it.

The preceding discussion in this chapter has mainly focused on the cloth fell position and the relations between different weaving parameters based on the theoretical methods and the mathematical models.

After identifying the various effecting parameters on the cloth fell, designing a way to measure and control the variations of this parameter is critical.

The proposed and presented methods for measuring the cloth fell movement and their advantageous and disadvantageous are discussed later in this chapter in detail.

2. A review of the cloth fell position and the interaction between weaving factors

It is necessary that a summary of the nomenclature used in this chapter be introduced. (Table 1)

Symbol	Definition	Units
a	Difference between actual and correct pickspacing	inches/pick
D	Minimum pickspacing (theoretical)	inches/pick
E ₁	Elastic modulus of warp	grammes/end
E ₂	Elastic modulus of fabric	grammes/end
k	Coefficient of weaving resistance	gramme inches
K	Cloth fell coefficient	square inches
l ₁	Free length of warp	inches
l ₂	Free length of fabric	inches
L	Cloth fell distance (c.f.d.)	inches
2m	Sweep of reed	inches
n	Number of picks woven	
P	Rate of take-up (correct pickspacing)	inches/pick
r	Distance between reed and cloth fell	inches
R	Weaving resistance	grammes/end
S	Pickspacing	inches/pick
t	Time	seconds
T ₀	Basic warp tension	grammes/end
T ₁	Instantaneous warp tension	grammes/end
T ₂	Instantaneous fabric tension	grammes/end
v	Angular velocity of main shaft	radians/second
χ	Instantaneous distance of the reed from its front position	inches

Table 1. Definition of the nomenclatures

2.1 The effect of take-up motion on cloth fell position

In the conventional power loom the way to obtain a desired pickspacing, is to make the rate of cloth take-up per pick equal to pickspacing by suitable adjustment of the take-up motion. During normal weaving, the amount of fabric woven is increased by a length P at every beat-up, and the function of the take-up motion is to take up this length so as to ensure that the cloth fell stays in the same position (a Greenwood & Cowhig, 1956).

In fact, during beat-up, the pickspacing is generally controlled by the action of the take-up mechanism (Zhonghuai & Mansour, 1989).

The equilibrium between the amount of fabric woven and the amount taken up will be disturbed if the instantaneous pickspacing has a value which differs from the correct pickspacing. In this case there will be a net increase in the free length of fabric of $S - P (= a)$ when the take-up has operated and the c.f.d. will have changed by an amount a . Thus

$$\frac{dL}{dn} = -a \quad (1)$$

Equation (1) will be referred to as the take-up equation and describes the function of the take-up motion in the most general way. When the pickspacing is correct, $a=0$ and the c.f.d. remains constant, as is the case in normal weaving. Thus, the function of the take-up motion is to maintain the c.f.d. constant when pickspacing is correct. The direct effect of the take-up motion is therefore confined to the c.f.d. and it can affect pickspacing only to the extent that the latter affects pickspacing. The relation between the rate of take-up and the c.f.d. is given by the take-up equation. The c.f.d. in turn is related to pickspacing by a cloth fell equation. This shows that the c.f.d. is a vital link between the rate of take-up and pickspacing and also explains the importance of the relation between c.f.d. and pickspacing (a Greenwood & Cowhig, 1956).

2.2 The effect of the cloth fell position on pickspacing

The fact that pickspacing depends on the c.f.d. is due to a simple geometrical cause and to a more complex physical cause and is peculiar to the positive reed motion.

2.2.1 The geometrical aspect of the cloth fell equation

This aspect exists because the new pick is always carried to the front position of the reed. The previous pick is, by definition, at the position of the cloth fell and therefore pickspacing, which is the distance between the new and the previous pick, will depend on the position of the latter, i.e., on the c.f.d. The geometrical aspect would be the only one if no force were required to beat up the new pick and is, in fact, important where the applied beat-up force is small, i.e., in the weaving of low-pick fabrics or with other fabrics when the cloth fell is too near the weaver so that a bad thin place is created (a Greenwood & Cowhig, 1956).

2.2.2 The physical aspect of the cloth fell equation

This aspect exists because in beating up the new pick a resistance is encountered, which increases as the new pick approaches the cloth fell. A higher beat-up intensity will therefore cause a closer pickspacing and vice versa. The beat-up intensity, in turn, depends on the c.f.d. (a Greenwood & Cowhig, 1956).

2.3 The relation between the cloth fell position and the intensity of beat-up

Three distinct theories have been put forward to account for the variation of the intensity of beat-up with the cloth fell position. The first one (velocity theory) relates to the fact that the reed velocity decreases as the reed approaches its front position. This means that the kinetic energy of slay at the impact of the reed with the cloth fell, and hence the intensity of the beat-up, depends on the c.f.d.

The second theory (contact theory) suggests that the intensity of beat-up depends on the length of the period of contact between the reed and the cloth fell. This period in turn depends on the c.f.d., and hence the intensity of beat-up depends on the c.f.d.

The third theory (excess tension theory) relates to the fact that the force of beat-up has to be balanced by an excess of warp tension over fabric tension. This excess can be created only by a displacement of the cloth fell during beat-up and this displacement in turn will depend on the c.f.d. Therefore the intensity of beat-up depends on c.f.d.

Neither the velocity nor the contact theory has ever been formulated in precise mathematical form. This makes a direct comparison on the theories somewhat difficult. It must also be noted that the three theories interpret the intensity of beat-up in terms of three different physical quantities, namely, energy, time and force, respectively.

The excess tension theory has the advantage of being capable of extension to include the other two effects.

The relation between the c.f.d. and the force of beat-up on the basis of the excess tension can be established from equations (2) and (3) for non-bumping and bumping conditions, respectively (a Greenwood & Cowhig, 1956).

$$R_s = (S - L) \left(E_1 / l_1 + E_2 / l_2 \right) \quad (2)$$

$$R_s = (S - L) E_1 / l_1 + T_0 \quad (3)$$

2.4 The relation between beat-up force and pickspacing

The beat-up force at any instant is equal to weaving resistance. The latter arises from many factors; the friction between warp and weft, the rigidity and tension of warp and weft, etc. The total weaving resistance, R, can be regarded as the sum of a frictional resistance and an elastic resistance, the difference between the two being as follows. The energy used in overcoming the frictional resistance is dissipated in heat and, to some extent, in the form of static electricity and, when the new pick has been forced to a point near the cloth fell, the frictional force will tend to keep it there. The energy used in overcoming the elastic resistance is stored in the form of potential energy and, when the new pick has been forced to a point near the cloth fell, the elastic resistance will tend to eject it from the fabric. In spite of these differences the elastic and frictional resistances have many common features. Both resistances increase as the new pick approaches the fell and tend to infinity for a finite value of the distance, r, of the new pick from the fell. Both increase with an increase in warp tension.

The distinction between elastic and frictional resistance is obviously of great importance in dealing fully with the phenomena which take place during beat-up, but this distinction becomes operative only after the beat-up is complete. During beat-up, the features common to both are dominant and, therefore, it was considered justifiable to simplify the treatment by dealing only with the total weaving resistance, R. The different and complex modes of action of the various components are also ignored, and it is assumed that the weaving resistance acts as a simple repulsive force between the cloth fell and the new pick.

For a mathematical treatment, it is necessary to express the weaving resistance, R, as a function of the distance, r, of the new pick from the cloth fell. Experimental technique on the running loom to determine this relationship is difficult and it would be unwise to expect too much from the results. On the other hand, it was also felt that to derive the relationship from theoretical considerations would lead to very complex mathematical expressions and be of little practical value. Therefore, to assume a simple relationship between R and r and to see how experimental results from more easily measured quantities would confirm this assumption. It is assumed that:

$$R = \frac{k}{r - D} \quad (4)$$

This equation takes account of the fact that R varies inversely with r and tends to infinity for a finite value of r . D and k are considered to be constants for a particular fabric. D can be considered the theoretical minimum pickspacing (the practical minimum will always be higher than D) and should be of the order of the yarn diameter. k is termed the coefficient of weaving resistance and is a measure of the difficulty of weft insertion into a given warp. Although as a first approximation k is considered constant, there is a probability that it will vary with warp tension and, possibly, also with loom speed, some loom settings, or atmospheric conditions. The magnitude of all these effects will have to be investigated experimentally.

Equation (4) will be called to inverse distance equation. It applies at any instant during beat-up and when the reed reaches its front position it becomes:

$$R_s = \frac{k}{S - D} \quad (5)$$

This gives the required relationship between beat-up force and pickspacing (a Greenwood & Cowhig, 1956).

2.5 The relation between cloth fell position and pickspacing

By substituting for R_s in equations (2) and (3), the followings relations are obtained for non-bumping and bumping conditions, respectively:

$$L = -\frac{K}{S - D} + S \quad (6)$$

$$L = -\frac{k / (S - D) - T_0}{E_1 / l_1} + S \quad (7)$$

where

$$K = \frac{k}{\left(\frac{E_1}{l_1} + \frac{E_2}{l_2} \right)} \quad (8)$$

When conditions are stable, equations (6) and (7) take on the form

$$L_p = -\frac{K}{P - D} + P \quad (9)$$

$$L_p = -\frac{k / (P - D) - T_0}{E_1 / l_1} + P \quad (10)$$

and can be used to determine the correct c.f.d. for any rate of take-up (a Greenwood & Cowhig, 1956).

2.6 The effect of warp tension on cloth fell position and pickspacing

2.6.1 The warp tension cycle

Fig. 1 shows a typical warp tension curve. During the whole weaving cycle, with the exception of beat-up, the warp tension is the same as the fabric tension. During beat-up, the warp rises to a peak and the fabric tension falls to a minimum. The tension value at which beat-up begins is, by definition, the basic warp tension (^aGreenwood & Cowhig, 1956). The fluctuation of the tension curve is the result of shedding, beat-up, take-up, and let-off motions. The effects of these factors are not simultaneous and vary in duration and magnitude. Among these, the shedding and the beat-up processes bring into being considerable tension loads, and the effect of shedding is of the longest duration compared with the others (Gu, 1984).

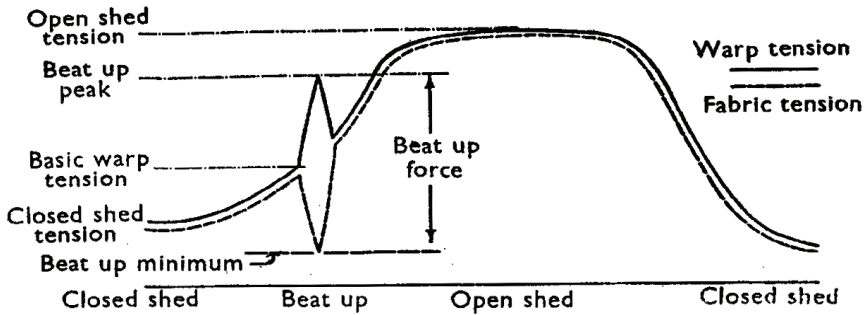


Fig. 1. Typical warp tension cycle

Outside the period of beat-up, the shape of the tension trace is determined by the shedding and reaches a peak at open shed and a minimum at closed shed. The whole tension cycle can thus be summed up in terms of five tension values, namely: open-shed tension, closed-shed tension, basic warp tension, beat-up peak and beat-up minimum (fabric). The difference between the beat-up peak and the beat-up minimum represents the applied beat-up force (according to the excess tension theory). The applied beat-up force in turn determines pickspacing by the inverse distance equation (^aGreenwood & Cowhig, 1956).

2.6.2 The effect of the warp tension cycle

The warp tension plays the contradictory effect during weaving. On the one hand, warp tension provides the only means of holding or supporting the cloth fell in position during beat-up. This is referred to as the supporting function. On the other hand, higher warp tension tends to increase the weaving resistance and can be said to oppose the entry of the new weft into the fabric. This is referred to as the opposing function. To introduce the opposing function it would be necessary to express the coefficient of weaving resistance as a function of warp tension. There is a great deal of evidence that the supporting function is by far the more important (^aGreenwood & Cowhig, 1956).

2.6.3 The setting of the let-off motion

The relation between the let-off motion and warp tension is somewhat similar to the relation between the take-up motion and the cloth fell position. When a loom is gaited up and

weaving started, a certain amount of fabric has to be woven before the warp tension attains the value for which the let-off motion is set. This value is maintained as long as the loom runs satisfactorily, but when the loom is stopped, the instantaneous warp tension may deviate greatly from the normal value because of relaxation or unsatisfactory letting back (a Greenwood & Cowhig, 1956).

2.6.4 The effect of the simultaneous variation in the cloth fell position and the warp tension on pickspacing

As mentioned in part 2.5, equations (6) and (7) show the instantaneous relation between c.f.d. and pickspacing under non-bumping and bumping conditions, respectively. Under normal weaving conditions, the pickspacing is always equal to the rate of take-up P , and to find the correct c.f.d. L_p for a given pickspacing, one need only to substitute P for S in equations (6) and (7) (equations (9) and (10)).

Equations (6) and (7) can be used to calculate the effect of a displacement of cloth fell from its correct position. Such a displacement is very often combined with a change in the basic warp tension from its normal value T_0 to some other value T_0' .

If the changes are small, the effect on pickspacing can be calculated by differentiating equations (6) or (7). This gives

$$dP = \frac{1}{1 + \frac{K}{(P-D)^2}} dL \quad (11)$$

$$dP = \frac{\frac{dL}{l_1} \frac{E_1}{l_1} - dT_0}{\frac{k}{(P-D)^2} + \frac{E_1}{l_1}} \quad (12)$$

for non-bumping and bumping conditions, respectively.

The effect of large changes in the c.f.d. can be calculated as follows, for non-bumping and bumping conditions, respectively:

The correct cloth fell position L_p is given by equations (9) and (10).

$$L - L_p = -\frac{K}{(S-D)} + S + \frac{K}{(P-D)} - P \quad (13)$$

$$L - L_p = -\frac{\frac{k}{(S-D)} - T_0'}{\frac{E_1}{l_1}} + S + \frac{\frac{k}{(P-D)} - T_0}{\frac{E_1}{l_1}} - P \quad (14)$$

These equations determine the deviation from correct pickspacing in terms of the deviation from the correct c.f.d.

From these calculations, it will be seen that under non-bumping conditions, pickspacing depends on the c.f.d. alone and is independent of warp tension, whereas under bumping

conditions both the c.f.d. and the warp tension are important (^b Greenwood & Cowhig, 1956).

2.6.5 The cloth fell displacement and the warp tension variation during loom stoppage

It is a well-known fact that, during a loom stoppage, the cloth fell tends to creep away from its correct position. To examine the effect of relaxation in the warp and the woven fabric on the position of the cloth fell and hence pickspacing, it was assumed that the cloth fell is fixed in its correct position during the stoppage and that, because of the difference in the properties of warp and fabric, the tension in the two materials falls from its original value T_0 to a lower value T_1 in the warp and T_2 in the fabric, where in general $T_1 \neq T_2$. Immediately before starting the loom, the cloth fell is released to find its equilibrium position. Equilibrium exists when the warp and fabric tensions are again equal at a value T'_0 and it is necessary to determine the displacement of the cloth fell which would bring T_1 and T_2 to the same value T'_0 . The displacement of the cloth fell is calculated by equation (15) and the common warp and fabric tension resulting from this displacement is given by equation (16).

$$dL = \frac{T_2 - T_1}{\frac{E_1}{l_1} + \frac{E_2}{l_2}} \quad (15)$$

$$T'_0 = \frac{T_1 \frac{E_2}{l_2} + T_2 \frac{E_1}{l_1}}{\frac{E_1}{l_1} + \frac{E_2}{l_2}} \quad (16)$$

Equations (15) and (16) apply only when a brake-type of let-off motion is used. In this case it will be seen that, if T_2 is smaller than T_1 , i.e., if the fabric relaxes more than the warp, the cloth fell will move away from the weaver. This is the more usual case. Thus the direction of the movement is determined by the relative values of T_1 and T_2 alone.

The effect of the displacement of the cloth fell on pickspacing is calculated by substituting for dL from equation (15) in equation (11) and for K from equation (8). This leads to:

$$dP = \frac{T_2 - T_1}{\frac{k}{(P-D)^2} + \left(\frac{E_1}{l_1} + \frac{E_2}{l_2} \right)} \quad (17)$$

In comparing the brake-type with the dead-weight type of let-off, it is often held in favour of the latter that it keeps warp tension constant during a stoppage.

Using the same simplified assumption as before, it will be assumed that the cloth fell is fixed in its correct position during the stoppage. Owing to the action of the dead weight, the warp tension in the present case remains constant at T_0 , whereas the fabric tension falls to a value T_2 as before. Immediately before starting the loom, the cloth fell is released and the dead weight brings the fabric tension back to its original value T_0 by stretching the fabric by an amount dL given by (^b Greenwood & Cowhig, 1956):

$$dL = \frac{T_0 - T_2}{\frac{E_2}{l_2}} \tag{18}$$

2.6.6 The effect of the let-off motion type

It will be seen on comparing equation (18) with equation (15) that, when the fabric relaxes more than the warp ($T_2 < T_1$), the displacement of the cloth fell will always be greater with a dead-weight than with a break-type let-off motion.

It may be said that the constancy of the warp tension in the dead-weight let-off is obtained at the expense of a greater movement of the cloth fell. Whether this is an advantage or not depends on the type of fabric. With a lighter type of fabric, which will normally be woven under non-bumping conditions, the cloth fell position is probably more important and therefore the brake-type let-off preferable. With a heavier type of fabric, warp tension becomes more critical and the dead-weight type may give better results (Greenwood & Cowhig, 1956).

2.7 The effect of free length of warp and fabric on cloth fell position and pickspacing

Equations (15) and (17) indicate that a long free length of warp and fabric will tend to increase cloth fell displacement and changes in pickspacing due to relaxation, respectively, i.e., it will tend to make setting-on places worse but equation (18) points out that just free length of fabric will affect on cloth fell displacement (Greenwood & Cowhig, 1956).

In addition, during weaving increasing in length of warp and fabric will affect on K and according to equation (11), will decrease the changes in pickspacing.

2.8 The effect of loom speed on cloth fell position

Three theories explained in section 2.3 differ in their prediction of the effect of loom speed on the cloth fell position.

According to the contact theory, a reduction in loom speed would cause a movement of the cloth fell towards the weaver; according to the velocity theory, it would cause a movement of the cloth fell away from the weaver; according to the excess tension theory, it would not cause any change in the cloth fell position.

To investigate these antonym effects, some experiments were carried out and their results are shown in Table 2. The weft used was 140/26 denier bright acetate and 56 picks per inch were inserted so that $P = 0.0154$.

Test Number	Loom Speed (Picks per Minute)	Cloth Fell Distance L (inches)
I	128	-0.151
	158	-0.139
	Difference 0.012	
II	128	-0.162
	158	-0.141
	Difference 0.021	

Table 2. The results of the investigation of loom speed effect

Table 2 shows that the cloth fell moves away from the weaver when the loom is running more slowly, as would be expected from the velocity theory; whereas the following argument shows that a much larger movement would be expected from the velocity theory. The results for the cloth fell position in the two tests agree well and for condition corresponding to a speed of 158 picks per minute, the position is taken as -0.140 inch.

At the time of reed impact with the fell, the reed distance from the fell and the front position of the reed is $P(=-0.154)$ and $X_1(= -0.140- 0.154= -0.155)$ (c Greenwood & Cowhig, 1956).

it is assumed that the motion of the reed near the cloth fell is single harmonic with an amplitude, m , so that:

$$X = m(\sin vt - 1) \quad (19)$$

So, the speed of the reed is given by:

$$\frac{dX}{dt} = mv \cos vt \quad (20)$$

$$\cos vt = \sqrt{\frac{2X}{m}} \quad (21)$$

Substituting for $\cos vt$ from equation (21) in equation (20), the speed of the reed at impact moment is given by (a. c Greenwood & Cowhig, 1956):

$$\frac{dX}{dt} = v\sqrt{2Xm} \quad (22)$$

From the velocity theory, one would expect that the cloth fell position would change with any alteration in loom speed, so that the velocity of the reed at the time of the impact with the fell should remain unaltered.

Thus

$$v_1(2X_1m)^{\frac{1}{2}} = v_2(2X_2m)^{\frac{1}{2}} \quad (23)$$

so that

$$X_2 = X_1 \left(\frac{v_1}{v_2} \right)^2 \quad (24)$$

Substituting numerical values, $X_2 = -0.155 (158/128)^2 = -0.237$ inch. Subtracting from this the value of P (0.0154 inch), the new cloth fell position should, on this calculation, be -0.222 inch. Thus, from the velocity theory one would expect a movement of the cloth fell of -0.082 inch, which is much greater than that actually observed in the above experiments (0.012 in test I and 0.021 in test II).

It is obvious that, for this particular loom and fabric, the observed effect of changes in loom speed on the cloth fell position cannot be explained by any of the three theories alone (c Greenwood & Cowhig, 1956).

3. Methods of measuring the cloth fell position

In general, proposed and presented methods for measuring the cloth fell movement are divided into two main categories:

1. Methods that measure the cloth fell movement during weaving.
2. Methods that measure the cloth fell movement during loom stoppage and try to prevent start-up marks. Such movements are due to difference in visco-elastic properties of warp threads and the cloth during loom stoppage.

These mentioned methods and their advantageous and disadvantageous are discussed later in this chapter in detail.

3.1 The methods of measuring the cloth fell position during weaving

3.1.1 Microscopic method

Early measurements of the cloth fell position were carried out by means of a microscope mounted on a rigid frame on the loom (c Greenwood & Cowhig, 1956). This method is difficult and time consuming.

3.1.2 Optical method

A source of light was placed under the loom and focussed on the cloth fell by a 5-inch focal length lens, the illuminated area being approximately 0.5-inch in diameter. A 4-inch focal length projector lens was mounted about 5 inches above the cloth in line with the source and the first lens. The image of the fell formed by this lens was thrown horizontally on the wall by a mirror inclined at 45° mounted 20 inches above the cloth surface. A white screen fixed to the wall enabled the image to be clearly seen and its position measured. It is essential to avoid movement and vibration in the lens and mirror, and so both were mounted on a frame of 2-inch steel tubing bolted firmly to the floor. To specify the position of the cloth fell, the loom was stopped with fully open shed and cloth fell position was read off on the screen, in terms of its distance from an arbitrary zero line. A diagram of the arrangement of this method is shown in Fig. 2 (c Greenwood & Cowhig, 1956).

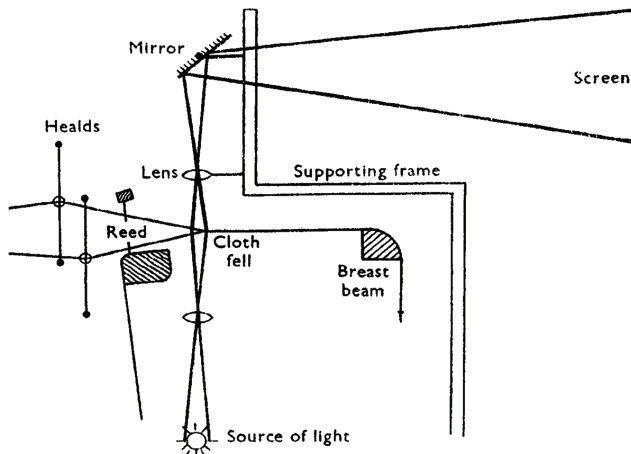


Fig. 2. Optical method for measuring the cloth fell position

The disadvantages of this method are as follows; there is no way to measure the cloth fell position dynamically during the loom running, so the loom has to be stopped to take the measurements (^a Azzam & Büsgen, 2006). Moreover, it is impossible to measure the cloth fell position immediately before beat-up, since at this stage the race board of slay obstructs the path of the light from the source of the fell (^c Greenwood & Cowhig, 1956; Azzam & Büsgen, 2006). In addition, the system is excessively complex, especially regarding the arrangement made to fix a reference point and adjustable pointer at the front position of the reed (^a Azzam & Büsgen, 2006).

3.1.3 Improved optical method

From Fig. 2, it can be seen that it is impossible to measure the cloth fell position immediately before beat-up. It was, therefore, necessary to apply a correction. The loom was stopped with open shed, the slay was left stationary and the healds were brought to beat-up position by loosening and rotating the shedding tappets. The corresponding change in the cloth fell position was measured and used as shedding correction (^c Greenwood & Cowhig, 1956).

3.1.4 Electronic needle wheel method

This method is a continuous measuring system for determining the movement of the cloth fell movement. The movement is measured in the immediate vicinity of the fell by a small wheel, placed on the fabric as close as possible to the fell, which follows the movement undergone by the cloth, as shown in Fig. 3, and is evaluated electronically (Kohlhass, 1981). The disadvantages of this method are the difficulty in fixation on the loom, the difference between the measuring point and the cloth fell is greater than 10 mm, and a great deal of electronics were used (^a Azzam & Büsgen, 2006).

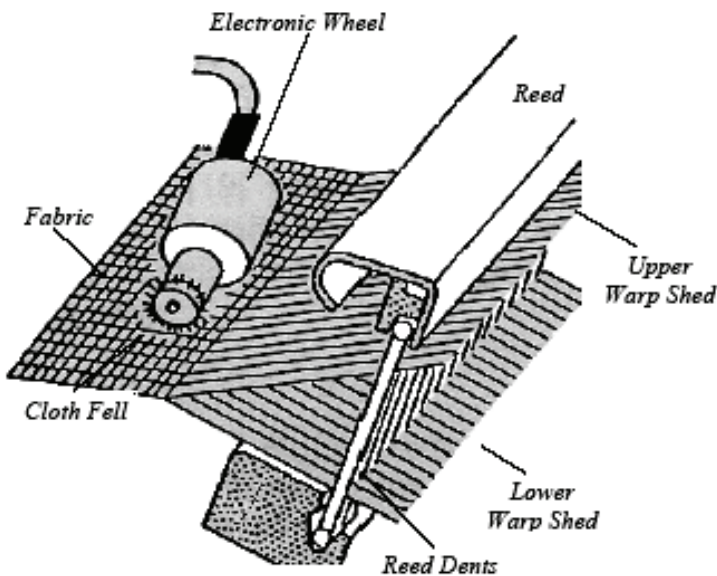


Fig. 3. Electronic needle wheel method for measuring the cloth fell movement

3.1.5 Using the high speed video system

The Kodak Ektapro High Speed Video System consists of a video camera, processor, controller, monitor, macro-objective, endoscope, personal computer, motion analysis package, and video recorder. The system provides a very sharp, clear depiction of the movement of the fell of the cloth during weaving (Weinsdörfer & Salama, 1992).

Also, a high speed camera at 1000 frames/sec has been used to record the cloth fell displacement during the beat-up. Fig. 4 shows the position of the cloth fell when the beat-up takes place. In this diagram the beat-up starts from 42° and ends around 58° (Mirjalili, 2003).

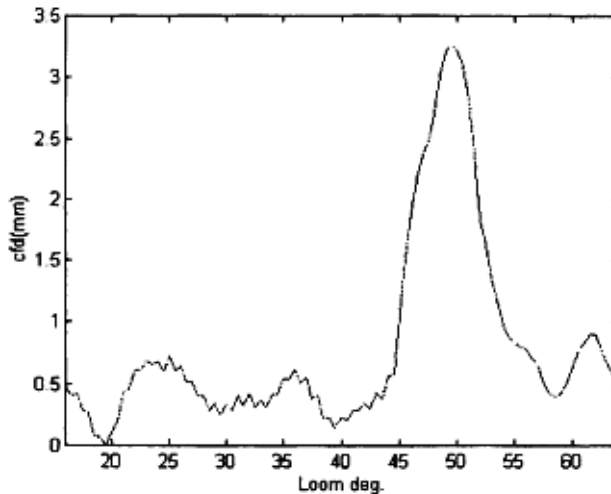


Fig. 4. Cloth fell displacement, c.f.d vs. loom degree

Uneconomical preparation and installation of this system on the loom are the great disadvantages of this method.

3.1.6 Using the lengths of cloth and warp thread

This method is based on the free lengths of warp and fabric. The desired lengths of cloth and warp thread are determined by averaging the actual values over a given number of weft insertions. The actual lengths of the cloth and warp are then continuously measured and compared with the desired values during weaving to compute warp and cloth offset values. A correction factor is determined based on the offset values and the elastic modulus of the warp thread and cloth. The cloth fell position is then corrected by adjusting the actual length of the cloth or the warp thread based on the correction factor (a Godert, 1996).

This method is also usable for measuring the cloth fell after loom stoppage and before loom restart and avoiding the start-up marks in fabrics.

3.1.7 Needle mechanical device

In this system, a simple and flexible needle mechanical device, fixed onto the loom frame and connected with the weave master to measure the cloth fell movement dynamically.

The measuring position for the needle was kept at 2-millimeter distance from the fabric support plate, as indicated in figure 5. This method is based on forced equilibrium. The

forces affecting the cloth fell will push the needle in the direction of force equilibrium; that means, if warp tension force is greater than the fabric tension force, the needle will be pushed towards the warp direction until beat-up takes place. In addition, if the fabric tension force is greater than the warp tension, then the needle will be pushed by the fell to move towards the fabric direction until shedding takes place. By using a special force-displacement calibration the cloth fell positions during shedding and beating could be calculated. In turn, the cloth fell movement could also be calculated. In fact, the difference between the cloth fell position due to beat-up and the cloth fell position due to open shed represents the cloth fell movement (Azzam & Büsgen, 2006).

However, this method is a satisfactory way to measure the cloth fell movement, it can not calculate the cloth fell distance.

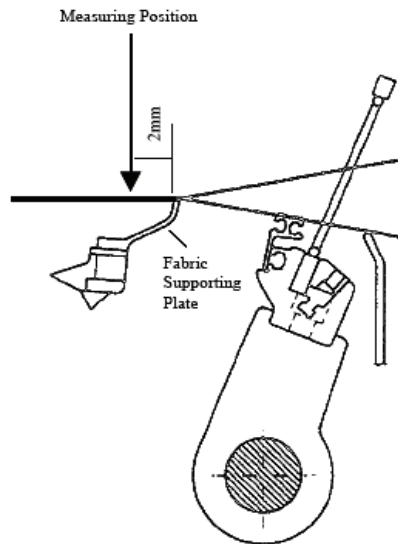


Fig. 5. Measuring position relative to the fabric support plate

3.2 The methods of measuring the cloth fell position during loom stoppage

The aim of this kind of studies is investigating the effect of cloth fell movement during loom stoppage on creating the start-up marks in fabrics woven after loom restart and controlling and preventing this fault.

Generally, the difference in relaxation between warp yarns and fabrics will cause a displacement of the cloth fell during loom stops. In addition to relaxation, cloth fell displacement is determined by the modulus of elasticity of warp yarn and fabric and by their relative lengths within the fabric warp yarn combination that exists on the loom (Vangheluwe & Kiekens, 1995).

3.2.1 Using the sensor needle

In this method the position of the cloth fell is sensed with a sensor needle that can be moved into and out of the cloth at a location proximate the fell during interruption of the weaving

operation. Upon insertion of the sensor needle into the cloth, it moves with the cloth and therewith measures cloth displacement while the loom is at rest. The sensor needle is attached to an actuation device capable of reciprocating the needle into and out of the cloth. The sensor needle is inductively coupled to a distance sensor which measures the needle displacement and therewith the displacement of the fell. In this manner, fell displacement while the loom is at rest can be measured and, before weaving is restarted, the position of the cloth, and therewith of the fell can be corrected (^b Godert, 1996).

3.2.2 Using the photography system

This test method was presented for measuring the cloth fell displacement during relaxation of fabric yarn combination on a tensile tester. The equipment consists of a CCD-camera, a frame grabber, and appropriate software. This study has been carried out on the tensile tester rather than on the loom, where oscillations can hinder the efficient use of a camera.

Fig. 6 shows the arrangement of the equipment. The camera takes one image per second during relaxation measurements. This image is sent to the frame grabber in the PC controlling the tensile tester. In this way, the images are known as a grid (the grid points being called pixels), in which each pixel carries a light intensity value of the total image. In this digitized image, rows of pixels are in the direction of the weft yarns, and columns of pixels are in the direction of the warp yarns. At first, the sum of the pixel values is calculated over the horizontal lines (rows) of the digitized image. Next, values are filtered to eliminate noise. The results in a graph show the position of the weft yarns in the fabric clearly as peaks in the sum of intensity along the warp yarn direction (Fig. 7).

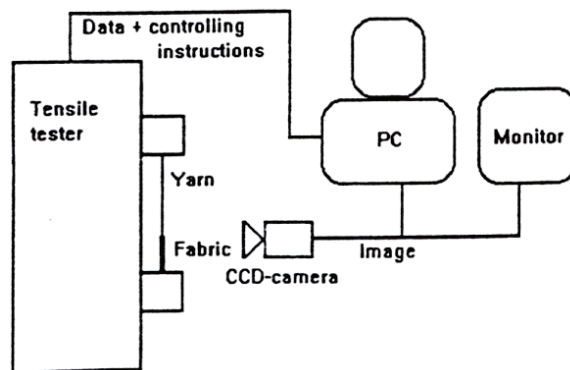


Fig. 6. Test equipment for measuring the cloth fell displacement

The position of the first weft yarn in the image determines the cloth fell. This position is compared with the cloth fell position of the first image that takes at the start of the relaxation. In fact, after calibration, cloth fell displacement is obtained in millimeters as a function of time during which relaxation is measured. This calibration is done by taking an image of a sheet of paper with lines on known distances, which is clamped in the tensile tester. A computer program converts the known distance between the lines to the number of pixels as measured between the lines. Therefore, the cloth fell displacement during relaxation will be measured (Vangheluwe & Kiekens, 1995).

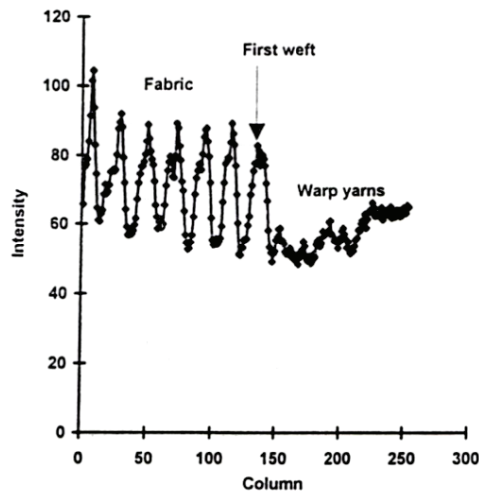


Fig. 7. Results obtained from image filtration

3.2.3 Using the laser analogue displacement sensor

A laser analogue displacement sensor was used, due to its comparatively small physical dimensions. This device, uses a fine laser beam to monitor the position of a target by detecting a spot of light falling on it. With a suitable amplifier, the device enables movements of the target position to be determined to an accuracy of $1\ \mu\text{m}$. The working distance, which is the separation between the target and the front edge of the detector is, $20\pm 2\ \text{mm}$. Within this range, the output signal of the sensor varies linearly with distance. Accordingly, a small lightweight target plate was made that could be placed very close to the cloth fell in such a way that it stayed stable during the loom stoppage period. As such, the movement of the target would be very nearly the same as that of the fell. The target had to be placed with precision on the fabric as soon as the loom stopped, and be removed immediately before the loom was restarted. The output of the sensor is a current signal, which can be easily converted into a voltage and amplified with a stable DC amplifier to enable detection of any movement of the target. A safeguard was provided that prevented the loom from being restarted without the target first being removed. The position of fixing this device on the loom and the cloth fell drift signal produced by the laser sensor are shown in Fig. 8 and Fig. 9, respectively. The output signal provided by the sensor shows the drift of the cloth fell that takes place during the loom stoppage. The rise of the trace indicates a corresponding movement of the fell towards the back of the loom.

The creep of the fell is dependent on the nature and duration of the loom stoppage and other factors. Hence the amount of cloth fell correction required before start-up varies, depending on the loom stoppage duration. Since the sensor enables this amount to be determined, it was possible to move the cloth fell back to where it would have been before the loom stopped. This was done by controlling the stepper motor on the take-up roller, as the number of steps of the motor rotation required could be determined from the required fell displacement. Following this, the let-off was adjusted to restore warp tension to its normal value (Islam & Bandara, 1998).

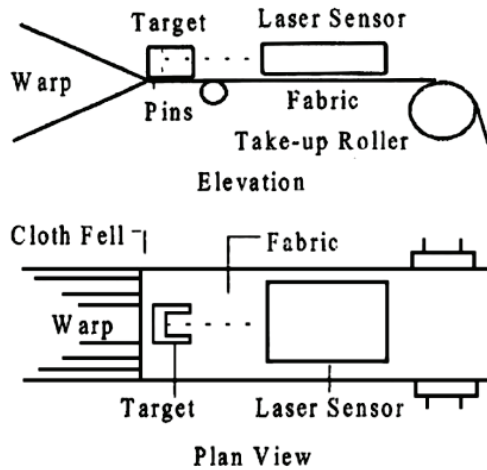


Fig. 8. Placement of the laser sensor on the loom

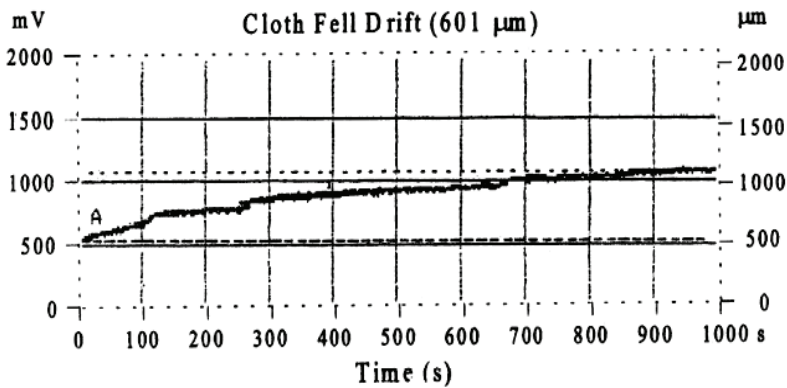


Fig. 9. Fell displacement on a narrow loom with viscose lining fabric

4. Conclusion

In this chapter the importance of the cloth fell position and the effective elements on cloth fell movement were described. After that some measurement methods for determining the cloth fell movement during weaving process and during loom stoppage were presented. However, today no economic method is available to measure the cloth fell position with the required accuracy on the loom.

With regarding to developing and progressing in online electronic systems based on advanced computer programs, It is our hope that a precise method with high speed processing will be designed not only for measuring and monitoring the cloth fell displacement dynamically but also for online controlling and correcting its faults during weaving process. This chapter can be a comprehensive and complete background to help researchers to get innovative ideas.

5. References

- ^a Azzam, H. A. & Büsgen, A. (2006), Dynamic Cloth Fell Movement, Part I: Critical Review, *Autex Research Journal*, Vol. 6 (No. 1): 14-22.
- ^b Azzam, H. A. & Büsgen, A. (2006), Dynamic Cloth Fell Movement, Part II: New Measuring Device, *Autex Research Journal*, Vol. 6 (No. 1): 23-29.
- ^a Godert, D. J. (1996), System and Method for Regulating the Cloth Fell Position in a Loom, Us 005 538 048.
- ^b Godert, D. J. (1995, 1996), Method and Weaving machine for Monitoring the Fell Position Following Weaving Operation Interruption, EP 0 682 132, 1995 and US 005 520 224, 1996.
- ^a Greenwood, K. & Cowhig, W. T. (1956), The Position of the Cloth Fell in Power Looms, Part I: Stable Weaving Conditions, *The Journal of the Textile Institute*, Vol. 47 (No. 5): 241-254.
- ^b Greenwood, K. & Cowhig, W. T. (1956), The Position of the Cloth Fell in Power Looms, Part II: Disturbed Weaving Conditions, *The Journal of the Textile Institute*, Vol. 47 (No. 5): 255-65.
- ^c Greenwood, K. & Cowhig, W. T. (1956), The Position of the Cloth Fell in Power Looms, Part III: Experimental, *The Journal of the Textile Institute*, Vol. 47 (No. 5): 274-286.
- Gu, H., (1984) Reduction of Warp Tension Fluctuation and Beat-up Strip Width in Weaving, *Textile Research Journal*, Vol. 54 (No. 3):143-148.
- Islam, A.T.M.S. & Bandara, M.P.U. (1999), Cloth Fell Control to Prevent Start-up Marks in Weaving, *The Journal of the Textile Institute*, Vol. 90, Part 1 (No. 3): 336-345.
- Kohlhass, O. (1981), Gerät zur Ermittlung der Warenrandbewegung, *Melliand Textilberichte*, Vol. 62 (No. 6): 457-460.
- Mirjalili, S. A. (2003), Computer Simulation of Warp Tension on a Weaving Machine, *Journal of Textile Engineering*, Vol. 49 (No. 1): 7-13.
- Vangheluwe, L. & Kiekens, P. (1995), Test Method for Cloth Fell Displacement Caused by Relaxation, *Textile Research Journal*, Vol. 65 (No. 9): 540-544.
- Weinsdörfer, H. & Salama, M. (1992), Messung der Warenrandbewegung beim Weben mit Hilfe eines High-Speed Video System, *Textile Praxis International*, Vol. 47 (No. 9): 812-814.
- Zhonghuai, Z. & Mansour, H. M. (1989), Theoretical Investigations of Beat-up, *Textile Research Journal*, Vol. 59 (No. 7): 395-404.

Artificial Neural Networks and Their Applications in the Engineering of Fabrics

Savvas Vassiliadis¹, Maria Rangoussi¹,
Ahmet Cay² and Christopher Provatidis³

¹*Department of Electronics, Technological Education Institute of Piraeus, Athens,*

²*Department of Textile Engineering, Ege University, Izmir,*

³*School of Mechanical Engineering, National Technical University of Athens,*

^{1,3}*Greece*

²*Turkey*

1. Introduction

Historically the main use of the textile fabrics has been limited mainly to clothing and domestic applications. The technical uses were of minor importance. However in the last decades the use of the textile structures has started to spread over other sectors like construction, medicine, vehicles, aeronautics, etc. The increased interest in technical applications have improved the fabric design and engineering procedures, given that the final products must be characterized by certain mechanical, electrical etc. properties. The performance of the fabrics should be predictable right from the design phase. The design of a fabric is focusing on the materials selection as well as on the definition of its structural parameters, so that the requirements of the end use be fulfilled.

These changes in the application field of the textile structures caused a move from the esthetic design to the total technical design, where the fabric appearance and the particular properties affecting its final performance are taken in account. However, the textile structures are highly complex. A textile fabric consists of yarns; yarns in turn consist of fibres. Thus the mechanical performance of the fabrics is characterized by the structural geometrical complexity and non-linearity, as well as from the non-linearities of the materials themselves. This double non-linear behaviour of the textile fabrics increases the difficulty in the fabric design and engineering processes. The complex structure and the difficulties introduced by the raw materials do not allow the use of precise analytical models for the technical design of the fabrics.

Fabric engineering activities are increasingly based on computational models that aim at the prediction of the properties and the performance of the fabrics under consideration. Various computational tools have been used in order to represent the fabrics in a computational environment and to predict their final properties. Among others, Finite Element Method (FEM) analysis has supported mainly the prediction of the behaviour of the complex textile structures under mechanical loads. In the case of classification problems Artificial Neural Networks (ANNs) have proved a very efficient tool for the fast and precise solution. ANNs have found an increasing application in the textile field in the classification as well as in the

prediction of properties and optimization problems (Chattopadhyay & Guha 2004). In parallel or complementarily to the ANNs, fuzzy logic and genetic algorithms techniques have been used in the textile field (Guruprasad & Behera, 2010). The applications of the ANNs in the textile classification and prediction problems cover the fields of fibres, yarns and fabrics as well as color, wet processing and clothing.

2. ANN applications in the textile engineering field

It is mainly since 1990 that the applications of ANNs in the textile engineering field have become more and more popular. Gradually it was proven that they can address successfully complex engineering problems. Many researchers have turned to ANNs when they were in front of a multiparameter and non-linear problem, without an obvious or straightforward analytical solution. In the following paragraphs, a thematic overview of the uses of the ANNs in the various textile fields will be presented.

2.1 Fibres

The implementation of the ANNs presupposes an initial phase of features extraction, which will be used later to feed the ANN. It includes the processing of the given data or measurements, typically in the form of a signal, an image etc. One of the most typical problems of the animal fibres classification has been faced using Artificial Neural Networks (She et al., 2002). In the case of cotton, ANNs have been used for the grading of the color of the raw fibres (Cheng et al., 1999; Xu et al., 2000; Kang et al., 2002). An attempt for the classification of the cotton lint has been also based on the use of ANNs (Mwasiagi et al., 2009). A method for the selection of cotton bales based on certain criteria was established (Majumdar et al., 2004). In the case of synthetic fibres, the ANNs have supported the identification of the production control parameters (Allan et al., 2001) and the prediction of the properties of the melt spun fibers (Kuo, 2004). ANNs have been used in conjunction with NIR spectroscopy for the identification of the textile fibres (Jasper & Kovacs 1994). A system for the optimization of the yarn production based on the blend characteristics and the process parameters has been developed based also on the use of ANNs (Sette & van Langenhove, 2002).

2.2 Yarns

The spinning of the staple fibres for the production of the yarns is a multistage procedure including many parameters, which influence the characteristics of the end product, the spun yarn. The examination of the image of the web produced by a carding machine and the detection of faults has been made possible in an automatic sense using ANN's (Kuo et al., 1999; Shiau et al., 2000). The autolevelling and thus the linear density control in the draw frame has been achieved using ANNs (Huang & Chang, 2001; Farooq & Cherif, 2008). In the main spinning phase, the optimization of the top roller diameter as well as the study of the ring ballon has been examined via the use of ANNs (Ghane et al., 2008; Tran et al., 2010).

The overall process performance in the case of the worsted spinning was estimated (Beltran et al., 2004), while the selection of the suitable parameters was the target of other researchers (Wu et al., 1994; Yin & Yu, 2007). The spinning process and its role on the prediction of the cotton-polyester yarn properties were examined using ANNs (Lu et al., 2007; Jackowska-Strumiłło et al., 2008). The effect of the fibres properties on the yarn characteristics is a topic

of great interest for many researchers, with different points of view or dealing with specific fibres or spinning method cases (Dayik, 2009; Jayadeva et al., 2003; Majumdar et al., 2006). A method based on a combination of Genetic Algorithms and Neural Networks has been used for the prediction and optimization of the yarns properties (Subramanian et al., 2007). In a similar sense, a combination of an adaptive neuro-fuzzy system has been developed for the prediction of fiber to yarn relation (Admuthe & Apte, 2010).

The prediction of the tensile properties of yarns is of main interests of the international research community. Many publications appeared dealing with the prediction of the tensile properties of the yarns under general (Ramesh et al., 1995; Guha et al., 2001; Majumdar & Majumdar, 2004; Nurwaha & Wang, 2008; Üreyen & Gürkan, 2008; Mwasiagi et al., 2008; Nurwaha & Wang, 2010) or under specific conditions, such as is the case of core spun yarns (Gharehaghaji et al., 2007), air-jet spun yarns (Zeng et al., 2004) or for the estimation of the torque of worsted yarns (Tran & Phillips, 2007). The ANN prediction method is compared with the Support Vector Machine (SVM) approach and conditions under which each method is better suited are investigated (Ghosh & Chatterjee, 2010). The warp breakage rate during the weaving is a complex function of the yarn properties and thus an application field of an ANN model (Yao, 2005). The prediction of the yarn evenness and hairiness is of great practical interest. ANNs have been used for the prediction of hairiness of worsted wool yarns (Khan et al., 2009) and of cotton yarns (Babay et al., 2005; Majumdar, 2010). In a similar way, ANNs have been used for the prediction of the evenness of ring spun worsted yarns (Wang & Zeng, 2008) and cotton yarns (Majumdar et al., 2008; Üreyen & Gürkan, 2008; Majumdar, 2010) or the evenness of blended rotor yarns (Demiryurek & Koc, 2009).

As it is known, when two yarn ends must be joined, instead of knotting they are subjected in the splicing process. Splicing positions are of special interest because they could affect heavily the mechanical performance of the yarn in total. Evaluation and comparison of the properties of the spliced yarns have been made based also on ANNs (Cheng & Lam, 2003). Later studies have used ANNs to predict the properties of the spliced yarns (Lewandowski & Drobina, 2008). Latest studies have contributed to the prediction of the spliced yarns tensile properties as well as to the prediction of the retained yarn diameter, thus covering the mechanical and the visible results of the presence of the splicing points in the yarn (Gürkan-Ünal et al., 2010). ANNs have also been used for the appearance analysis of false twist textured yarn packages (Chiu et al., 2001), for the prediction of yarn shrinkage (Lin, 2007) or for the modelling of the relaxation behaviour of yarns (Vangheluwe et al., 1996).

2.3 Fabrics

Textile fabrics are often the final product of the textile process. Their properties must directly meet the user requirements; obviously, the prediction of their properties and their final behaviour is very important. The fabrics are complex structures, if their micromechanical structure is considered. The structural complexity in conjunction with the materials complexity do not usually permit the development of Computer Aided Engineering tools for the support of the design phase, as it usually the case in other engineering fields such as mechanical, structural, naval, electrical, etc. Therefore, a lot of effort has been given towards the development of computational tools for the prediction of the behaviour of the fabrics (Basu et al., 2002).

The inspection of the fabrics for the detection of faults is a very important operation, traditionally carried out by skilled operators. Many attempts have been made in order to

perform the inspection automatically. Consequently the task of automated defects detection is popular and many research teams have focused their interest on it, while many of them have used ANNs to support the fault detection task, (Tsai et al., 1995; Sette & Bullard, 1996; Tilocca et al., 2002; Kumar, 2003; Islam et al., 2006; Shady et al., 2006; Behera & Mani, 2007; Mursalin et al., 2008). Another similar approach is the combined use of fuzzy systems (Choi et al., 2001; Huang & Chen, 2003) or wavelet packet bases (Hu & Tsai, 2000; Jianli & Baoqi, 2007). Defects can be detected also by a dynamic gray cloth inspecting machine system (Kuo et al., 2008). The detection and recognition of the patterns on a fabric is of the same class of problems and thus a candidate for the use of ANNs (Jeon et al., 2003; Chiou et al., 2009; Liu et al., 2009). Using the same principles, stitch inspection can be achieved (Yuen et al., 2009). Drapability is far the most complex mechanical property of the fabrics and it is essential for many applications of the textile fabrics. The prediction of the drape has been made using ANNs (Fan et al., 2006). In parallel the engineering of the drapability of the fabrics became possible though a predictive tool (Stylios & Powel, 2003). Fabric hand is a property that combines the mechanical properties of a fabric with the sensory perception of the fabric by the humans when they touch it. It is difficult to give an objective description of the fabric handle, because a subjective evaluation takes place in practice. However, there have been developed some complex systematic approaches for the definition of the fabric hand, which include the full set of the low stress mechanical properties of the fabrics. Obviously the prediction of the fabric hand is equivalent to the prediction of the low stress mechanical properties of the fabrics. The prediction of the fabric hand is a complex, highly non-linear problem and therefore an early target for the application of ANNs (Youssefi & Faez, 1999; Hui et al., 2004; Shyr et al., 2004; Matsudaira, 2006). The data from the FAST system were used to approach the hand of the fabrics (Sang-Song & Tsung-Huang, 2007), while fuzzy logic has been combined with ANN for the evaluation of the fabric hand (Park et al., 2000; Park et al., 2001). ANNs in combination with fuzzy logic have been used in the case of the prediction of the sensory properties of the fabrics, as well (Jequirim et al., 2009). Closely related applications are the objective evaluation of the textile fabric appearance (Cherkassky & Weinberg, 2010) and the emotion based textile indexing using ANNs (Kim et al., 2007). The prediction of the simpler mechanical properties of the textile fabrics is an essential technical requirement. ANNs have been used for the prediction of the tensile strength (Majumdar et al., 2008) and for the initial stress-strain curve of the fabrics (Hadizadeh et al., 2009). The same problem has been solved using an adaptive neuro-fuzzy system (Hadizadeh et al., 2010). The shear stiffness of the worsted fabrics (Chen et al., 2009) and their compression properties have been successfully modelled (Murthyguru, 2005; Gurumurthy, 2007). In general, the prediction of the properties of a fabric enables the support of the design phase, (Behera & Muttagi, 2004). The prediction of bursting using ANNs for knitted fabrics (Ertugrul & Ucar, 2000) as well as for woven fabrics (Vassiliadis et al., 2010) has been achieved with satisfactory results. The permeability of the woven fabrics has been modelled using ANNs as well (Tokarska, 2004; Çay et al., 2007). Further on, the impact permeability has been studied (Tokarska & Gniotek, 2009) and the quality of the neural models has been assessed (Tokarska, 2006). The pilling propensity of the fabrics has been predicted (Beltran et al., 2005) and the pilling of the fabrics has been evaluated (Chen & Huang, 2004; Zhang et al., 2010), while the presence of fuzz fibres has been modelled (Ucar & Ertugrul, 2007). The evaluation of the wrinkle of the fabrics has been realized on an objective basis with a system based on ANNs (Su & Xu, 1999; Kim, 1999; Mori & Komiyama, 2002). Prediction of the spirality of the relaxed knitted fabrics

(Murrells et al., 2009) as well as knit global quality (Slah et al., 2006) and subjective assessment of the knit fabrics (Ju & Ryu, 2006) have been implemented.

Prediction of the thermal resistance and the thermal conductivity of the textile fabrics has been realized with the help of ANNs (Bhattacharjee & Kothari, 2007; Fayala et al., 2008). Moisture and heat transfer in knitted fabrics has been also studied similarly (Yasdi et al., 2009). Engineering of fabrics used in safety and protection applications is supported by ANNs (Keshavaraj et al., 1995; Ramaiah et al., 2010). Prediction of the fabrics end use is also possible via the same method (Chen et al., 2001). Optimization of the application of a repellent coating has also been approached by the ANN model (Allan et al., 2002).

2.4 Color

The color measurement, comparison, evaluation and prediction are major actions in the dyeing and finishing field of the textile process. Although color measurement is possible in the laboratory with the help of specialized equipment like the spectrophotometers, few capabilities exist for the prediction of the color changes or the final color appearance, because the problem is multivariable. A model for the prediction of color change after the spinning process has been developed (Thevenet et al., 2003). The prediction of the color and the color solidity of a jigger dyed cellulose based fabric has been achieved by using cascade ANNs. In the field of printing, the color recipe specification has been made possible using radial basis function neural networks (Rautenberg & Todesco, 1999). The pigment combinations for the textile printing can be determined (Golob et al., 2008), the color of the printed fabric images can be identified and the color separation can take place by using different ANN types (Xu & Lin, 2002; Kuo et al., 2007). The prediction of CIELAB values is possible for color changes after chemical processes (Balci & Ogulata, 2009), for nylon 6,6 and for stripped cotton fabrics (Balci et al., 2008). The optimization of the processing conditions and the prediction of the dyeing quality of nylon and lycra fabrics and the classification of dyeing defects have been carried out with the help of ANNs and fuzzy neural networks respectively (Kuo & Fang, 2006; Huang & Yu, 2001).

2.5 Making up and clothing

Clothing articles are the end product of the main stream of the textile production flow. Although precision of the prediction of properties is not that critical as in technical applications, estimation of the final properties is essential for the clothing design, the selection of raw materials and their required properties. One of the most important factors affecting the garment quality is related to the seam, the result of the sewing process. Indeed, prediction of the seam strength is very important, especially for parachutes (Oanl et al., 2009). The thread consumption is predicted via an ANN model (Jaouadi et al., 2006), while the seam puckering is evaluated and the sewing thread is optimized through ANN models, respectively (Mak & Li, 2007; Lin, 2004). The prediction of the sewing performance is also possible using ANNs (Hui & Ng, 2005; Hui et al., 2007; Hui & Ng, 2009).

The human psychological perceptions of the clothing sensory comfort and the analysis of the tactile perception of the textile materials can be carried out using ANN approaches (Wong et al., 2003; Karthikeyan & Sztandera, 2010). Prediction of the performance of the fabrics in garment manufacturing and fit garment design have been realized based on ANN systems (Hu et al., 2009; Gong & Chen, 1999). Cases of special interest, like the selection of the optimal interlinings, or of broad interest, like the simulation of a textile supply chain, have been successfully modelled by ANNs (Jeong et al., 2000; Nuttle et al., 2000).

2.6 Nonwovens

The nonwoven is a specific category of fabrics, made directly of fibres and not of yarns. The nonwoven fabrics find many technical applications and their role is essential. The nonwoven fabrics undergo a process of inspection in order to ensure quality of the delivered material. A visual inspection system has been based on wavelet texture analysis and robust bayesian ANNs (Liu et al., 2010), or similarly wavelet transforms and ANNs (Huang & Lin, 2008), while a neuro-fractal approach has been used for the recognition and classification of nonwoven web images (Payvand et al., 2010). Many quality issues are addressed via ANN methods, like the structure-properties relations of the nonwoven fabrics (Chen et al., 2007), the construction of a quality prediction system (Kuo et al., 2007), the modeling of the compression properties of needle-punched nonwoven fabrics (Debnath & Madhusoothanan, 2008), the simulation of the drawing of spunbonding nowoven process (Chen et al., 2008) and also the objective evaluation of the pilling on nonwoven fabrics (Zhang et al., 2010).

3. Artificial Neural Networks

3.1 Functionalities of interest for textile engineering

Artificial Neural Networks (ANNs) are algorithmic structures derived from a simplified concept of the human brain structure. They belong to the Soft Computing family of methods, along with fuzzy logic / fuzzy control algorithms and genetic algorithms, (Zadeh, 1994). They all share an iterative, non-linear search for optimal or suboptimal solutions to a given problem, without the presupposition of a model of any type for the underlying system or process, (Keeler, 1992). Various different ANN types have already been successfully employed in a wide variety of application fields, (Haykin, 1998). Major ANN functionalities are

- i. Function approximation: this functionality is exploited in system input-output modeling and prediction, and
 - ii. Classification: this functionality is exploited in pattern recognition / classification problems, (Lippman, 1987).
- In their capacity as function approximators, ANNs have long been studied as to the required properties of the target function as well as to the structure of the ANN, in order to guarantee convergence of the – typically iterative – approximation algorithm. The first brain-inspired ANN structure was proposed by McCulloch and Pitts in 1943, along with a proof that it could approximate any deterministic function, (Hertz et. al., 1991). In light of the Cybenko theorem, (Cybenko, 1989), ANNs are recognized today as ‘universal approximators’, i.e. they can approximate arbitrarily closely any function on a compact subset of R^n , under certain general assumptions on the function. The property was proved for a specific ANN structure (the standard multilayer feed-forward network with a single hidden layer that contains a finite number of hidden neurons, with a sigmoid activation function and a linear output layer). Similar results exist for arbitrary activation functions, (Hornik, 1989) and other ANN structures, as well, (e.g., Lin, 1994). A common prerequisite for the ANN to operate as approximator is the linearity of its output node(s).

Under their function approximator form, ANNs have served as a powerful modeling tool, able to capture and represent almost any type of input-output relation, either linear or nonlinear. The shortcoming of such an ANN-based modeling solution is that the model is implicit. Indeed, rather than formulating an explicit input-output analytic

expression, either linear or nonlinear, an ANN processes examples of inputs and outputs, to capture and store knowledge on the system. It can subsequently simulate the system, or predict output values; yet, it cannot offer a closed-form description of the system.

In a textiles context, the function approximation capacity of ANNs is of great practical interest because a variety of quantities that characterize yarns and/or fabrics depend on (i.e., are functions of) the yarn or fabric consistency, structure and weaving characteristics. Air permeability of a woven fabric, for example, depends on such parameters as warp and weft yarn density and mass per unit area. These dependencies do not always lend themselves to accurate description by an analytic mathematical function; yet, the ability to estimate or predict the value of such a quantity of interest given the yarn or fabric parameters – before actually constructing the yarn or fabricating the fabric – is highly desirable in the textiles design and production phases. Research has turned to ANNs for estimation and prediction tasks in various textile applications, (Stylios & Parsons-Moore, 1993), (Stylios & Sotomi, 1996), (Ertugul & Ucar, 2000), (Majumdar, 2004), (Lin, 2007), (Bhattacharjee & Kothari, 2007), (Gurumurthy, 2007), (Guruprasad & Behera, 2010).

- In their capacity as classifiers, on the other hand, ANNs have found extensive and successful application in virtually all pattern recognition tasks, including 1-D and 2-D signal (image) processing applications, clustering, etc. In such problems, unknown input data are classified as belonging to one of a finite number of known classes or categories. ANN structures with an output layer of nodes (neurons) of the ‘competitive’ type are suitable for classification tasks. Individual binary outputs of the output layer nodes are vectorized in order to enumerate the class where incoming data belong, in typical classification problems. Single and multiple-layer perceptrons, self-organizing maps and other types of ANN structures serve as classifiers. Among them, of practical interest are networks that compute probabilities that a given input belongs to one of the considered classes, rather than deterministic outputs. They can thus substitute multi-expert decision algorithms, such as majority-voting, etc. Probabilities can subsequently be handled in a variety of ways to obtain final answers in the output.

The classification capacity of ANNs in a textiles context finds extended use in classification of yarn or fabric types or other visual properties, such as color, defects, weaving / knitting pattern, percentage consistency in various materials and the like, (Guruprasad & Behera, 2010). These tasks are affordable in time and equipment investment thanks to the recent technological advances (a) in image capturing equipment of high quality and very low cost and (b) in hardware processors of increased processing power that allow for real or quasi-real time applications.

3.2 Architecture and training algorithms

The structure or ‘architecture’ of an ANN contains a number of nodes, called neurons, organized in a number of layers and interconnected to form a network. Neurons are rather simple algorithmic structures that can perform parallel computation for data processing and knowledge representation, (Brasquet & LeCloirec, 2000). Weighted averaging, followed by linear or non-linear (thresholding) operations, with the possibility of feedback between layers, constitute the main processing operations in an ANN. The acquired knowledge is stored as the weight values of the nodes. The real power of this model, therefore, lies in the

mesh of simple but highly interconnected nodes rather than the power or sophistication of each node. Although inspired from the way neurons are interconnected in the human brain and nervous system to transfer messages by chemo-electrical procedures, no further analogy between ANNs and the human brain operation is claimed as to the functionalities achieved.

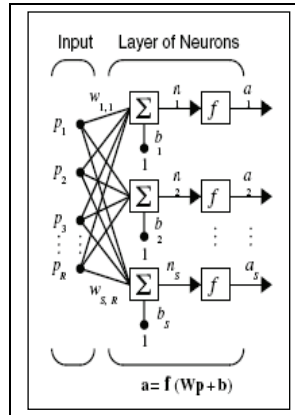


Fig. 1. A sample ANN architecture (one single layer of S nodes or neurons).

The architecture of a single layer of nodes for a sample ANN is shown in Figure 1, (Matlab, 2005). There exist S nodes in this layer. In the i -th node, a linear combination of a vector of R inputs $[p_1, \dots, p_R]$ is computed. In it, inputs are weighted by weights $[w_{i1}, \dots, w_{iR}]$ and a bias term b_i is added. The scalar value produced undergoes a transformation by a generally nonlinear activation function $f(\cdot)$ to yield the corresponding i -th output, for all $i = 1, 2, \dots, S$. Sigmoid, log-sigmoid, hard-limiter or even linear types of functions are employed, resulting in accordingly varying properties of the network.

In general, the ANN architecture is characterized by:

- A large number of simple, neuron-like processing elements;
- A large number of weighted connections between elements. The weights of these connections store the 'knowledge' of the network. The adaptive adjustment of the weight values, while moving down an error surface to a minimum point, constitutes the 'learning process' of the network;
- Highly parallel and distributed control; and
- An emphasis on learning internal system representations automatically, (Rich & Knight, 1991).

Apart from the topology and node characteristics (type of activation function, etc.), an ANN model is specified by the training rules or training algorithm employed to adapt its weights. These rules define an initial set of values for the weights and indicate how weights should be iteratively adapted to improve the performance of the network by minimizing the error between actual and ideal outputs, when the network is presented with a set of known inputs. A variety of different network models have already been proposed and used in practical applications, such as the Perceptron, the Multilayer Perceptron, the Hopfield network, the Carpenter-Grossberg classifier, the Back-propagation network, the Self-organizing Map, the Radial Basis Function Network, the Probabilistic Network, etc., (Ramesh et al., 1995), (Lippman, 1987).

In terms of operation, an ANN undergoes a training phase, where a rich set of examples matched in pairs of input - output values and called the 'training set' is presented to the network input. The weights in the nodes of the network are iteratively optimized by a gradient-type algorithm, so as to produce correct outputs for all inputs in the training set. As iterations proceed, the algorithm leads to sets of weights that minimize the error between ideal and actual ANN outputs – usually, in the least squares sense. Once trained, the network enters the so-called test phase, where it is 'questioned' to produce outputs for unknown inputs presented to it. Decisions are made (i.e., outputs are produced) on the basis of the experience gained by the network over the training set. During the test phase, the network is expected to 'generalize' successfully, i.e., to exploit the experience stored in its elements during the training phase in order to make correct decisions on incoming data that are similar but not identical to the training set data. Satisfactory generalization implies

- a correct choice of the network type in relation to the problem at hand and
- a successful training phase, in the sense that:
 - the training set was rich and informative enough to represent adequately the space of the input vectors, and
 - the training algorithm was allowed an adequate number of iteration to converge.

Major reasons for non-convergence of the training algorithm are

- i. the choice of an inappropriate ANN structure (e.g., one with too many / not enough nodes or too many / not enough layers of nodes), and
- ii. the unavailability of a rich training set, which means that more data or measurements are necessary to solve the problem at hand.

The second problem is more crucial in practice, as it is not always straightforward how more data are to be obtained or measured in real field applications. The first problem, on the other hand, can be efficiently addressed by simulations during the design phase of the whole application.

In order to illustrate the above, an example is provided in the following section, where an ANN is employed to predict or estimate a fabric property in terms of a set of structural weaving parameters of the yarns used and of the fabric itself.

4. A sample application of ANNs in fabric air permeability prediction

4.1 Problem description

Vacuum drying is a method for removing the water content from wet fabrics by suction. In a typical industrial fabric production process, vacuum drying is a pre-drying stage, positioned before the main drying unit, which operates by heating the wet fabric (stenter). The behavior of woven fabrics during vacuum drying is primarily influenced by their air permeability. Air permeability can be calculated from the porosity of the fabric. This approach, however, is not used in practice, because of known difficulties in determining basic porosity calculation parameters, such as the shape factor. Alternatively, air permeability can be measured in the laboratory after the production of the fabric. Of practical interest, however, is the possibility to predict air permeability during the design phase, based on technical, micro-structural characteristics of the fabric. This would allow for the prediction of the behavior of a fabric during vacuum drying and would thus support a realistic and optimized planning of the production process.

Air permeability depends both on the material(s) of the yarn and on the structural parameters of the fabric, through a generally complex, nonlinear relation, (Backer, 1951). In

order to 'capture' this relation and use it later as a predictor, the nonlinear approach of ANNs is adopted, (Cay et. al., 2007). Given the construction process of woven fabrics, three structural parameters are intuitively more attractive for this task, namely,

- warp yarn density,
- weft yarn density and
- mass per unit area.

They are advantageous in that their values either are predefined in the weaving process (warp and weft densities) or can be easily and accurately measured (mass per unit area), while at the same time they influence directly the properties of the woven fabric.

4.2 Network type selection

As discussed in section 3, the choice of the appropriate type of ANN depends on the peculiarities of the problem investigated. Several types of ANNs are promising candidates for the problem under consideration. In fact, any neural network that can take on the form of a universal function approximator will do. These are networks whose output layer nodes operate linearly and can therefore produce practically any real value in the output – as opposed to the limited output values possible when nonlinear / thresholding nodes are employed in the output layer.

The major network families in this class are

1. Multilayer Perceptrons,
2. Radial Basis Function Networks; more specifically, Generalized Regression Neural Networks, (Chen et al., 1991), and
3. Elman Networks, (Elman, 1990).

Among these three alternatives, Generalized Regression Neural Networks (GRNNs), are selected because

- they are known to approximate arbitrarily closely any desired function with finite discontinuities, and
- although they require an increased number of nodes in their architecture, they can be designed in far less time than necessary for the design and training of, e.g., a multiplayer perceptron.

GRNNs work by measuring how far a given sample pattern lies from patterns in the training set, in the N-dimensional space defined by the cardinality of the input set. When a new pattern is presented to the network, it is compared in the N-dimensional space to all patterns in the training set to determine how far in distance it lies from each one of them. The output that is predicted by the network is proportional to all outputs produced by the training set. The proportion value depends upon the distance between the incoming pattern and the given patterns in the training set. Euclidean or city-block distance metrics are used.

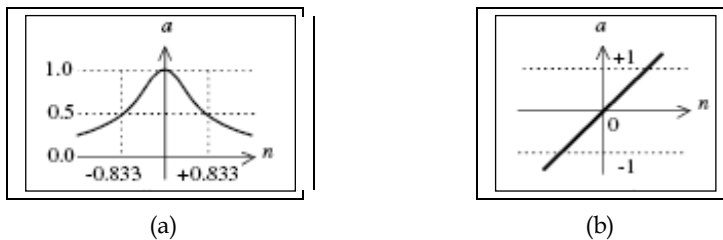


Fig. 2. A radial basis (a) and a linear (b) neuron transfer function.

In terms of structure, a GRNN contains two layers of neurons, each consisting of N neurons, where N is the cardinality of the training set (number of the input - output pairs available for training). The first, hidden layer consists of radial basis function (RBF) neurons while the second, output layer consists of linear neurons of special structure. Thanks to the later, the network can produce any real value in its output. Figure 2a shows a RBF neuron sample transfer function. An RBF neuron 'fires' or produces an output of 1 when its input lies on or fairly close to its central coordinates. Thanks to its symmetry and finite radial support controlled by a spread parameter, it responds only to local inputs, i.e. those befalling within a neighbourhood of controlled radius. Figure 2b shows a linear neuron sample transfer function. The linear layer of a GRNN is special in that its weights are set equal to the output values contained in the training set. When a value equal or close to 1 is produced by the first layer and propagated to the second layer, it produces by means of an inner product operation a significantly non-zero value at a certain output and practically zero values at the rest of the outputs.

During the design phase of the GRNN, the centres of the RBF neurons in the first layer are set equal to the input vectors in the training set. During the test phase, when an unknown input close (similar) to one of the training set inputs appears, the corresponding RBF neuron (or neighbouring set of neurons) fires a value equal or close to 1. The second layer performs an inner product between the vector of the first layer outputs and the vector of training set outputs. Training set outputs matched with values close to 1 in this inner product contribute significantly to the output, while the contribution of the rest is negligible. This is how the GRNN generalizes from the training set to unknown inputs.

The major shortcoming of a GRNN is that both its layers consist of a number of nodes equal to the number N of vectors in the training set. Given the fact that the training set should be rich enough to be representative of the input space, this number may grow large for a given application. As a counter-balance, however, it has been proved that the GRNN can be designed to produce zero error for any given training set in a very short time.

4.3 Experimental setup

A set of different samples of woven fabrics are produced and tested experimentally. All fabric types used are made of 100% cotton yarns and they are of plain weave structure. The warp and weft yarn linear densities are Ne 40 and Ne 50, respectively. The warp and weft yarn densities of the samples vary in incremental steps. Six (6) different weft densities and five (5) different warp densities are combined to produce a set of $6 \times 5 = 30$ different fabric types in total.

The air permeability of these fabrics is measured under constant pressure drop. Actually, rather than being directly measured, the air permeability is estimated by the measurement of air velocity. Air permeability in ($\text{cm}^3/\text{s}/\text{cm}^2$) is measured via the standard BS5636 method, using the Shirley FX 3300-5 air permeability tester. For each one of the thirty (30) fabric types constructed, the air permeability measurement is repeated across five (5) different samples of the same fabric, thus producing a total of $30 \times 5 = 150$ measurements. The five measurements of the same fabric are averaged to produce an average air permeability value, in order to reduce non-systematic measurement errors. The structural fabric parameters, the respective air permeability values (averages across five samples) and the standard deviation of the measurements are given in the Table I.

As it can be seen in Table 1, air permeability values decrease when warp and weft yarn densities increase - an expected behaviour because the dimensions of the pores through

which air flows are getting smaller when moving from looser towards tighter fabric types, where resistance to the airflow is higher.

Warp and weft yarn densities and mass per unit area form the input vector to the ANN. Therefore, each input – output pair in the training set contains a vector of these three inputs and a single output (air permeability). As mentioned earlier, air permeability measurements are averaged across sets of five samples for each fabric type. Therefore the data set consists of thirty (30) independent combinations of values of the three independent input variables along with the respective averaged air permeability value per case.

Sample No.	Warp yarn density (ends/cm)	Weft yarn density (picks/cm)	Mass per unit area (gr/m ²)	Average Air permeability (cm ³ /s/cm ²)	STDEV of Air permeability	Sample No.	Warp yarn density (ends/cm)	Weft yarn density (picks/cm)	Mass per unit area (gr/m ²)	Average Air permeability (cm ³ /s/cm ²)	STDEV of Air permeability
1	54	20	101.0	45.74	1.80	16	60	35	141.4	4.56	0.41
2	54	25	110.3	27.02	2.44	17	60	40	151.2	2.12	0.07
3	54	30	119.5	15.68	0.68	18	60	45	153.7	1.70	0.05
4	54	35	127.3	8.76	0.39	19	63	20	109.0	27.68	0.55
5	54	40	136.7	4.37	0.15	20	63	25	119.1	15.24	0.64
6	54	45	144.1	2.90	0.40	21	63	30	129.1	7.23	0.13
7	57	20	101.2	47.94	1.83	22	63	35	148.5	3.22	0.42
8	57	25	111.1	27.52	0.78	23	63	40	150.3	1.89	0.08
9	57	30	120.5	14.84	0.97	24	63	42	154.4	1.61	0.05
10	57	35	130.7	8.99	0.48	25	66	20	111.2	27.28	1.68
11	57	40	142.0	3.98	0.24	26	66	25	123.0	14.42	1.39
12	57	45	146.3	2.68	0.12	27	66	30	134.0	6.90	0.21
13	60	20	107.9	33.98	1.16	28	66	35	144.4	3.19	0.17
14	60	25	118.7	17.01	0.79	29	66	40	155.0	1.65	0.06
15	60	30	129.5	9.75	0.41	30	66	42	160.2	1.38	0.05

Table 1. Structural parameters and corresponding air permeability measurements for 30 fabric types.

Twenty-four (24) out of the thirty (30) cases are used for training while the remaining six (6) cases are retained for testing. This leads to a GRNN architecture of 24 neurons in each of the two layers. Furthermore, in order to reduce the dependency of the results on a specific partition of the data into training and testing sets, a five-ways cross validation test is carried out, i.e., the data are partitioned in five (5) different ways and finally results are averaged across all five (5) partitions. Figure 4 show results of one out of the five (5) different experiments of the five-ways cross-validation. The upper plot shows results where the

training set per se is used as the test set, while the lower plot shows results where the test set is disjoint to the training set. Within each plot, stars (*) and circles (o) indicate measured and estimated air permeability values, respectively, while dots (·) indicate the ANN performance error (difference between measured and estimated air permeability values).

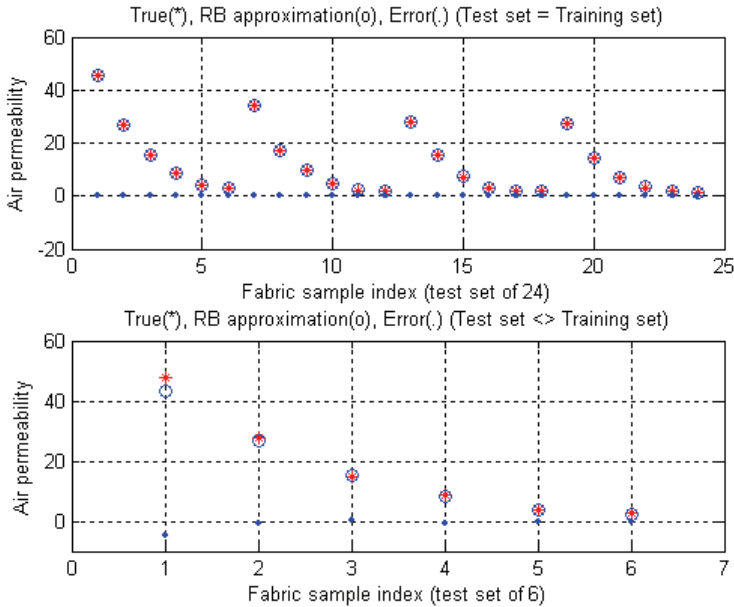


Fig. 4. Air permeability estimated (approximated) by the GRNN (partition no. 2).

As it can be seen in Figure 4, the network employed approximates air permeability values with a very low output error – a result observed regardless of the specific data partition into training and test sets. Error (sum-of-squares) values, given in Table 2, are indeed very low.

Data Partition No.	Error (sum-of-squares)
1	16.62
2	22.64
3	17.10
4	17.52
5	94.49
Average error (sum-of-squares)	33.27

Table 2. Sum-of-squares error across five partitions and average.

Although the relation under investigation is clearly non-linear, due to the complex dynamics involved in the underlying physical phenomena, a multiple linear regression is performed on the data of Table 1, in order to obtain

- a. a crude linear approximation of the relation sought and
- b. a clue as to the relative importance of the three intuitively chosen structural parameters within this relation.

```

The regression equation is
C4 = 105 - 0,679 C1 - 0,392 C2 - 0,355 C3

Predictor    Coef    SE Coef    T    P
Constant    105,04    16,36    6,42    0,000
C1          -0,6793    0,7280   -0,93    0,359
C2          -0,3920    0,5694   -0,69    0,497
C3          -0,3551    0,3655   -0,97    0,340

S = 5,59416    R-Sq = 84,0%    R-Sq(adj) = 82,2%

Analysis of Variance

Source      DF      SS      MS      F      P
Regression    3    4285,9    1428,6    45,65    0,000
Residual Error 26    813,7     31,3
Total        29    5099,6

Source  DF  Seq SS
C1      1  3825,8
C2      1  430,6
C3      1   29,5

Unusual Observations

Obs    C1    C4    Fit    SE Fit    Residual    St Resid
1     20,0  45,74  34,42    2,54     11,32     2,27R
7     20,0  47,94  33,17    2,05     14,77     2,84R

R denotes an observation with a large standardized
residual.

```

Table 3. Multiple linear regression analysis on the data of Table 1.

The results are given in Table 3. Data in columns C1, C2, C3 contain weft densities, warp densities and mass per unit area data, respectively, while column C4 contains average air permeability values.

In Table 3, the P-value in the Analysis of Variance section is less than 10^{-3} , showing that the regression per se is indeed significant, i.e. there does exist an influential relation between the dependent variable (air permeability) and the three independent variables selected here. The R^2 value is 84% (adjusted R^2 is 82,2%), showing that 84% of the variability in the air permeability data is 'explained' by the linear combination of the specific three independent variables. This percentage is high enough to indicate that a linear relation could certainly be used as a crude approximation of the true relation and, at the same time, low enough to justify the investigation of nonlinear alternatives to explain the remaining variability in the data.

It is interesting to notice that the (appropriately scaled) average error produced by the ANN approach in Table 2 ($33.68 \cdot 30 / 6 = 168.4$) compares favourably to the respective error produced by the multiple linear regression approach (813.7). The later is a very encouraging result, as it justifies the extra effort required by the nonlinear approach. Indeed, in terms of the multiple linear regression, it can be claimed that the ANN structure leaves unexplained only the ($168.4 / 5099.6 =$) 3,3% of the total variability in the air permeability data, thus offering a five times better result than the respective 16% of the linear regression approach.

An error pattern apparent in the lower plot of Figure 4 associates looser fabric types (towards the left side of the horizontal axis) with error values higher than the respective error values for dense fabrics (towards the right side of the horizontal axis). For loose fabrics the pores or openings between the yarns are bigger so the yarn mobility is higher, thus the pore dimensions become bigger because of the deformation during the airflow. On the contrary, dense fabrics have very small pores and high resistance to airflow and can preserve their compactness during airflow.

Finally, Figure 5 shows the strong correlation between the measured and the predicted by the ANN air permeability values.

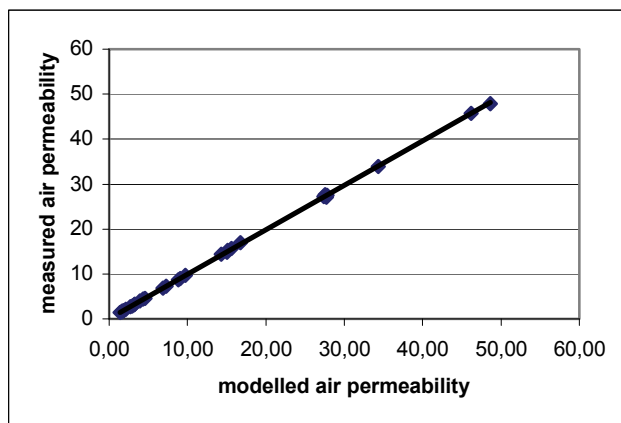


Fig. 5. Correlation between measured and ANN-predicted air permeability values.

5. Conclusions – future trends

An extended overview of the application of artificial neural networks methods for the solution of textile problems is provided in an attempt to cover this evolving field up to the current research and technology advances. It is clear to the reader that related publications on the field are produced in increasing numbers from the research community. Starting from the decade of the nineties a continuously increasing number of ANN applications has provided solutions to complex and multivariable textile problems. It seems that the textile community has been familiarized with this powerful tool and it trusts it more and more. The continuous increase of the computational power of the personal computers reduces the drawback of the computational cost that the use of ANNs requires. Therefore, it is expected that ANNs will augment their percentage of participation in solving complex textile problems and they will support the design and the computer aided engineering concepts in the textile field.

6. References

- Admuthe L.S. & Apte S. (2010). Adaptive Neuro-fuzzy Inference System with Subtractive Clustering: A Model to Predict Fiber and Yarn Relationship, *Text. Res. J.*, 80(9), pp 841-846.

- Allan G., Yang R., Fotheringham A. & Mather R. (2001). Neural modelling of polypropylene fibre processing: Predicting the structure and properties and identifying the control parameters for specified fibres, *J. of Materials Science*, 36 pp. 3113 – 3118.
- Allan G., Fotheringham A. & Weedall P. (2002), The Use of Plasma and Neural Modelling to Optimise the Application of a Repellent Coating to Disposable Surgical Garments, *AUTEX Res. J.*, Vol. 2, No2.
- Babay, A. , Cheikhrouhou, M. , Vermeulen, B. , Rabenasolo, B. & Castelain, J. M.(2005). Selecting the optimal neural network architecture for predicting cotton yarn hairiness, *J. of the Text. Inst.*, 96: 3, pp. 185 – 192.
- Backer, S. (1951). The relationship between the structural geometry of a textile fabric and its physical properties, Part IV: Intercise geometry and air permeability, *Text. Res. J.*, vol. 2, pp. 703-714.
- Balci O., Ogulata S.N., Sahin C. & Ogulata R.T. (2008). Prediction of CIELab Data and Wash Fastness of Nylon 6,6 Using Artificial Neural Network and Linear Regression Model, *Fibers and Polymers*, Vol.9, No.2, pp. 217-224.
- Balci O., Ogulata S.N., Sahin C. & Ogulata R.Y. (2008). An Artificial Neural Network Approach to Prediction of the Colorimetric Values of the Stripped Cotton Fabrics, *Fibers and Polymers*, Vol.9, No.5, pp. 604-614.
- Balci O. & Ogulata R.T. (2009). Prediction of CIELab Values and Color Changing Occurred After Chemical Finishing Applications by Artificial Neural Networks on Dyed Fabrics, *Tekstil ve Konfeksiyon*, 1, pp. 61-69.
- Balci O. & Ogulata R.T. (2009). Prediction of the Changes on the CIELab Values of Fabric after Chemical Finishing Using Artificial Neural Network and Linear Regression Models, *Fibers and Polymers*, Vol.10, No.3, pp. 384-393.
- Basu A., Chellamani, K. P. & Ramesh P.R. (2002). Fabric Engineering by Means of an Artificial Neural Network, *J. of the Text. Inst.*, 93:3, pp. 283 – 296.
- Behera B.K. & Mani M.P. (2007). Characterization and Classification of Fabric Defects Using Discrete Cosine Transformation and Artificial Neural Network, *Ind. J. of Fibre & Text. Res.*, Vol. 32, pp. 421-426.
- Behera B.K. & Muttagi S.B. (2004). Performance of Error Back Propagation vis-à-vis Radial Basis Function Neural Network: Part I: Prediction of Properties for Design Engineering of Woven Suiting Fabrics, *J. of the Text. Inst.*, 95:1, pp. 283 – 300.
- Behera B.K. & Muttagi S.B. (2004). Performance of Error Back Propagation vis-à-vis Radial Basis Function Neural Network: Part II: Reverse Engineering of Woven Fabrics, *J. of the Text. Inst.*, 95: 1, pp. 301 – 317.
- Beltran R., Wang L. & Wang X. (2004). Predicting Worsted Spinning Performance with an Artificial Neural Network Model, *Text. Res. J.*, 74(9), pp 757-763.
- Beltran R., Wang L. & Wang X. (2005). Predicting the Pilling Propensity of Fabrics through Artificial Neural Network Modeling, *Text. Res. J.*, 75(7), pp 557-561.
- Bhattacharjee D. & Kothari V.K. (2007). A Neural Network System for Prediction of Thermal Resistance of Textile Fabrics, *Text. Res. J.*, 77(1), pp 4-12.
- Brasquet, C., LeCloirec, P. (2000). Pressure drop through textile fabrics-experimental data modeling using classical models and neural networks. *Chemical Engineering Science*, 55, pp. 2767-2778.
- Çay A., Vassiliadis S., Rangoussi M. & Tarakçioğlu I. (2007). Prediction of the Air Permeability of Woven Fabrics using Neural Networks, *Int. J. of Cloth. Sc. & Techn.* Vol. 19, No 1, pp 18-35.

- Chattopadhyay R. & Guha A. (2004). Artificial Neural Networks: Applications to Textiles, *Textile Progress*, 35:1, 1-46.
- Chen, S., Cowan, C.F.N., and Grant, P.M. (1991). Orthogonal least-squares learning algorithm for radial basis function networks, *IEEE Transactions on Neural Networks*, vol. 2(2), pp. 302-309.
- Chen T., Li L., Koehl L., Vroman P. & Zeng X. (2007). A Soft Computing Approach to Model the Structure - Property Relations of Nonwoven Fabrics, *J. of Applied Polymer Science*, Vol. 103, pp. 442-450.
- Chen T., Wang K. & Wu L., (2009). Artificial Neural Network Modeling for the Weft Shear Stiffness of Worsted Fabrics, *3rd Int. Symp. on Intell. Inf. Techn. Appl.* v. 1, pp.211-215.
- Chen T., Zhang C., Chen X. & Li L.(2009). An Input Variable Selection Method for the Artificial Neural Network of Shear Stiffness of Worsted Fabrics, *Statistical Analysis and Data Mining*, Vol. 1 (5), pp 287-295.
- Chen T., Zhang C., Li L. & Chen, X. (2008). "Simulating the drawing of spunbonding nonwoven process using an artificial neural network technique", *J. of the Text. Inst.*, 99: 5, pp. 479 - 488.
- Chen X. & Huang X.B. (2004). Evaluating Fabric Pilling with Light-Projected Image Analysis, *Text. Res. J.*, 74(11), pp 977-981.
- Chen Y., Zhao T. & Collier B. J. (2001). Prediction of Fabric End-use Using a Neural Network Technique, *J. of the Text. Inst.*, 92: 2, pp. 157 - 163.
- Cheng K.P.S. & Lam H.L.I. (2003). Evaluating and Comparing the Physical Properties of Spliced Yarns by Regression and Neural Network Techniques, *Text. Res. J.*, 73(2), pp 161-164.
- Cheng L., Ghorashi H., Duckett K., Zapletalova T. & Watson M. (1999). Color Grading of Cotton Part II: Color Grading with an Expert System and Neural Networks, *Text. Res. J.*, 69(12), pp 893-903.
- Cherkassky A. & Weinberg A. (2010). Objective Evaluation of Textile Fabric appearance. Part 2: SET Opti-grade Tester, Grading Algorithms and Testing, *Text. Res. J.*, 80(2), pp 135-144.
- Chiu S.H., Chen H.M., Chen J.Y. & Wen C.Y. (2001). Appearance Analysis of False Twist Textured Yarn Packages Using Image Processing and Neural Network Technology, *Text. Res. J.*, 71(4), pp 313-317.
- Chiou Y.-C., Lin C.- S. & Chen G.-Z. (2009). Automatic texture inspection in the classification of papers and cloths with neural networks method, *Sens. Review*, 29/3, pp. 250-259.
- Choi H.T., Jeong S.H., Kim S.R., Jaung J.Y. & Kim S.H. (2001). Detecting Fabric Defects with Computer Vision and Fuzzy Rule Generation. Part II: Defect Identification by a Fuzzy Expert System, *Text. Res. J.*, 71(7), pp 563-573.
- Cybenko, G. (1989). Approximations by superpositions of sigmoidal functions. *Mathematics of Control, Signals, and Systems*, no. 4, pp. 303-314.
- Dayik M. (2009). Prediction of Yarn Properties Using Evaluation Programing", *Text. Res. J.*, 79(11), pp. 963-972.
- Debnath S. & Madhusootheran M. (2008). Modeling of Compression Properties of Needle-Punched nonwoven Fabrics Using Artificial Neural Network, *Ind. J. of Fibre & Text. Res.*, Vol. 33, pp. 392-399.
- Demiryurek O. & Koc E. (2009). Predicting the Unevenness of Polyester/Viscose Blended Open-end Rotor Spun Yarns Using Artificial Neural Network and Statistical Models, *Fibers and Polymers*, Vol.10, No.2, pp. 237-245.

- Elman, J.L. (1990). Finding structure in time, *Cognitive Science*, vol. 14, pp. 179-211.
- Ertugrul S. & Ucar N. (2000). Predicting Bursting Strength of Cotton Plain Knitted Fabrics Using Intelligent Techniques, *Text. Res. J.*, 70(10), pp 845-851.
- Fan J., Newton E., Au R. & Chan S.C.F. (2001). Predicting Garment Drape with a Fuzzy-Neural Network, *Text. Res. J.*, 71(7), pp 605-608.
- Farooq A. & Cherif C. (2008). Use of Artificial Neural Networks for Determining the Leveling Action Point at the Auto-leveling Draw Frame, *Text. Res. J.*, 78(6), pp 502-509.
- Fayala F., Alibi H., Benltoufa S. & Jemni A. (2008). Neural Network for Predicting Thermal Conductivity of Knit Materials, *J. of Eng. Fibers and Fabrics*, Vol. 3, Issue 4, pp. 53-60.
- Furferi R. & Carfagni M. (2010). Prediction of the Color and of the Color Solidity of a Jigger-dyed Cellulose-based Fabric: A Cascade Neural Network Approach, *Text. Res. J.*, 80, pp --.
- Ghane M., Semnani D., Saghafi R. & Beigzadeh H. (2008). Optimization of Top Roller Diameter of Ring Machine to Enhance Yarn Evenness by Using Artificial Intelligence, *Ind. J. of Fibre & Text. Res.*, Vol. 33, pp. 365-370.
- Gharehaghaji A.A., Shanbeh M. and Palhang M. (2007). Analysis of Two Modeling Methodologies for Predicting the Tensile Properties of Cotton-covered Nylon Core Yarns, *Text. Res. J.*, 77(8), pp 565-571.
- Ghosh A. & Chatterjee P. (2010). Prediction of Cotton Yarn Properties Using Support Vector Machine, *Fibers and Polymers*, Vol.11, No.1, pp. 84-88.
- Golob D., Osterman D.P. & Zupan J. (2008). Determination of Pigment Combinations for Textile Printing Using Artificial Neural Networks, *Fibr. & Text. in East. Eur.*, Vol. 16, No. 3 (68), pp 93-98.
- Gong R.H. & Chen, Y. (1999). Predicting the Performance of Fabrics in Garment Manufacturing with Artificial Neural Networks, *Text. Res. J.*, 69(7), pp 477-482.
- Guha A., Chattopadhyay, R. & Jayadeva (2001). Predicting Yarn Tenacity: A Comparison of Mechanistic, Statistical, and Neural Network Models, *J. of the Text. Inst.*, 92: 2, pp. 139 - 145.
- Gürkan Ünal P., Özdil N. & Taskin C. (2010). The Effect of Fiber Properties on the Characteristics of Spliced Yarns Part I: Prediction of Spliced Yarns Tensile Properties, *Text. Res. J.*, 80(5), pp 429-438.
- Gürkan Ünal P., Arikan C., Özdil N. & Taskin C. (2010). The Effect of Fiber Properties on the Characteristics of Spliced Yarns: Part II: Prediction of Retained Spliced Diameter, *Text. Res. J.*, 80, pp--.
- Gurumurthy B.R. (2007). Prediction of Fabric Compressive Properties Using Artificial Neural Networks, *AUTEX Res. J.*, Vol. 7, No 1.
- Guruprasad R. & Behera B.K. (2010). Soft Computing in Textiles, *Ind. J. of Fibre & Text. Res.*, Vol. 35, pp. 75-84.
- Hadizadeh M., Jeddi A.A.A. & Tehran M.A. (2009). The Prediction of Initial Load-extension Behavior of Woven Fabrics Using Artificial Neural Network, *Text. Res. J.*, 79(17), pp 1599-1609.
- Hadizadeh M., Tehran M. A. & Jeddi A.A.A. (2010). Application of an Adaptive Neuro-fuzzy System for Prediction of Initial Load/Extension Behavior of Plain-woven Fabrics, *Text. Res. J.*, 80(10), pp 981-990.
- Haykin, S. (1998). *Neural Networks: A Comprehensive Foundation*, Prentice Hall, ISBN 0132733501, New York.

- Hertz, J., Krogh, A. & Palmer, R.G. (1991). *Introduction to the Theory of Neural Computation*, Addison-Wesley Longman Publishing Co., Boston, MA, USA.
- Hornik, K., Stinchcombe, M. & White, H. (1989). Multilayer Feedforward Networks are universal approximators. *Neural Networks*, vol. 2, pp.359-366.
- Hu M.C. & I.S. Tsai I.C. (2000). Fabric Inspection Based on Best Wavelet Packet Bases, *Text. Res. J.*, 70(8), pp 662-670.
- Hu Z. H., Ding Y.S, Yu X. K., Zhang W. B. & Yan Q. (2009). A Hybrid Neural Network and Immune Algorithm Approach for Fit Garment Design, *Text. Res. J.*, 79(14), pp 1319-1330.
- Huang C.C. & Chen I.C. (2001). Neural-Fuzzy Classification for Fabric Defects, *Text. Res. J.*, 71(3), pp 220-224.
- Huang C.C. & Chang K.T. (2001). Fuzzy Self-Organizing and Neural Network Control of Sliver Linear Density in a Drawing Frame, *Text. Res. J.*, 71(11), pp 987-992.
- Huang C.C. & Lin T.F. (2008). Image Inspection of Nonwoven Defects Using Wavelet Transforms and Neural Networks, *Fibers and Polymers*, Vol.9, No.5, 633-638
- Huang CC. & Yu W.H. (2001). Fuzzy Neural Network Approach to Classifying Dyeing Defects, *Text. Res. J.*, 71(2), pp 100-104.
- Hui C.L., Lau T.W., Ng S.F. & Chan K.C.C. (2004). Neural Network Prediction of Human Psychological Perceptions of Fabric Hand, *Text. Res. J.*, 74(5), pp 375-383.
- Hui C.-L. & Ng S.-F. (2005). A new approach for prediction of sewing performance of fabrics in apparel manufacturing using artificial neural networks, *J. of the Text. Inst.*, 96: 6, pp. 401 - 405.
- Hui P.C.L., Chan K.C.C., Yeung K.W. & Ng F.S.F. (2007). Application of artificial neural networks to the prediction of sewing performance of fabrics, *Int. J. of Cloth. Sc. & Techn.*, Vol. 19 No. 5, pp. 291-318.
- Hui C.L. & Ng S.F. (2009). Predicting Seam Performance of Commercial Woven Fabrics Using Multiple Logarithm Regression and Artificial Neural Networks, *Text. Res. J.*, 79(18), pp 1649-1657.
- Islam M.A., Akhter S., Mursalin T.E. & Amin M.A. (2006). A Suitable Neural Network to Detect Textile Defects, King et al. (Eds.): *ICONIP 2006*, Part II, LNCS 4233, pp. 430 - 438, Springer.
- Jackowska-Strumillo L., Cyniak D., Czekalski J. & Jackowski T. (2008). Neural Model of the Spinning Process Dedicated to Predicting Properties of Cotton-Polyester Blended Yarns on the Basis of the Characteristics of Feeding Streams, *Fibr. & Text. in East. Eur.*, Vol. 16, No. 1 (66).
- Jasper W.J. & Kovacs E. (1994). Using Neural Networks and NIR Spectro-photometry to Identify Fibers, *Text. Res. J.*, August 1994; vol. 64, 8: pp. 444-448.
- Jaouadi M., Msahli S., Babay A. & Zitouni B. (2006). Analysis of the modeling methodologies for predicting the sewing thread consumption, *Int. J. of Cloth. Sc. & Techn.*, Vol. 18 No. 1, pp. 7-18.
- Jayadeva, Guha, A. & Chattopadhyay, R. (2003). A Study on the Capability of a Neural Network Ranking Fibre Parameters Having an Influence on Yarn Properties, *J. of the Text. Inst.*, 94: 3, pp. 186 - 193.
- Jeguirim S.E.G., Dhouiib A.B., Sahnoun A. Cheikhrouhou M. Schacher L. & Adolphe D. (2009). The use of fuzzy logic and neural networks models for sensory properties prediction from process and structure parameters of knitted fabrics, *J. Intell. Manuf.*, DOI 10.1007/s10845-009-0362-y.

- Jeon B. S., Bae J. H. & Suh M. W. (2003). Automatic Recognition of Woven Fabric Patterns by an Artificial Neural Network, *Text. Res. J.*, 73(7), pp 645-650.
- Jeong S.H., Kim J.H. & Hong C.J. (2000). Selecting Optimal Interlinings with a Neural Network, *Text. Res. J.*, 70(11), pp 1005-1010.
- Jianli, Liu & Baoqi, Zuo (2007). Identification of fabric defects based on discrete wavelet transform and back-propagation neural network, *J. Text. Inst.*, 98(4), pp. 355 - 362.
- Ju J. & Ryu H. (2006). A Study on Subjective Assessment of Knit Fabric by ANFIS, *Fibers and Polymers*, Vol.7, No.2, pp. 203-212.
- Kang T.J. & Kim S.C. (2002). Objective Evaluation of the Trash and Color of Raw Cotton by Image Processing and Neural Network, *Text. Res. J.*, 72(9), pp. 776-782.
- Karthikeyan B. & Sztandera L. M. (2010). Analysis of tactile perceptions of textile materials using artificial intelligence techniques, Part 2: reverse engineering using genetic algorithm coupled neural network, *Int. J. of Cloth. Sc. & Techn.*, Vol. 22 No. 2/3, pp. 202-210.
- Keeler, J. (1992). Vision of Neural Networks and Fuzzy Logic for Prediction and Optimisation of Manufacturing Processes, In: *Applications of Artificial Neural Networks III*, vol. 1709, pp. 447-456.
- Keshavaraj R., Tock R.W. & Nusholtz G.S. (1995). A Simple Neural Network Based Model Approach for Nylon 66 Fabrics Used in Safety Restraint Systems: A Comparison of Two Training Algorithms, *J. of Applied Polymer Science*, Vol. 57, pp. 1127-1144.
- Khan Z., Lim A.E.K., Wang L., Wang X. & Beltran R. (2009). An Artificial Neural Network-based Hairiness Prediction Model for Worsted Wool Yarns, *Text. Res. J.*, 79(8), pp 714-720.
- Kim E.H. (1999). Objective Evaluation of Wrinkle Recovery, *Text. Res. J.*, 69(11), pp. 860-865.
- Kim N.Y., Shin Y. & Kim E.Y. (2007). Emotion-Based Textile Indexing Using Neural Networks, J. Jacko (Ed.): Human-Computer Interaction, Part III, *HCI 2007*, LNCS 4552, pp. 349-357, Springer.
- Kumar A. (2003). Neural Network Based Detection of Local Textile Defects, *Pattern Recognition*, 36 pp.1645 - 1659.
- Kuo C.F.J. & Fang C.-C. (2006). Optimization of the Processing Conditions and Prediction of the Quality for Dyeing Nylon and Lycra Blended Fabrics, *Fibers and Polymers*, Vol.7, No.4, pp. 344-351.
- Kuo C.F.J., Hsiao K.I. & Wu Y.S. (2004). Using Neural Network Theory to Predict the Properties of Melt Spun Fibers, *Text. Res. J.*, 74(9), 2004, pp 840-843.
- Kuo C.F. J., Su T.L., Chang C.D. & Lee C.H. (2008). Intelligence Control of On-line Dynamic Gray Cloth Inspecting Machine System Module Design. II. Defects Inspecting Module Design, *Fibers and Polymers*, Vol.9, No.6, pp. 768-775.
- Kuo C.-F. J., Su T.L., Chiu C.-H. & Tsai C.-P. (2007). Analysis and Construction of a Quality Prediction System for Needle-Punched Non-woven Fabrics, *Fibers and Polymers*, Vol.8, No.1, 66-71.
- Kuo C.-F. J., Su T.L. & Huang Y.J. (2007). Computerized Color Separation System for Printed Fabrics by Using Backward-Propagation Neural Network, *Fibers and Polymers*, Vol.8, No.5, pp. 529-536.
- Kuo C.F.J., Wang C.C. & Hsieh C.T. (1999). Theoretical Control and Experimental Verification of Carded Web Density Part III: Neural Network Controller Design, *Text. Res. J.*, 69(6), pp 401-406.

- Lewandowski S. & Drobina R. (2008). Prediction of Properties of Unknotted Spliced Ends of Yarns Using Multiple Regression and Artificial Neural Networks. Part I: Identification of Spliced Joints of Combed Wool Yarn by Artificial Neural Networks and Multiple Regression, *Fibr. & Text. in East. Eur.*, 16, 5 (70) pp. 33-39.
- Lewandowski S. & Drobina R. (2008). Prediction of Properties of Unknotted Spliced Ends of Yarns Using Multiple Regression and Artificial Neural Networks. Part II: Verification of Regression Models, *Fibr. & Text. in East. Eur.*, 16,6 (71) pp. 20-27.
- Lin, D.-T. (1994). *The Adaptive Time-Delay Neural Network: Characterization and Applications to Pattern Recognition, Prediction and Signal Processing*. PhD thesis, University of Maryland, USA.
- Lin J.J. (2007). Prediction of Yarn Shrinkage using Neural Nets, *Text. Res. J.*, 77(5), pp 336-342.
- Lin T.H. (2004). Construction of Predictive Model on Fabric and Sewing Thread Optimization, *J. of Textile Engineering*, Vol. 50, No. 1, pp. 6-11.
- Lippman, R.P. (1987). An introduction to computing with neural nets. *IEEE ASSP Magazine*, pp. 4-22.
- Liu S., Wan O. & Zhang H. (2009). Fabric Weave Identification Based on Cellular Neural Network, *The Sixth Int. Symposium on Neural Networks*, AISC 56, pp. 563-569.
- Liu J., Zuo B., Vroman P., Rabenasolo B., Zeng X. & Bai L. (2010). Visual Quality Recognition of Nonwovens using Wavelet Texture Analysis and Robust Bayesian Neural Network, *Text. Res. J.*, 80, pp -.
- Lu Z.-J., Yang J.-G., Xiang Q. & Wang X.-L. (2007). Support Vector Machines for Predicting Worsted Yarn Properties, *Ind. J. of Fibre & Text. Res.*, Vol. 32, pp. 173-178.
- Majumdar A., Majumdar P.K. & Sarkar B. (2004). Selecting Cotton Bales by Spinning Consistency Index and Micronaire Using Artificial Neural Networks, *AUTEX Res. J.*, Vol. 4, No1, pp. 2-8.
- Majumdar P.K. & Majumdar A. (2004). Predicting the Breaking Elongation of Ring Spun Cotton Yarns Using Mathematical, Statistical, and Artificial Neural Network Models, *Text. Res. J.*, 74(7), pp 652-655.
- Majumdar A., Majumdar P.K. & Sarkar B. (2006). An investigation on yarn engineering using artificial neural networks, *J. of the Text. Inst.*, 97: 5, pp. 429 - 434.
- Majumdar A., Ciocoiu M. & Blaga M. (2008). Modelling of Ring Yarn Unevenness by Soft Computing Approach, *Fibers and Polymers*, Vol.9, No.2, 210-216.
- Majumdar A., Ghosh A., Saha S.S., Roy A., Barman S., Panigrahi D. & Biswas A. (2008). Empirical Modelling of Tensile Strength of Woven Fabrics, *Fibers and Polymers* 2008, Vol.9, No.2, 240-245.
- Majumdar A. (2010). Modeling of Cotton Yarn hairiness Using Adaptive Neuro-Fuzzy Inference System", *Ind. J. of Fibre & Text. Res.*, Vol. 35, pp. 121-127.
- Mak K.L. & Li W. (2007). Objective Evaluation of Seam Pucker on Textiles by Using Self-organizing Map. *IAENG International J. of Computer Science*, 35:1, IJCS_35_1.
- Matlab, (2005), MATLAB 7 R14, *Neural Network Toolbox User's Guide*, The MathWorks Inc., Natick, MA, USA.
- Matsudaira M. (2006). Fabric Handle and Its Basic Mechanical Properties, *J. of Textile Engineering*, Vol 52, No 1, pp. 1-8.
- Mori T. & Komiyama J. (2002). Evaluating Wrinkled Fabrics with Image Analysis and Neural Networks, *Text. Res. J.*, 72(5), pp. 417-422.

- Murrells C.M., Tao X.M., Xu B.G. & Cheng K.P.S. (2009). An Artificial Neural Network Model for the Prediction of Spirality of Fully Relaxed Single Jersey Fabrics, *Text. Res. J.*, 79(3), pp 227-234.
- Mursalin T.E., Eishita F.Z. & Islam A. R. (2008). Fabric Defect Inspection System Using Neural Network and Microcontroller, *J. of Theoretical and Applied Information Technology*, Vol4, No7.
- Murthyguru, (2005). Novel Approach To Study Compression Properties in Textiles, *AUTEX Res. J.*, Vol. 5, No 4.
- Mwasiagi J.I., Huang X. & Wang X. (2008). Performance of Neural Network Algorithms during the Prediction of Yarn Breaking Elongation, *Fibers and Polymers*, Vol.9, No.1, pp. 80-86.
- Mwasiagi J. I. , Wang X. H. & Huang X. B. (2009). The Use of K-means and Artificial Neural Network to Classify Cotton Lint, *Fibers and Polymers*, Vol.10, No.3, 379-383.
- Nurwaha D. & Wang X.H. (2008). Comparison of the New Methodologies for Predicting the CSP Strength of Rotor Yarn, *Fibers and Polymers*, Vol.9, No.6, pp. 782-784.
- Nurwaha D. & Wang X.H. (2010). Prediction of Rotor Spun Yarn Strength from Cotton Fiber Properties Using Adaptive Neuro-Fuzzy Inference System Method, *Fibers and Polymers*, Vol.11, No.1, pp. 97-100.
- Nuttle, H.L.W., King R.E., Hunter N.A., Wilson J.R. & Fang S.C. (2000). Simulation Modeling of the Textile Supply Chain. Part I: The Textile-plant Models, *J. of the Text. Inst.*, 91: 1, pp. 35 - 50.
- Onal L., Zeydan M., Korkmaz M. & Meeran S. (2009). Predicting the Seam Strength of Notched Webbing for Parachute Assemblies Using the Taguchi's Design of Experiment and Artificial Neural Networks, *Text. Res. J.*, 79(5), pp 468-478.
- Park S.W., Hwang Y.G., Kang B.C. & Yeo S.W. (2000). Applying Fuzzy Logic and Neural Networks to Total Hand Evaluation of Knitted Fabrics, *Text. Res. J.*, 70(8), pp 675-681.
- Park S.W., Hwang Y. G., Kang B.C. & Yeo S.W. (2001). Total handle evaluation from selected mechanical properties of knitted fabrics using neural network, *Int. J. of Cloth. Sc. & Techn.*, Vol. 13 No. 2, pp. 106-114.
- Payvandy P., Yousefzadeh-Chimeh M. & Latifi M. (2010). A note on neurofractal-based defect recognition and classification in nonwoven web images", *J. of the Text. Inst.*, 101: 1, pp. 46 - 51.
- Ramaiah G.B., Chennaiah R.Y. & Satyanarayanan G.K. (2010). Investigation and modeling on protective textiles using artificial neural networks for defence applications, *Materials Science and Engineering B* 168 pp.100-105.
- Ramesh M.C., Rajamanickam R. & Jayaraman S. (1995). The Prediction of Yarn Tensile Properties by Using Artificial Neural Networks, *J. Text. Inst.*, 86: 3, pp. 459 - 469.
- Rautenberg S. & Todesco J.L. (1999). Color Recipe Specification in the Textile Print Shop Using Radial Basis Function Networks, *Engineering Applications of Bio Inspired ANN*, pp 884-892, Springer.
- Rich, E. & Knight, K. (1991). *Artificial Intelligence*, McGraw-Hill, New York, USA, pp. 487-524.
- Sang-Song L. & Tsung-Huang L. (2007). FAST System Approach to Discriminate the Characterized Generic Hand of Fabrics, *Ind. J. Fibr. & Text. Res.*, Vol. 32, pp. 344-350.
- Sette S. & Boullart L. (1996). Fault detection and quality assessment in textiles by means of neural nets, *Int. J. of Cloth. Sc. & Techn.*, Vol. 8 No. 1/2, pp. 73-83.

- Sette S. & van Langenhove L. (2002). Optimising the Fibre-to-Yarn Production Process: Finding a Blend of Fibre Qualities to Create an Optimal Price/Quality Yarn, *AUTEX Res. J.*, Vol. 2, No2, pp 57-63.
- Shady E., Gowayed Y., Abouiiiana M., Youssef S. & Pastore C. (2006). Detection and Classification of Defects in Knitted Fabric Structures, *Text. Res. J.*, 76(4), 2006, pp 295-300.
- She F.H., Kong L.X., Nahavandi S. & Kouzani A.S. (2002). Intelligent Animal Fiber Classification with Artificial Neural Networks, *Text. Res. J.*, 72(7), pp 594-600.
- Shiau Y.-R., Tsai I-S. & Lin C.-S. (2000). Classifying Web Defects with a Back-Propagation Neural Network by Color Image Processing, *Text. Res. J.*, 70(7), 2000, pp. 633-640.
- Shyr T.W., Lin J.Y. & Lai S.S. (2004). Approaches to Discriminate the Characteristic Generic Hand of Fabrics, *Text. Res. J.*, 74(4), pp 354-358.
- Slah M., Amine H. T. & Faouzi, S. (2006). A new approach for predicting the knit global quality by using the desirability function and neural networks, *J. of the Text. Inst.*, 97:1, pp. 17 - 23.
- Stylios, G. & Parsons-Moore, R. (1993). Seam pucker prediction using neural computing. *Intl. J. of Clothing Science and Technology*, vol. 5, no.5, pp. 24-27.
- Stylios G.K. & Powell N.J. (2003). Engineering the drapability of textile fabrics, *Int. J. of Cloth. Sc. & Techn.*, Vol. 15 No. 3/4, pp. 211-217.
- Stylios, G. & Sotomi, J.O., (1996). Thinking sewing machines for intelligent garment manufacture. *Intl. J. of Clothing Science and Technology*, vol. 8 (1/2), pp. 44-55.
- Su J. & Xu B. (1999). Fabric wrinkle evaluation using laser triangulation and neural network classifier, *Opt. Eng.* 38, pp. 1688.
- Subramanian S.N., Venkatachalam A. & Subramaniam V. (2007). Prediction and Optimization of Yarn Properties Using Genetic Algorithm/Artificial Neural Network, *Ind. J. of Fibre & Text. Res.*, Vol. 32, pp. 409-413.
- Thevenet L., Dupont D. & Jolly-Desodt A.M. (2003). Modeling Color Change after Spinning Process Using Feedforward Neural Networks, *Color Research and Application*, Vol. 28, No 1, pp. 50-58.
- Tilocca A., Borzone P., Carosio S. & Durante A. (2002). Detecting Fabric Defects with a Neural Network Using Two Kinds of Optical Patterns, *Text. Res. J.*, 72(6), pp 545-550.
- Tokarska M. (2004). Neural Model of the Permeability Features of Woven Fabrics, *Text. Res. J.*, 74(12), pp 1045-1048.
- Tokarska M. (2006). Assessing the Quality of Neural Models Using a Model of Flow Characteristics of Fabrics as an Example, *AUTEX Res. J.*, Vol. 6, No 3.
- Tokarska M. & Gniotek K. (2009). Determination of Woven Fabric Impact Permeability Index, *Ind. J. of Fibre & Text. Res.*, Vol. 34, pp. 239-244.
- Tran C.-D. & Phillips D. G. (2007). Predicting torque of worsted singles yarn using an efficient radial basis function network-based method, *J. of the Text. Inst.*, 98: 5, pp. 387 - 396.
- Tran C.-D. , Phillips D. G. & Fraser W. B. (2010). Stationary solution of the ring-spinning balloon in zero air drag using a RBFN based mesh-free method, *J. of the Text. Inst.*, 101: 2, pp. 101 – 110.
- Tsai I-S., Lin C.H. & Lin J.J. (1995). Applying an Artificial Neural Network to Pattern Recognition in Fabric Defects, *Text. Res. J.*, vol. 65, 3: pp. 123-130.
- Vangheluwe L., Sette S. and Kiekens, P.(1996). Modelling Relaxation Behaviour of Yarns Part II: Back Propagation Neural Network Model, *J. of the Text. Inst.*, 87: 2, pp. 305 - 310.

- Vassiliadis S., Rangoussi M., Kremenakova D., Belkhir M., Boukhris M.A. & Louda O. (2010). Prediction of Bursting Strength of Fabrics using Neural Networks, *International Conference of Applied Research in Textile, CIRAT-4, Monastir, Tunisia*.
- Ucar N. & Ertugrul S. (2007). Prediction of Fuzz Fibers on Fabric Surface by Using Neural Network and Regression Analysis, *Fibr. & Text. in East. Eur.*, 15, 2 (61) pp. 58-61.
- Üreyen M.E. & Gürkan P. (2008). Comparison of Artificial Neural Network and Linear Regression Models for Prediction of Ring Spun Yarn Properties. I. Prediction of Yarn Tensile Properties, *Fibers and Polymers*, Vol.9, No.1, pp. 87-91.
- Üreyen M.E. & Gürkan P. (2008). Comparison of Artificial Neural Network and Linear Regression Models for Prediction of Ring Spun Yarn Properties. II. Prediction of Yarn Hairiness and Unevenness, *Fibers and Polymers*, Vol.9, No.1, pp. 92-96.
- Xu B. & Lin S. (2002). Automatic Color Identification in Printed Fabric Images by a Fuzzy-Neural Network, *AATCC Review*, 2(9), 42-45, 2002.
- Xu B., Su J., Dale D.S. & Watson M.D. (2000). Cotton Color Grading with a Neural Network, *Text. Res. J.*, 70(5), pp 430-436.
- Yao G., Guo J. & Zhou Y. (2005). Predicting the Warp Breakage Rate in Weaving by Neural Network Techniques, *Text. Res. J.*, 75(3), pp. 274-278.
- Yazdi M.M, Semnani D. & Sheikhzadeh M. (2009). Moisture and Heat Transfer in Hybrid Weft Knitted Fabric with Artificial Intelligence, *J. of Applied Polymer Science*, Vol. 114, pp. 1731-1737.
- Yin X.G. & Yu W. (2007). Selection and Evaluation of Input Parameters of Neural Networks Using Grey Superior Analysis, *Text. Res. J.*, 77(6), pp 377-386.
- Youssefi M., & Faez K. (1999), "Fabric Handle Prediction Using Neural Networks", *Proceedings of the IEEE-EURASIP Workshop on Nonlinear Signal and Image Processing (NSIP'99)*, Antalya, Turkey,, Bogaziçi University Printhouse, ISBN 975-518-133-4.
- Yuen C.W.M., Wong W.K., Qian S.Q., Fan D.D., Chan L.K. & Fung E.H.K. (2009). Fabric Stitching Inspection Using Segmented Window Technique and BP Neural Network, *Text. Res. J.*, 79(1), pp 24-35.
- Wang K.F. & Zeng Y. (2008). A Wavelet Neural Network Applied to Textile Spinning, *Aspects of Mathematical Modelling, Mathematics and Biosciences in Interaction*, pp. 363-369.
- Wong A.S.W., Li Y., Yeung P.K.W. & Lee P.W.H. (2003). Neural Network Predictions of Human Psychological Perceptions of Clothing Sensory Comfort, *Text. Res. J.*, 73(1), pp 31-37.
- Wu, P., Fang, S.-C., Nuttle, H.L.W., King, R.E. & Wilson, J.R. (1994). Decision surface modeling of textile spinning operations using neural network technology, *Textile, Fiber and Film Industry Techn. Conf., IEEE 1994 Annual*, pp.0-19, 4-5 May 1994.
- Zadeh, L. (1994). *Soft Computing and Fuzzy Logic*, IEEE Software, vol. 11, no.1-6, pp. 48-56.
- Zeng Y.C., Wang K.F. & Yu C.W. (2004). Predicting the Tensile Properties of Air-Jet Spun Yarns, *Text. Res. J.*, 74(8), pp 689-694.
- Zhang J., Wang X. & Palmer S. (2010). Performance of an Objective Fabric Pilling Evaluation Method, *Text. Res. J.*, 77(6), pp -.
- Zhang J., Wang X. & Palmer S. (2010). Objective Pilling Evaluation of Nonwoven Fabrics, *Fibers and Polymers*, Vol.11, No.1, pp. 115-120.